Rep. Prog. Phys. 55 (1992) 1241–1309. Printed in the UK

Phase transitions in lyotropic colloidal and polymer liquid crystals

G J Vroege and H N W Lekkerkerker

Van 't Hoff Laboratory, University of Utrecht, Padualaan 8, 3584 CH Utrecht, The Netherlands

Abstract

An overview is given of theory and experiments on liquid crystal phases which appear in solutions of elongated colloidal particles or stiff polymers. The Onsager (1949) virial theory for the isotropic–nematic transition of thin rodlike particles is treated comprehensively along with extensions to polydisperse solutions and soft interactions. Computer simulations of liquid crystal phases in hard particle fluids are summarized and used to assess the quality of statistical mechanical theories for stiff particles at higher volume fraction—like the inclusion of higher virial coefficients, y-expansion, scaled particle theory and density functional theory. Both computer simulations and density functional theory indicate formation of more highly ordered smectic phases. The range of experimental applicability is strongly widened by the extension of the virial theory to wormlike chains by Khokhlov and Semenov (1981, 1982). Finally, experimental results for a number of carefully studied, charged and uncharged colloids and polymers are summarized and compared to theoretical results. In many cases the agreement is semi-quantitative.

This review was received in July 1991.

0034-4885/92/081241+69$18.00

Contents

1. Introduction

Although liquid crystals have been known for more than a century (Reinitzer 1888) a real upsurge in interest can be traced to the last 25 years. One reason for this is the use of liquid crystals in device applications such as displays. Another reason for an increased study of liquid crystals is the wealth of different possible phases with orientational order and/or partial positional order which appear beside the more common gaseous, liquid and crystalline phases. These liquid crystal phases presented the opportunity to study all types of subtle problems in the theory of phase transitions, in particular critical phenomena (Pershan 1988).

In this review we shall not treat the low molecular weight liquid crystals referred to above but their high molecular weight counterparts consisting of polymers or colloidal particles and of those only the liquid crystalline phases which are formed in solutions of these particles (the so called *lyotropic* liquid crystals). In parallel with the history of low molecular weight liquid crystals, lyotropic liquid crystalline phases were recognized a long time ago, namely in solutions of inorganic particles (V_2O_5 by Zocher (1925)) and biological particles (tobacco mosaic virus by Bawden *et al* (1936)) but there is an increased interest over the last decade. Partially this originates from industrial applications like the wet spinning of ultrastrong fibres (e.g. polyaramids, for reviews see Kwolek *et al* (1987) and Northolt and Sikkema (1990)), partially from biological problems like, for example, the dense packing of DNA in virus heads (Earnshaw and Casjens 1980). Apart from these applications, the phase transitions observed for lyotropic liquid crystals are of interest in their own right allowing a satisfactory theoretical description as a result of the low concentrations at which these phases appear and the relatively simple way in which the interaction between the particles may be described.

The *thermotropic* variety of liquid crystalline polymers (which show liquid crystal phase transitions by variation of the temperature) will not be covered in this review. The basic reason for this is that the vast amount of work which has been performed since the discovery of the thermotropic main chain polymers (e.g. polyesters (Jackson and Kuhfuss 1976)) has mainly focused on the materials science, whereas a description from the viewpoint of statistical mechanics—as is the emphasis in our paper—has proven very difficult up to now.

As alluded to above our starting point in this review is the statistical mechanical theory of phase transitions in liquid crystals. This field was opened by the seminal work of Onsager in the 1940s (Onsager 1942, 1949) who recognized that the isotropic–nematic phase transition for stiff slender particles may be treated within a virial expansion of the free energy—in contrast to the gas–liquid transition. For very thin, rigid, hard particles the transition occurs at very low volume fraction and the virial expansion may be truncated after the second virial term, leading to an exact theory for infinitely thin particles. We therefore describe the Onsager theory in depth and extension in section 2, combineing it with later work within the second virial approach. For somewhat shorter particles the second virial theory is no longer adequate, so section 3 deals with attempts to go beyond it. In recent years, computer simulations have played an important role in this respect, which we also summarize in section 3. Computer simulations of hard particles show that it is possible to obtain more highly ordered phases like the layered smectic phases without attractive interactions between the particles. Section 4 describes the density functional formalism which is, in principle, able to include these more highly ordered phases. For the

application of virial theories a strong impediment has been its limitation to rigid particles. This has changed with its extension to semiflexible (wormlike chain) polymers by Khokhlov and Semenov (1981, 1982), which is treated in section 5. Finally, in section 6 we compare the theory to available experimental results.

In this review we have chosen a didactic presentation for our material. This forces us to refrain from presenting all lines of attack. Specifically, we do not discuss the lattice-based theories of Flory and coworkers (Flory 1956, Flory and Abe 1978, Abe and Flory 1978, Flory and Frost 1978, Frost and Flory 1978, Flory 1978, Flory and Ronca 1979, Warner and Flory 1980, Flory 1984) or alternative lattice theories like DiMarzio (1961). Although these theories present an ingenious model which may describe many features of liquid crystalline polymers qualitatively (like e.g. behaviour at higher densities, with attractive interactions and for bidisperse systems), they do not lead to the exact result of Onsager for infinitely thin hard rods. There are also some other models based on the wormlike chain which we can only mention here: an extension of the Flory theory to wormlike chains (Ronca and Yoon 1982, 1984, 1985) and theories using a Maier–Saupe potential (Ten Bosch *et al* 1983, 1987, Warner *et al* 1985). As a last point we want to draw attention to some monographs and review papers on liquid crystals (De Gennes 1974, Stephen and Straley 1974, Chandrasekhar 1977, Luckhurst and Gray 1979, Vertogen and De Jeu 1988, Frenkel 1991) and liquid crystalline polymers (Straley 1973a, Blumstein 1978, Grosberg and Khokhlov 1981, Ciferri *et al* 1982, Miller 1982, Samulski and DuPré 1983, Gordon and Platé 1984, Khokhlov and Semenov 1985, Odijk 1986a, Ciferri and Marsano 1987, Semenov and Khokhlov 1988, DuPré and Yang 1991), which might be helpful for the reader.

2. Virial theory of the isotropic–nematic transition

2.1. Imperfect gas

At the beginning of this century the virial expansion was introduced by Kamerlingh Onnes (1901) as an empirical systematic correction to the pressure P of an ideal gas at higher (number) densities ρ

$$\frac{P}{kT} = \rho + B_2\rho^2 + B_3\rho^3 + \cdots \tag{1}$$

where B_2 and B_3 are the second and third virial coefficients respectively. Later, and especially in the 1930s, much work was done to provide this density expansion with a theoretical background, starting from statistical mechanics. As derivations of the virial expansion are found in many textbooks of statistical mechanics (Mayer and Mayer 1940, Hansen and McDonald 1986, McQuarrie 1976, Feynman 1972) we briefly summarize some relevant formulae. In the following we assume pairwise interaction u between particles so that the potential energy U can be written as a summation over pairs

$$U = \sum_{i<j} u(i,j). \tag{2}$$

Starting either from the canonical or the grand-canonical partition function, both of which contain the Boltzmann factor $\exp(-U/kT)$, it was shown that a virial series

for the pressure could be made. In view of the pairwise potential energy (2) we expect functions $\exp(-u(i,j)/kT)$ to appear in the derived expressions for the virial coefficients. They indeed show up as the so-called Mayer functions (Mayer and Mayer 1940)

$$\Phi(i,j) = \exp(-u(i,j)/kT) - 1 \tag{3}$$

which vanish outside the range of the potential. The virial coefficients B_n are proportional to irreducible cluster integrals β_{n-1} of these Mayer functions. The second virial coefficient contains interactions between two particles

$$B_2 = -\beta_1/2 = -\frac{1}{2V}\int\int \Phi(1,2)\,\mathrm{d}\boldsymbol{r}_1\,\mathrm{d}\boldsymbol{r}_2 \tag{4}$$

as it is the coefficient for the quadratic term in ρ. The third virial coefficient involves all clusters with simultaneous interactions between three particles

$$B_3 = -2\beta_2/3 = -\frac{1}{3V}\int\int\int \Phi(1,2)\Phi(1,3)\Phi(2,3)\,\mathrm{d}\boldsymbol{r}_1\,\mathrm{d}\boldsymbol{r}_2\,\mathrm{d}\boldsymbol{r}_3. \tag{5}$$

Note that for a cluster, in which one pair does not interact, the corresponding Mayer function is 0 and this cluster does not contribute to B_3 (although it does to B_2). In 1937 and later it was hoped that virial expansions could be used to describe the gas–liquid phase transition (Mayer and Mayer 1940). This hope was not fulfilled, but we shall see that at the same time Onsager (1942, 1949) recognized it to be useful in the description of the isotropic–nematic phase transition in solutions of thin rods.

2.2. *Non-ideal solutions*

As Van 't Hoff's law says there is a striking similarity between an ideal gas and an ideal solution when we replace the pressure of the gas, P, by the osmotic pressure of the solution, Π. The analogy also holds for the imperfect case when we use the *potential of mean force* $w(i,j)$ between two solute particles instead of the direct potential $u(i,j)$ (Onsager 1933, McMillan and Mayer 1945, Hill 1956). This procedure takes an average over all possible configurations of the solvent molecules accounting for interactions among themselves and with the solute particles. Using $w(i,j)$ in the Mayer function

$$\Phi(i,j) = \exp(-w(i,j)/kT) - 1 \tag{6}$$

virial expansion (1) and virial coefficients (4) and (5) now hold for the osmotic pressure. For phase transitions it is more appropriate to use a virial expansion of the Helmholtz free energy of the solute ΔF

$$\frac{\Delta F}{NkT} = \frac{\mu^0(T,\mu_0,\mu_1,\ldots)}{kT} + \ln(\Lambda^3\rho) - 1 + B_2\rho + \tfrac{1}{2}B_3\rho^2 + \cdots \tag{7}$$

where μ^0 is the reference chemical potential of the solute, which depends on the chemical potentials of the solvent components $\mu_0, \mu_1, \ldots$ and Λ is the de Broglie wavelength. The virial series for the (osmotic) pressure (1) is obtained by the usual thermodynamic relation

$$\Pi = -(\partial\Delta F/\partial V)_{N,T,\mu_0,\mu_1,\ldots}. \tag{8}$$

In the context of nematic liquid crystals we must account for the possibility of a non-uniform orientational distribution function $f(\Omega)$, which gives the probability of finding a (rigid) particle with an orientation characterized by solid angle Ω. This distribution function must be normalized

$$\int f(\Omega)\,\mathrm{d}\Omega = 1. \tag{9}$$

In the isotropic phase all orientations are equally probable which implies

$$f_{\mathrm{iso}}(\Omega) = \frac{1}{4\pi} \tag{10}$$

is compatible with the normalization (9). As a consequence of this non-uniform $f(\Omega)$ in the nematic phase, we must subtract T multiplied by an *orientational entropy*

$$S_{\mathrm{or}} = -Nk \int f(\Omega) \ln[4\pi f(\Omega)]\,\mathrm{d}\Omega \equiv -Nk\sigma[f] \tag{11}$$

from the free energy. A second effect is that all cluster integrals (which now depend on the orientations of the particles through w) must be averaged to obtain the virial coefficients, e.g.

$$B_2 = -\tfrac{1}{2} \iint \beta_1(\Omega, \Omega') f(\Omega) f(\Omega')\,\mathrm{d}\Omega\,\mathrm{d}\Omega'. \tag{12}$$

Onsager (1949) derived these expressions by considering particles of different orientations as belonging to different species. Equation (11) is then the entropy of mixing and (12) the natural expression for B_2 of a mixture.

Sometimes there is confusion about the validity of the virial series for long particles. It may be useful to stress that—although some derivations are not correct—the derivation by Doi and Edwards (1986) is satisfactory. We must find the free energy under the condition that the orientational distribution is given by $f(\Omega)$. The configurational partition function Z may then be factorized into an ideal part (without interactions)

$$Z_0 = \frac{1}{N!} \int_f \mathrm{d}\Omega^N\,\mathrm{d}\boldsymbol{r}^N \tag{13}$$

and an interaction part

$$Z_1 = \int_f \exp\left(-\sum_{i<j} w(i,j)/kT\right) \mathrm{d}\Omega^N\,\mathrm{d}\boldsymbol{r}^N \Big/ \int_f \mathrm{d}\Omega^N\,\mathrm{d}\boldsymbol{r}^N \tag{14}$$

$$\equiv \left\langle \exp\left(-\sum_{i<j} w(i,j)/kT\right)\right\rangle_f . \tag{15}$$

The condition that the orientational distribution must be $f(\Omega)$ is denoted by the subscript f on the integral. Z_0 leads to the ideal term $\ln\rho - 1$ and the restriction on the orientational distribution to the extra entropic term (11). The interaction

part Z_1 can be approximated by taking each of the $N(N-1)/2$ pair interactions independently from all others

$$Z_1 \simeq \prod_{i<j} \langle \exp(-w(i,j)/kT) \rangle_f \tag{16}$$

$$\simeq \langle 1 + \Phi(1,2) \rangle_f^{N(N-1)/2}$$

$$\simeq \left[1 - \frac{1}{V} \int \beta_1(\Omega_1, \Omega_2) f(\Omega_1) f(\Omega_2) \, d\Omega_1 \, d\Omega_2 \right]^{N(N-1)/2}$$

$$\simeq \exp\left[-N\rho \tfrac{1}{2} \int \beta_1(\Omega_1, \Omega_2) f(\Omega_1) f(\Omega_2) \, d\Omega_1 \, d\Omega_2 \right] \tag{17}$$

where we used (6) and (4). The standard relation $F = -kT \ln Z$ gives us expression (12) for B_2. Van Kampen (1961) devised an elegant method to derive higher order terms in the virial series from correction factors to (16). Although his method was developed for gases it may be used to extend the above results analogously.

Finally, we may now summarize the foregoing in the following expression for the free energy

$$\frac{\Delta F}{NkT} = \frac{\mu^0}{kT} + \ln(\Lambda^3 \rho) - 1 + \int f(\Omega) \ln[4\pi f(\Omega)] \, d\Omega$$

$$- \tfrac{1}{2} \rho \iint \beta_1(\Omega, \Omega') f(\Omega) f(\Omega') \, d\Omega \, d\Omega' + \cdots . \tag{18}$$

As we shall see later, this expression for the free energy is sufficient to show an isotropic–nematic phase transition. As examples we will first consider hard rods and subsequently charged rods.

2.3. Virial coefficients of hard rods

Hard particles are characterized by particularly simple potentials and Mayer functions

$$\begin{aligned} w &= \infty \qquad \Phi = -1 \qquad \text{for overlapping particles} \\ w &= 0 \qquad \Phi = 0 \qquad \text{for non-overlapping particles.} \end{aligned} \tag{19}$$

This makes cluster integral β_1 the negative of the excluded volume v_{excl} of both particles involved

$$\beta_1(\Omega, \Omega') = \frac{1}{V} \iint \Phi \, d\boldsymbol{r}_1 \, d\boldsymbol{r}_2 = \int_{\text{overlap}} (-1) \, d\boldsymbol{r}_{12} = -v_{\text{excl}}(\Omega, \Omega'). \tag{20}$$

As a model for hard rods we may take spherocylinders (consisting of cylinders of diameter D and length L capped with two hemispheres).

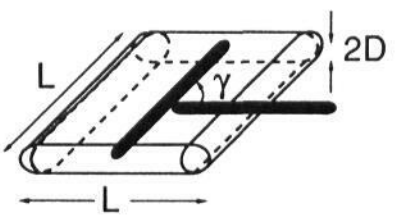

Figure 1. The excluded volume of two spherocylinders.

The volume excluded to a second spherocylinder due to the presence of the first is sketched in figure 1 and is dependent on the angle $\gamma(\Omega,\Omega')$ between both cylinders

$$-\beta_1(\Omega,\Omega') = 2L^2D|\sin\gamma| + 2\pi D^2L + \tfrac{4}{3}\pi D^3. \tag{21}$$

Note that the last two terms are end corrections which are at least of order D/L smaller than the leading term. The end corrections depend on the exact form of the rods near the ends and are, for example, different for simple cylinders. For thin rods these end effects are of minor importance, thus giving

$$-\beta_1(\Omega,\Omega') \sim 2DL^2|\sin\gamma| \tag{22}$$

where $\sim$ denotes an asymptotic relationship (only giving the leading term).

The next step would be to determine B_3. However, before turning to that problem it is good to realize that a virial series only makes sense if it is rapidly convergent. We might ask whether this is feasible in the case of thin rods. Let us first consider the *isotropic* phase. With the help of equations (10), (22) and (12) we find

$$\begin{aligned} B_2^{\mathrm{iso}} &= -\frac{1}{2}\iint -2DL^2|\sin\gamma|\frac{1}{4\pi}\frac{1}{4\pi}\,\mathrm{d}\Omega\,\mathrm{d}\Omega' \\ &= \frac{\pi}{4}DL^2. \end{aligned} \tag{23}$$

It is this (excluded) volume which determines when the rods are strongly interacting, rather than the proper volume of the rod, being $v_0 = (\pi/4)D^2L$. This will be the case, when the number density of rods reaches the order of 1 rod per v_{excl} or $B_2^{\mathrm{iso}}\rho = \mathcal{O}(1)$. When we now write equation (7) as

$$\frac{\Delta F^{\mathrm{iso}}}{NkT} = \frac{\mu^0}{kT} + \ln(\Lambda^3\rho) - 1 + B_2^{\mathrm{iso}}\rho + \frac{B_3^{\mathrm{iso}}}{2(B_2^{\mathrm{iso}})^2}(B_2^{\mathrm{iso}}\rho)^2 + \cdots \tag{24}$$

we see that the condition for rapid convergence is that $B_n^{\mathrm{iso}}/[(n-1)(B_2^{\mathrm{iso}})^{n-1}]$ be small (for all $n > 2$). When we look at equation (5) we see that to obtain the third virial coefficient we can start from a configuration in which two rods overlap (this gives a contribution of $\mathcal{O}(L^2D)$, just like the second virial coefficient) and subsequently put the third rod in the overlap area of the first two rods (so that the centre point of the third rod probes a volume of $\mathcal{O}(LD^2)$). Onsager (1949) gave some further geometric arguments and estimated the following scaling behaviour

$$\frac{B_3^{\mathrm{iso}}}{(B_2^{\mathrm{iso}})^2} \sim \frac{D}{L}\left(\ln\frac{L}{D} + \text{constant}\right) \tag{25}$$

which means it is small in the limit of thin rods ($L \gg D$). By a combination of analytical and numerical work, Straley (1973b) verified the smallness of equation (25) for large L/D ratios. For higher virial coefficients the number of integrations increases so drastically that a Monte Carlo simulation is more suitable. Frenkel's (1987a, 1988) results for different L/D are given in table 1, which show that the ratios indeed decrease but the limit that all higher virial coefficients may be neglected is only reached for very high L/D.

Table 1. Reduced third, fourth and fifth virial coefficients of hard spherocylinders, as a function of the length-to-breadth ratio L/D (from Frenkel (1987a)).

L/D	B_3/B_2^2	B_4/B_2^3	B_5/B_2^4
0	0.625	0.286 95	0.110 25
5	0.4194	0.0528	0.0110
10	0.3133	−0.0157	0.0229
10^2	0.0698	−0.0291	0.0325
10^3	0.0106	−0.0045	0.0051
10^4	0.001 45	−0.000 50	0.000 61
10^5	0.000 172	−0.000 049	0.000 03
10^6	0.000 021	−0.000 005	0.000 011

In the *nematic* phase we expect even more stringent requirements on L/D. In the extreme case of perfectly parallel (sphero)cylinders v_{excl} is no longer much larger than v_0 (as is readily seen from equation (21) when $\gamma = 0$) and B_3 scales like v_0^2. The relative importance of the higher virial coefficients is much more like the case of spheres (see the first row of table 1) and may never be neglected. The crucial question now is whether the clusters in the nematic phase are similar to those in the isotropic phase or to those in the perfectly aligned state. Luckily, we shall see in the next section that at the phase transition the order is moderately high but independent of L/D. Thus by making L/D so large that all typical angles are much larger than D/L, we can be confident that higher virial coefficients may be neglected. This point makes Onsager's (second virial) theory an exact theory for $L/D \to \infty$.

2.4. *The isotropic–nematic transition for thin hard rods*

Let us first introduce a dimensionless concentration

$$c \equiv (B_2^{\text{iso}}\rho) \overset{(23)}{=} \frac{\pi}{4} L^2 D \frac{N}{V} = \frac{L}{D} v_0 \frac{N}{V} = \frac{L}{D}\phi \tag{26}$$

where ϕ is the volume fraction of the rods. Combining this with equations (18) and (22) we have

$$\frac{\Delta F[f]}{NkT} \simeq \text{constant} + \ln c + \sigma[f] + c\rho[f] \tag{27}$$

where $\sigma[f]$ is related to the orientational entropy as given in equation (11). For hard particles $-c\rho[f]$ is also entropic in nature, namely a *packing entropy*,

$$\rho[f] \equiv \frac{4}{\pi} \iint |\sin\gamma| f(\Omega) f(\Omega')\, \mathrm{d}\Omega\, \mathrm{d}\Omega'. \tag{28}$$

The isotropic–nematic transition originates from a competition between these two types of entropy: for low concentrations the orientational entropy dominates and is maximized by an *isotropic* distribution, whereas for high concentrations the packing entropy becomes more important which favours a *nematic* distribution. For the isotropic phase σ and ρ are easily found from equations (10), (11), (23) and (28)

$$\sigma_{\text{iso}} = 0 \qquad \rho_{\text{iso}} = 1. \tag{29}$$

For a given concentration c the free energy must be a minimum. There are two different ways to find this minimum:

(i) choosing a (normalized) *trial function* with one or more variational parameters, then calculating the free energy as a function of these parameters and then minimizing the free energy with respect to these parameters;

(ii) considering ΔF as a functional of f, while taking into account the normalization condition (9) by adding $\lambda' \int f(\Omega)\,\mathrm{d}\Omega$ (λ' being a Lagrange undetermined multiplier) and then minimizing the resulting expression *formally*. This means the functional derivative must be 0 or

$$\frac{\delta}{\delta f}\left(\frac{\Delta F[f]}{NkT}\right) = \lambda'. \tag{30}$$

Before examining both routes in more detail, we must realize that—when we are considering a nematic phase—the distribution function must satisfy its symmetry properties, namely cylindrical symmetry around the director (f does not depend on azimuthal angle φ) and inversion symmetry (θ and $\pi - \theta$ are equivalent). This implies that $f(\Omega)$ can be taken as $f(\theta)$.

2.4.1. Trial functions. Here, we prescribe a fixed functional form for $f(\theta)$, which may be accommodated by one (or more) variational parameter(s). Of course, the success of the method largely depends upon the form chosen. Onsager (1949) chose the following function

$$f_{\mathrm{O}}(\cos\theta) = \frac{\alpha \cosh(\alpha \cos\theta)}{4\pi \sinh\alpha} \tag{31}$$

which works quite well. For illustrative purposes we shall use a Gaussian distribution function (Odijk 1986a) here

$$\begin{aligned} f_{\mathrm{G}}(\theta) &\sim N \exp\left(-\tfrac{1}{2}\alpha\theta^2\right) \qquad 0 \leqslant \theta \leqslant \pi/2 \\ &\sim N \exp\left(-\tfrac{1}{2}\alpha(\pi-\theta)^2\right) \qquad \pi/2 \leqslant \theta \leqslant \pi \end{aligned} \tag{32}$$

$N = N(\alpha)$ is a normalization constant (see appendix A). Similar functions have also been used, e.g. (Straley 1973b)

$$f_{\mathrm{S}}(\theta) \sim N \exp(-A \sin^2\theta). \tag{33}$$

Note that for large α (or A) these functions are asymptotically equal to f_{O}. In this case the distribution functions are strongly peaked and therefore suitable for strongly ordered nematics. In appendix A we describe how an asymptotic expression (valid for large α) can be derived for ΔF

$$\frac{\Delta F(\alpha)}{NkT} \sim \text{constant} + \ln\alpha - 1 + \frac{4c}{\sqrt{\pi\alpha}}. \tag{34}$$

Minimizing this expression with respect to α leads to

$$\alpha \sim \frac{4c^2}{\pi}. \tag{35}$$

This dependence of α on c means that the typical angle of a rod with the director $\sqrt{\langle\theta^2\rangle}$ is inversely proportional to the concentration (see equation (192)). Finally, the

usual measure of the ordering in the nematic phase is the nematic order parameter given by

$$S \equiv \langle P_2(\cos\theta)\rangle \sim \langle 1 - \tfrac{3}{2}\theta^2\rangle \overset{(192)}{\sim} 1 - \frac{3}{\alpha}. \tag{36}$$

In his original publication Onsager used trial function (31) and also calculated ΔF by means of asymptotic expansions valid for large α. The leading terms of these expansions are equal to those obtained by the Gaussian trial function, but Onsager took into account three further terms, which gave better results for the phase transition (see later).

2.4.2. Formal minimization of the free energy. When we minimize equation (27) formally, we obtain an integral equation

$$\ln[4\pi f(\theta)] = \lambda - \frac{8c}{\pi}\int |\sin\gamma(\Omega,\Omega')| f(\theta')\,\mathrm{d}\Omega' \tag{37}$$

which is nonlinear because of the presence of the logarithmic term. $\lambda \equiv \lambda' - 1$ is as yet undetermined and must be determined by requiring that $f(\theta)$ fulfils the normalization (9). If we exponentiate equation (37) we can see $f(\theta)$ as a Boltzmann distribution of rods in the field

$$U_{\mathrm{scf}}[\theta] = kT\frac{8c}{\pi}\int |\sin\gamma(\Omega,\Omega')| f(\theta')\,\mathrm{d}\Omega' \tag{38}$$

which is called a self-consistent field, because it depends on f itself. An exact solution to equation (37) has not yet been found, but in literature two ways of solving it numerically have appeared:

(i) *Series expansion.* For a series expansion it is convenient to observe that the φ'-integration in equation (37) may be carried out independently from f, which only depends on θ'. The resulting integral may be written as a bilinear expansion in Legendre polynomials $P_{2n}(\cos\theta)$ (Kayser and Raveché 1978)

$$K(\theta,\theta') \equiv \int_0^{2\pi} |\sin\gamma|\,\mathrm{d}\varphi' = 2\pi\sum_{n=0}^{\infty} c_{2n} P_{2n}(\cos\theta) P_{2n}(\cos\theta') \tag{39}$$

with $c_0 = \pi/4$, $c_2 = -5\pi/32$, etc. This makes the Legendre polynomials the appropriate orthogonal polynomials for expanding f. However, nonlinear equation (37) contains f as well as its logarithm, both of which may be expanded (Lasher 1970)

$$f(\theta) = \sum_{n=0}^{\infty} a_{2n} P_{2n}(\cos\theta) \tag{40}$$

or (Lekkerkerker *et al* 1984)

$$\ln[f(\theta)] = \sum_{n=0}^{\infty} \alpha_{2n} P_{2n}(\cos\theta). \tag{41}$$

Unfortunately, the expansion coefficients a_{2n} and α_{2n} are not simply related. Therefore the solution method must be iterative using either equation (40) or (41), estimating its coefficients and substituting it in the right-hand side of equation (37) to obtain a new estimate for f. In doing this it is necessary to obtain the averages $\langle P_{2n} \rangle$ numerically. There is not much difference in using equation (40) or (41) except that (41) ensures that f is positive definite, even for the truncated expansions used in practice.

(ii) *Purely numerical.* This method (Herzfeld *et al* 1984) assumes a grid of angles θ and θ' and uses the exponentiated form of (37) to solve it iteratively

$$f_{m+1}(\theta) = \frac{\exp[-(8c/\pi) \int K(\theta, \theta') f_m(\theta') \, \mathrm{d} \cos \theta']}{\int \exp[-(8c/\pi) \int K(\theta, \theta') f_m(\theta') \, \mathrm{d} \cos \theta'] \, \mathrm{d} \cos \theta} \tag{42}$$

where $K(\theta, \theta')$ (see equation (39)) is now also determined numerically (but only once) for all combinations of θ and θ'. A disadvantage of equation (42) is the fact that the numerical integration must be carried out for all θ instead of all P_{2n} (the number of which required to obtain full convergence is much smaller at the phase transition). Convergence properties of iteration scheme (42) have been studied by Herzfeld *et al* (1984).

Kayser and Raveché (1978) performed a *bifurcation analysis* on equation (37). A trivial solution of equation (37) is the isotropic solution (10) and bifurcation analysis determines at which concentration another solution can branch from the isotropic one. Near the branching (or bifurcation) point such a function is only infinitesimally (denoted by ϵ) different from the isotropic state

$$f(\theta) = \frac{1}{4\pi}(1 + \epsilon h(\theta)) \tag{43}$$

where $h(\theta)$ must be orthogonal to $1/4\pi$ to fulfil equation (9). Substituting in equation (37) and linearizing in ϵ gives

$$h(\theta) = -\frac{8c}{\pi} \int |\sin \gamma| \frac{h(\theta')}{4\pi} \mathrm{d}\Omega' \overset{(39)}{=} -\frac{4c}{\pi} \sum c_{2n} P_{2n}(\cos \theta) \langle P_{2n} \rangle_h \tag{44}$$

where $\langle P_{2n} \rangle_h = \int_{-1}^{1} P_{2n}(\cos \theta) h(\theta) \, \mathrm{d} \cos \theta$. From the orthogonality properties of Legendre polynomials (Abramowitz and Stegun 1964)

$$\int_{-1}^{1} P_m(\cos \theta) P_n(\cos \theta) \, \mathrm{d} \cos \theta = \frac{2}{2m+1} \delta_{mn} \tag{45}$$

it is easily seen that all even Legendre polynomials fulfil equation (44), but each only at one special value of c. The lowest of these values of c—called branching or bifurcation points c^*—is

$$c^* = \left[-\frac{4c_2}{\pi} \langle P_2 \rangle_{P_2} \right]^{-1} = \left[-\frac{4}{\pi} \left(-\frac{5\pi}{32} \right) \frac{2}{5} \right]^{-1} = 4 \tag{46}$$

with

$$h(\theta) = P_2(\cos \theta). \tag{47}$$

When we determine the free energy of distribution function (43) in combination with (47) we find

$$\frac{\Delta F}{NkT} = \ln c + c + \frac{1}{40}(4 - c)\epsilon^2 \tag{48}$$

from which we immediately see that at $c = c^* = 4$ the isotropic state changes from a local minimum to a local maximum. This explains the possibility of a second branch at $c = 4$ and shows at the same time that for concentrations above $c = 4$ the isotropic state becomes absolutely unstable (note that equation (37) only ensures an extremum of ΔF, not necessarily a minimum).

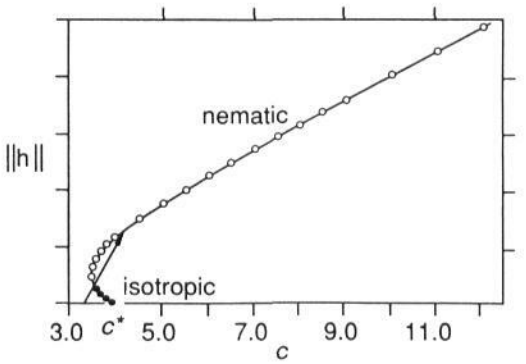

Figure 2. The norm of the anisotropic part of the distribution function ($||h|| \equiv (\int h^2(\theta)\,d\Omega)^{1/2}$) against scaled concentration c (Kayser and Raveché 1978). We have indicated the location of the phase transition by an arrow.

Kayser and Raveché (1978) followed the anisotropic branch, which turned out to go to lower concentrations at first: its complete behaviour is sketched in figure 2. The first part of the anisotropic branch is also a maximum of the free energy and thus no physical solution to equation (37). Therefore we expect a sudden jump from the isotropic to the anisotropic branch which implies a first-order phase transition.

2.4.3. The coexistence relations. For each concentration c the system of hard rods must be at the minimum of the free energy. Above a certain concentration this minimum is obtained by a state in which part of the system is isotropic and the other part nematic (with different concentrations c_i and c_a; from now on we denote properties of the isotropic and nematic phase with subscripts i and a respectively). To be in mechanical and chemical equilibrium both phases must have the same osmotic pressure and the same chemical potential

$$\Pi_i(c_i) = \Pi_a(c_a) \qquad \mu_i(c_i) = \mu_a(c_a). \tag{49}$$

We find Π from equations (8), (26) and (27);

$$\Pi = \frac{kT}{v_0(L/D)}\,(c + c^2\rho[f]) \tag{50}$$

and μ from the similar thermodynamic relation $\mu = (\partial \Delta F/\partial N)_{V,T,\mu_0,\mu_1,\ldots}$

$$\mu = kT\,(\text{constant} + \ln c + \sigma[f] + 2c\rho[f])\,. \tag{51}$$

For the isotropic phase μ and Π are simple (see equation (29))

$$\frac{\Pi_i v_0(L/D)}{kT} = c_i + c_i^2 \tag{52}$$

$$\frac{\mu_i}{kT} = \text{constant} + \ln c_i + 2c_i. \tag{53}$$

As seen earlier, one way to describe the anisotropic state is to use a Gaussian distribution function which leads to (equations (193) and (194) in combination with (35))

$$\frac{\Pi_a v_0(L/D)}{kT} \sim c_a + c_a^2\rho(\alpha) \sim 3c_a \tag{54}$$

$$\frac{\mu_a}{kT} \sim \text{constant} + \ln c_a + \sigma(\alpha) + 2c_a\rho(\alpha) \sim \text{constant} + 3\ln c_a + 3 + \ln\left(\frac{4}{\pi}\right). \tag{55}$$

These expressions must be equated to the isotropic expressions (52) and (53) while we must realize that the constant is the same in both phases. From this we find the following coexisting concentrations (Odijk 1986a)

$$c_i = 3.45 \qquad c_a = 5.12 \tag{56}$$

implying (via equation (35))

$$\alpha = 33.4 \tag{57}$$

which is reasonably large (thus justifying the use of the Gaussian trial function). Correspondingly, the order parameter of the nematic phase is also high

$$S = 0.910. \tag{58}$$

The Onsager trial function may also be used, which gives the following results (Onsager 1949)

$$c_i = 3.340 \qquad c_a = 4.486 \qquad \alpha = 18.58 \qquad S = 0.848 \tag{59}$$

which shows that the results depend critically on the exact form of the distribution function.

Of course we can also apply the methods of section 2.4.2 to obtain f numerically. As we do not know the right c_a, we choose an arbitrary value, calculate f, $\sigma[f]$ and $\rho[f]$ and use equations (49)–(51) in an iterative fashion in order to obtain in the end values for c_i and c_a which fulfil the coexistence relations (Lekkerkerker *et al* 1984)

$$c_i = 3.290 \qquad c_a = 4.191 \qquad S = 0.7922. \tag{60}$$

In the bifurcation diagram figure 2 we have indicated the coexisting phases.

Up to now we have only considered hard rods of fixed length. However, in practice it is difficult to obtain purely monodisperse samples. Therefore we shall look into the influence of polydispersity on the phase transition in the next section. Furthermore, many of the rodlike polymers of biological and some of synthetic origin turn out to be charged, the effects of which will be studied in section 2.6.

2.5. *Polydispersity*

In an experimental situation, the particles will hardly ever be monodisperse. In this section we will see that this may have rather strong effects on the isotropic–nematic phase transition. Let us consider a system which consists of particles with equal diameters D but different lengths L_j. The mole fraction of species j is given by $x_j \equiv N_j/N$, where $N = \sum_j N_j$ is the total number of particles present. In this case the excluded volume between a rod of length L_j and another of length L_k is a simple generalization of equation (22)

$$v_{\text{excl}} = -\beta_1(\Omega,\Omega') \sim 2DL_jL_k|\sin\gamma| = q_jq_k2DL_1^2|\sin\gamma|. \tag{61}$$

All terms still have the same dependence on $|\sin\gamma|$ and we have related them all to the excluded volume between two rods of the shortest length (which we take to be L_1) via $q_j \equiv L_j/L_1$. The expression for the free energy (equation (27)) is now simply generalized

$$\frac{\Delta F}{NkT} \simeq \text{constant} + \ln c + \sum_j x_j \ln x_j + \sum_j x_j\sigma_j + c\sum_j\sum_k x_jx_kq_jq_k\rho_{jk} \tag{62}$$

where $\sum_j x_j \ln x_j$ is an entropy of mixing since we now have different species and

$$\sigma_j \equiv \int f_j(\theta)\ln[4\pi f_j(\theta)]\,\mathrm{d}\Omega \tag{63}$$

$$\rho_{jk} \equiv \frac{4}{\pi}\iint |\sin\gamma| f_j(\theta)f_k(\theta')\,\mathrm{d}\Omega\,\mathrm{d}\Omega'. \tag{64}$$

Each species has its own distribution function $f_j(\theta)$ which must be normalized separately

$$\int f_j(\theta)\,\mathrm{d}\Omega = 1. \tag{65}$$

Note that in this section we relate the dimensionless concentration c to the excluded volume for the shortest rods

$$c \equiv \frac{\pi}{4}L_1^2D\frac{N}{V}. \tag{66}$$

We can formally minimize this free energy with respect to all distribution functions $f_j(\theta)$ and obtain a set of coupled nonlinear integral equations

$$\ln[4\pi f_j(\theta)] = \lambda_j - \frac{8c}{\pi}q_j\sum_k x_kq_k\int|\sin\gamma|f_k(\theta')\,\mathrm{d}\Omega' \qquad (j = 1,2,\ldots). \tag{67}$$

The sum over k at the right-hand side is identical in all equations. Therefore this term may be eliminated, giving

$$q_k\ln[4\pi f_j(\theta)] - q_k\lambda_j = q_j\ln[4\pi f_k(\theta)] - q_j\lambda_k. \tag{68}$$

Since λ_j and λ_k are undetermined multipliers which must be fixed by the normalization conditions (65), we may relate each distribution function to the distribution function of the shortest rods

$$f_j(\theta) = \frac{[f_1(\theta)]^{q_j}}{\int [f_1(\theta')]^{q_j}\, \mathrm{d}\Omega'}. \tag{69}$$

This implies that we do not have to solve the entire set of equations (67) but only one equation

$$\ln[4\pi f_1(\theta)] = \lambda_1 - \frac{8c}{\pi} \sum_k x_k q_k \frac{\int |\sin\gamma| [f_1(\theta')]^{q_k}\, \mathrm{d}\Omega'}{\int [f_1(\theta')]^{q_k}\, \mathrm{d}\Omega'} \tag{70}$$

which is still a formidable task, the more so because we now have a coexistence equation for the chemical potential of each species

$$\begin{aligned} \mu_{\mathrm{i}}^j &= \mu_{\mathrm{a}}^j \qquad \mu^j = (\partial \Delta F / \partial N_j)_{V,T,N_{k\neq j},\mu_0} \\ \Pi_{\mathrm{i}} &= \Pi_{\mathrm{a}} \qquad \Pi = -(\partial \Delta F / \partial V)_{T,N_k,\mu_0}. \end{aligned} \tag{71}$$

On top of this the composition (the set of x_j) may be different in both phases. This indicates it will be very hard to calculate phase transitions in these systems.

One thing which is relatively easy to perform is a bifurcation analysis on equation (70). By writing $f_1 = (1/4\pi)(1 + \epsilon h_1)$ as in equation (43) and following the discussion below it, we find for a perturbation $h_1(\theta) = P_2(\cos\theta)$

$$c^* = 4 / \sum_j x_j q_j^2. \tag{72}$$

Since c is—rather arbitrarily—scaled like equation (66) we get a better physical insight by looking at the volume fraction at which bifurcation occurs

$$\phi^* = 4D \frac{\sum_j N_j L_j}{\sum_j N_j L_j^2} = \frac{4D}{\overline{L}^{\mathrm{w}}} \propto (\overline{M}^{\mathrm{w}})^{-1} \tag{73}$$

from which we observe a reciprocal proportionality with the weight-average molecular weight $\overline{M}^{\mathrm{w}}$ of the polymer sample. This means that a few longer rods may shift the phase transition to a lower volume fraction. We must realize that with a bifurcation analysis we do not find the actual phase transition. However, as the analysis predicts when the isotropic phase will become absolutely unstable, we expect it to give some indication about the phase transition.

For bidisperse systems numerical calculations for two different length ratios ($L_2/L_1 = 2$ and 5) were performed (Lekkerkerker *et al* 1984, Birshtein *et al* 1988). In figure 3 we illustrate the phase separation for $L_2/L_1 = 2$. We note the following features:

(i) *strong fractionation effect* (the longer rods preferentially go into the anisotropic phase);

(ii) *widened biphasic gap* (in a mixture of rods of two different lengths the concentration difference between isotropic and nematic phases may be much larger than in the case of one component);

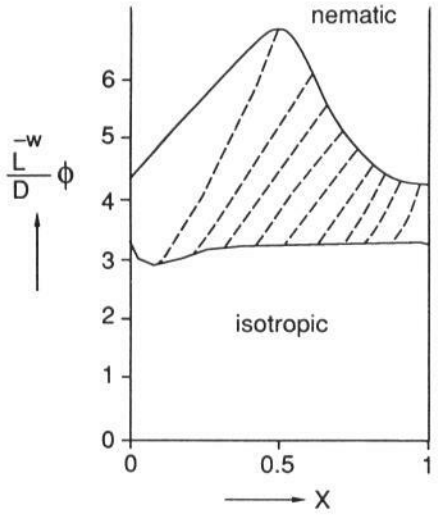

Figure 3. Volume fraction scaled by the weight-averaged length against mole fraction of the longer rods for a bidisperse mixture of rods ($L_2/L_1 = 2$). The broken lines indicate in which two phases compositions falling in the two-phase region will divide.

(iii) *weak variation in* $\overline{L}^{w}\phi_i/D$ (this implies that the molecular weight dependence of the bifurcation density (see equation (73)) is a good indication for the onset of phase separation);

(iv) *strong order of longer rods* (in the nematic phase the order parameter of the longer rods is always rather high, whereas that of the shorter rods can be quite small, especially in compositions in which there are few short rods).

For length ratio 5 similar (but more pronounced) results were found with two additional points:

(v) *a re-entrant nematic phase* (for some compositions the system shows a phase sequence of *isotropic–nematic–(re-entrant) isotropic–(re-entrant) nematic* as a function of concentration);

(vi) *two nematic phases* (for some compositions the system shows a biphasic region where the system separates into two different nematic phases, or even a three-phase region in which an isotropic phase coexists with two nematic phases (Birshtein *et al* 1988)).

Since these numerical calculations several theoretical studies (Odijk and Lekkerkerker 1985, McMullen *et al* 1985, Odijk 1986a, 1986b, Sluckin 1989) of bidisperse and polydisperse systems have been performed for special regions of the phase diagram. All of these use Gaussian trial functions (32) with different α for the different components j (to be called α_j). However, if these Gaussian functions were to be the proper distribution functions there should be a relation between different α_js (from equation (69))

$$q_j\alpha_k = q_k\alpha_j. \tag{74}$$

In most cases the calculated α_js do not fulfil equation (74) which means these results should be considered with some reserve.

2.6. Charged rods

In the preceding sections we only considered hard-core interactions, to which we will now add electrostatic repulsion. When the rods are charged (i.e. they are polyelectrolytes), there is an additional soft repulsion because of the electrostatic interaction between the polyelectrolytes and their surrounding double layers (Onsager 1949, Stroobants *et al* 1986a). In the remainder of this section we closely follow the discussion in Stroobants *et al* (1986a) for rods. Although the potential of mean force w for two charged rods is, in general, very difficult to evaluate, we are helped by the fact that we only need to know the Mayer function $\Phi = \exp(-w/kT) - 1$. Φ is insensitive to the exact form of the potential when $w/kT \gg 1$, in which case $\Phi \simeq -1$ and it does always contribute to B_2 in the same way (see equation (4)). This implies that we only need to know an accurate form of the potential of mean force for configurations where only the outer parts of the double layers overlap. In the outer part of the double layer of a long rod the electric potential ψ^e is low and it therefore takes the Debye–Hückel form for cylindrical symmetry (Philip and Wooding 1970)

$$\frac{e\psi^e}{kT} \sim \Gamma K_0(\kappa r) \tag{75}$$

where e is the elementary charge, r is the distance from the centre line of the rod, κ^{-1} is the Debye screening length and K_0 is a modified Bessel function. Note that the proportionality constant Γ is also determined by the potential in the inner part of the double layer (which has to fulfil the nonlinear Poisson–Boltzmann equation instead of its linearized Debye–Hückel version). Because a line charge with linear charge density ν_{eff} (i.e. number of charges per unit length) in the Debye–Hückel limit also gives a far-field form like equation (75) (Brenner and Parsegian 1974)

$$\frac{e\psi^e}{kT} \sim 2\nu_{\text{eff}} Q K_0(\kappa r) \tag{76}$$

it is possible to associate an effective Debye–Hückel line charge with our rod provided we choose

$$\nu_{\text{eff}} = \frac{\Gamma}{2Q} \tag{77}$$

Q is the Bjerrum length $e^2/4\pi\epsilon_0\epsilon kT$ with ϵ the dielectric permittivity. Because we argued that the contact between the outer parts of the double layers determines the second virial coefficient, we can approximate w by the interaction between two effective line charges (at a shortest distance x and mutual angle γ) in the Debye–Hückel approximation, which is well known (Brenner and Parsegian 1974, Stigter 1977, Fixman and Skolnick 1978):

$$\frac{w^{\text{el}}}{kT} = \frac{2\pi\nu_{\text{eff}}^2 Q \mathrm{e}^{-\kappa x}}{\kappa \sin\gamma} = \frac{\pi\Gamma^2 \mathrm{e}^{-\kappa x}}{2(\kappa Q)\sin\gamma} \equiv \frac{A' \mathrm{e}^{-\kappa(x-D)}}{\sin\gamma}. \tag{78}$$

The last equality forms the definition of A':

$$A' \equiv \frac{\pi\Gamma^2 \mathrm{e}^{-\kappa D}}{2\kappa Q} \tag{79}$$

Not surprisingly the potential of mean force (78) decays with the Debye length, while the factor $(\sin\gamma)^{-1}$ is proportional to the interaction area between the two crossed rods. Note that as a consequence of the latter factor two charged rods tend to rotate to a perpendicular configuration. Although strictly speaking equation (78) is only valid for infinitely extended line charges and therefore cannot be used for parallel configurations, the contribution of these configurations to the second virial coefficient is negligible anyway.

To fix A' it is necessary to know Γ. For weakly charged polyelectrolytes this is simple because it is possible to use the Debye–Hückel approximation for a charged cylinder with diameter D and surface charge density $\nu/\pi D$ (Hill 1955)

$$\frac{e\psi^{e}_{DH}}{kT} = \frac{4\nu Q K_0(\kappa r)}{\kappa D K_1(\kappa D/2)} \tag{80}$$

valid if this does not exceed 1 for $r = D/2$. In (80) ν is the actual linear charge density and K_1 is a modified Bessel function. Comparing (75) and (80) it is possible to derive a closed expression for A' from equation (79)

$$A'_{DH} = \frac{8\pi\nu^2 Q e^{-\kappa D}}{\kappa^3 D^2 K_1^2(\kappa D/2)}. \tag{81}$$

In two limits (thick and thin double layer) it is possible to simplify this with asymptotic expressions for $K_1(\kappa D/2)$ (Abramowitz and Stegun 1964)

$$A'_{DH} \sim 2\pi\nu^2 Q\kappa^{-1} \qquad (\kappa D \ll 1) \tag{82}$$

$$A'_{DH} \sim (8\nu^2 Q/D)\kappa^{-2} \qquad (\kappa D \gg 1). \tag{83}$$

For more strongly charged polyelectrolytes it is necessary to solve the full Poisson–Boltzmann equation. In that case it is useful to employ the approximate analytical solution given by Philip and Wooding (1970), from which Γ and A' are obtained by a simple numerical procedure.

With expression (78) for the potential of mean force it is possible to evaluate the cluster integral from equation (4) splitting the integration in a hard-core part and an electrostatic part outside the hard core (Onsager 1949)

$$\begin{aligned}\beta_1(\Omega,\Omega') &= -2DL^2\sin\gamma + 2L^2\sin\gamma\int_D^\infty [\exp(-w^{el}/kT) - 1]\,dx \\ &= -2DL^2\sin\gamma - 2\kappa^{-1}L^2\sin\gamma[\ln(A'/\sin\gamma) + C_E + E_1(A'/\sin\gamma)]\end{aligned} \tag{84}$$

with Euler's constant $C_E = 0.577\,215\ldots$ and E_1 the exponential integral (Abramowitz and Stegun 1964). For $A' > 2$ the argument of E_1 is always larger than 2, in which range the exponential integral may be neglected. Stroobants *et al* (1986a) divided the effect of charge into two parts. The first becomes apparent when we determine the second virial coefficient in the isotropic state (equation (12) with (10))

$$B_2^{iso} = \tfrac{1}{4}\pi DL^2 + \tfrac{1}{4}\pi\kappa^{-1}L^2[\ln A' + C_E + \ln 2 - \tfrac{1}{2}] \tag{85}$$

$$\equiv \tfrac{1}{4}\pi L^2 D_{eff} \tag{86}$$

indicating that in the isotropic state—because of the repulsion—charge generates a larger effective diameter of the rods (Onsager 1949)

$$D_{\text{eff}} = D\left[1 + \frac{\ln A' + C_{\text{E}} + \ln 2 - \frac{1}{2}}{\kappa D}\right]. \tag{87}$$

The second effect is only present in the anisotropic state (Stroobants *et al* 1986a)

$$B_2^{\text{aniso}} = \tfrac{1}{4}\pi D_{\text{eff}} L^2(\rho[f] + h\eta[f]) \tag{88}$$

with $\rho[f]$ defined by equation (28). Apart from the larger effective diameter we see the second effect in the extra term

$$\eta[f] \equiv \frac{4}{\pi}\iint[-\sin\gamma\ln(\sin\gamma) - (\ln 2 - \tfrac{1}{2})\sin\gamma]f(\Omega)f(\Omega')\,\mathrm{d}\Omega\,\mathrm{d}\Omega' \tag{89}$$

which is called the twisting effect as it originates from the factor $(\sin\gamma)^{-1}$ in equation (78). The relative importance of this effect is determined by the twisting parameter

$$h \equiv (\kappa D_{\text{eff}})^{-1}. \tag{90}$$

To illustrate the dependence of effective diameter D_{eff} and twisting parameter h on polyelectrolyte properties and salt concentration we give two representative examples in tables 2 and 3. As we might expect, D_{eff} increases with decreasing salt concentration (equivalent to increasing screening length κ^{-1}) and increasing charge density ν. For thin double layers ($\kappa D \gg 1$) the charge is completely screened and D_{eff} is nearly equal to D.

Table 2. Ratio of effective and hard-core diameter D_{eff}/D and twisting parameter h (in brackets) as a function of ionic strength and linear charge density ν for a cylinder with $D = 20$ Å in an aqueous solution at 25 °C. Γ was determined from Philip and Wooding (1970). If no values are given, $A' < 2$.

		ν (Å^{-1})				
M	κ^{-1} (Å)	1	0.4	0.2	0.1	0.04
0.001	96	27 (0.18)	26 (0.19)	24 (0.20)	21 (0.23)	13 (0.37)
0.003	56	15 (0.19)	14 (0.19)	13 (0.21)	11 (0.26)	6.2 (0.45)
0.01	30	8.0 (0.19)	7.6 (0.20)	6.7 (0.23)	5.2 (0.29)	—
0.03	17.6	4.8 (0.18)	4.4 (0.20)	3.8 (0.23)	2.8 (0.31)	—
0.1	9.6	2.9 (0.17)	2.6 (0.19)	2.1 (0.22)	—	—
0.3	5.6	2.0 (0.14)	1.7 (0.16)	1.5 (0.19)	—	—
1	3.0	1.5 (0.10)	1.3 (0.12)	—	—	—

The variation of twisting parameter h is less easy to predict. From equations (87) and (90) we have

$$h = [\kappa D + \ln A' + 0.7703]^{-1} \tag{91}$$

which is certainly small for thin double layers ($\kappa D \gg 1$). For large A' (usually implying thick double layers, $\kappa D \ll 1$) h would also be small, although in practice

Table 3. The same as table 2 for diameter $D = 100$ Å.

		ν (Å^{-1})				
M	κ^{-1} (Å)	1	0.4	0.2	0.1	0.04
0.001	96	6.7 (0.14)	6.3 (0.15)	5.7 (0.17)	4.6 (0.21)	3.0 (0.32)
0.003	56	4.1 (0.13)	3.8 (0.15)	3.3 (0.17)	2.7 (0.21)	—
0.01	30	2.6 (0.12)	2.3 (0.13)	2.0 (0.15)	1.6 (0.19)	—
0.03	17.6	1.8 (0.10)	1.6 (0.11)	1.4 (0.12)	—	—
0.1	9.6	1.4 (0.07)	1.3 (0.08)	1.1 (0.09)	—	—
0.3	5.6	1.2 (0.05)	1.1 (0.05)	—	—	—
1	3.0	1.1 (0.03)	—	—	—	—

not as small as for thin double layers because of the logarithmic dependence on A'. An indication of the location of the maximum value of h can be acquired in the Debye–Hückel approximation. From equations (82) and (83) we see that the dependence of A' on κ^{-1} varies between a second and a first power:

$$A' \sim \kappa^{-\omega} \qquad (1 < \omega < 2). \tag{92}$$

Substituting in (91) and determining its maximum gives (Stroobants *et al* 1986a)

$$\kappa^{-1} \sim D/\omega \tag{93}$$

which means we may expect a maximum for h for a Debye screening length on the order of the diameter. Apparently, this is also correct for table 2, although the Debye–Hückel approximation is not valid there. In practice, h will not be much larger than 0.6.

The total free energy for a solution of charged rods can be represented analogously to equation (27) by use of equation (88)

$$\frac{\Delta F[f]}{NkT} \simeq \text{constant} + \ln c + \sigma[f] + c(\rho[f] + h\eta[f]) \tag{94}$$

with the number density ρ now scaled by the isotropic effective excluded volume (86)

$$c \equiv \tfrac{1}{4}\pi L^2 D_{\text{eff}} \rho. \tag{95}$$

Note that here we expect the higher virial coefficients to be insignificant for a small ratio D_{eff}/L, which may be a much stricter condition than small D/L (see e.g. the upper left corner of table 2). Stroobants *et al* (1986a) determined the phase transition for this free energy. As scaled concentration (95) now takes the place of scaled concentration (26) the effect of the larger effective diameter is to shift the phase transition to lower particle concentrations. On the other hand the anisotropic state is destabilized by the twisting effect: charged rods want to be perpendicular. This second effect of charge is seen in figure 4. However, it is good to realize that, in general, the stabilizing effect on the nematic state of a larger effective diameter dominates the destabilizing twisting effect (e.g. compare table 2 and figure 4).

Sato and Teramoto (1991) extended this theory of electrostatic interaction between infinite line charges by incorporating end effects in the second virial coefficient, although their interpolation method is arbitrary to some extent. A paper by Odijk

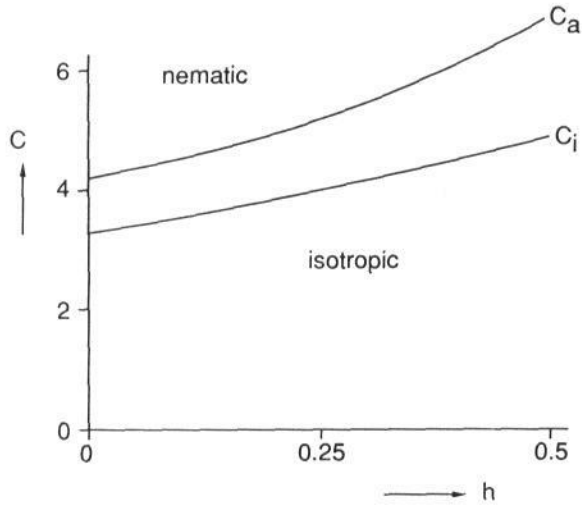

Figure 4. The effect of electrostatic twisting on the isotropic–nematic phase transition. Note that we plot *effective* concentration (95) against h.

(1990) to obtain the end effects in the isotropic state (for $\kappa^{-1} > D$) shows how intricate this type of calculation is, although his final result is very simple

$$B_2^{\text{iso}} = \tfrac{1}{4}\pi L^2 D_{\text{eff}} + \pi L D_{\text{eff}}^2 + \cdots \qquad (A' \text{ large}) \tag{96}$$

where the first correction term is also given by that for a spherocylinder of effective diameter D_{eff} (cf equations (21) and (23)).

Nyrkova and Khokhlov (1986) performed a qualitative study of the phase behaviour in the case that the infinite line charge model of equations (78) and (88) can no longer be applied and/or for low linear charge densities (low A'). Of the various different regimes they discerned the most remarkable is the one for which

$$D < \kappa^{-1} < L \qquad \kappa^{-1}/L < A' < 6 \tag{97}$$

where they claim the occurrence of two nematic phases of different degrees of ordering. Although later (Semenov and Khokhlov 1988) they restricted this regime somewhat further, this phenomenon is interesting and deserves more elaborate study.

2.7. *Attractive interaction*

Now we have seen that electrostatic repulsion may be treated satisfactorily at least in some cases the next question would be how to deal with attractive interactions like Van der Waals forces. Although a similar expression to equation (78) has been given for non-retarded Van der Waals attraction between long thin (although macroscopic) rods (Parsegian 1972) which might be used as a potential of mean force, it is very hard to develop a similar theory for the isotropic–nematic transition. This stems from the fact that parallel configurations show the largest attraction so they cannot be neglected as in the electrostatic interaction but instead they dominate the problem. The latter observation was used by Khokhlov (1979) and Grosberg and Khokhlov (1981) in formulating a simple model to incorporate attraction. They imposed an

attractive square-well potential around the hard core of the rods and showed that the behaviour of the second virial coefficient is determined by this simplified attraction only for nearly parallel configurations. Although they claim to be able to predict a triple point at which an isotropic phase coexists with two anisotropic phases within the second virial approximation, this must be considered with some reservation: in a situation with many nearly parallel configurations the second virial term no longer exceeds the higher virial terms as we have seen in section 2.3.

Therefore the incorporation of attraction requires a method valid beyond the second virial approximation. In this respect the lattice theory of Flory (1956) is more successful: besides a more or less athermal isotropic–nematic transition at higher temperatures it predicts the formation of a second highly ordered nematic phase at lower temperatures, where attractions play a more important role.

3. Computer simulations and hard-core models for liquid crystals at higher volume fraction

3.1. Introduction

As discussed in section 2 the isotropic–nematic phase transition in systems of long thin hard rods can be treated accurately within the second virial approximation. However, for short rods the contributions of the higher virial terms to the free energy can no longer be neglected. The incorporation of these higher virial coefficients in the theory of the isotropic–nematic liquid crystal transition requires extensive numerical calculations. Nevertheless, attempts to assess the influence of the third virial coefficient on the isotropic–nematic phase transitions have been made (Straley 1973b, Tjipto-Margo and Evans 1990).

Another route towards a theoretical treatment of liquid crystal phase transitions in systems of rodlike particles is the adaptation of the methods of liquid state theory. Computer simulations carried out during the last 35 years have provided ample evidence that the structural arrangements of molecules in a liquid are determined predominantly by the short-ranged harshly repulsive intermolecular forces. These interactions can be conveniently modelled by hard-core interactions. In particular fluids of hard spheres have played an important role in the development of theories for the liquid state (Hansen and McDonald 1986). A similar role is played by assemblies of hard rodlike particles (hard ellipsoids, hard (sphero)cylinders) in the development of theories for liquid crystal phases. Using computer simulations Frenkel and coworkers (Frenkel *et al* 1984, Frenkel and Mulder 1985, Frenkel 1987a, 1987b, 1988, 1989, Frenkel *et al* 1988, Allen *et al* 1989, Veerman and Frenkel 1990) have shown that systems of rodlike particles with purely repulsive interactions do indeed exhibit liquid crystal behaviour. These simulations have inspired a large amount of theoretical work and serve as reference points for a large number of recent calculations on liquid crystal phase transitions. We, therefore, first summarize the most relevant results of these simulations. Subsequently, we discuss a number of theoretical works on the liquid crystal phase transitions in fluids of hard rodlike particles and compare them with the simulation results.

One has to keep in mind that the whole subject is in a state of rapid development and many of the calculations are based on assumptions the validity of which is hard to assess. We therefore limit ourselves to the main developments.

3.2. Computer simulations of hard-core models for liquid crystals

As mentioned earlier, it is commonly accepted that the structure of simple liquids is largely determined by short-ranged repulsive intermolecular forces (Hansen and McDonald 1986). For this reason much of attention has been devoted to the simplest possible model representing such forces, i.e. the hard sphere fluid. Not only does this model provide insight into the essential structural features of simple liquids, the freezing of atomic liquids can also be understood on the basis of the fluid–solid transition of hard spheres (Longuet-Higgins and Widom 1964). It is therefore natural to ask to what extent the properties of liquid crystals can be modelled by fluids of hard-core particles. Pioneering simulations of hard spherocylinders with $L/D = 2$ were carried out by Vieillard-Baron (1974). However, in that system no nematic ordering was observed. More recently Frenkel and coworkers (see earlier references), Allen *et al* (1989) and Allen and Wilson (1989) reported on simulations for both hard ellipsoids of revolution (HE) and hard spherocylinders (HSC). Since there exist comprehensive reviews on computer simulations of hard-core models for liquid crystals (Frenkel 1987a, 1987b, 1988, Allen and Wilson 1989), we shall be brief here. For details of the simulations and the calculation of thermodynamic properties such as pressures and free energies we refer to the original papers.

Table 4. Simulation results for the isotropic–nematic phase transition in a fluid of hard ellipsoids of revolution (v_0: volume per particle).

a/b	$(\rho v_0)_{iso}$	$(\rho v_0)_{nem}$	Pv_0/kT
2.75[a]	0.561	0.570	15.7
3[a]	0.507	0.517	9.79
5[b]	0.37		—
10[b]	0.21		—

[a] Frenkel and Mulder (1985).
[b] Allen and Wilson (1989). Transition densities estimated from the behaviour of the order parameter.

The HE can be conveniently parametrized by their length-to-breadth ratio a/b where a and b denote the major and minor axes of the ellipsoids. Here we will focus on the results for the prolate ellipsoids, for which simulations were performed for axial ratios $a/b = 1.25$, 2, 2.75, 3, 5, 10. For $a/b = 1.25$ and 2 no isotropic–nematic phase transition is observed, but a direct transition from the isotropic to the solid state (for $a/b = 1.25$ the almost spherical ellipsoids freeze into an orientationally disordered ('plastic') solid which only at higher density transforms into a solid with both positional and orientational order). For $a/b = 2.75$ and higher an isotropic–nematic phase transition is observed. In table 4 we give the coexistence densities and pressure for these phase transitions. Upon further increasing the density a transition from the nematic into a solid phase is observed. A sketch of the 'phase diagram' for prolate HE based on these discussed simulation results and including, as a limiting case, the fluid-to-solid transition of hard spheres ($a/b = 1$) is presented in figure 5. So we see that a simple fluid of HE already displays four distinct phases: isotropic fluid, nematic fluid, plastic solid and ordered solid. This naturally raises the question whether in other hard-core models further liquid crystal phases could possibly be identified.

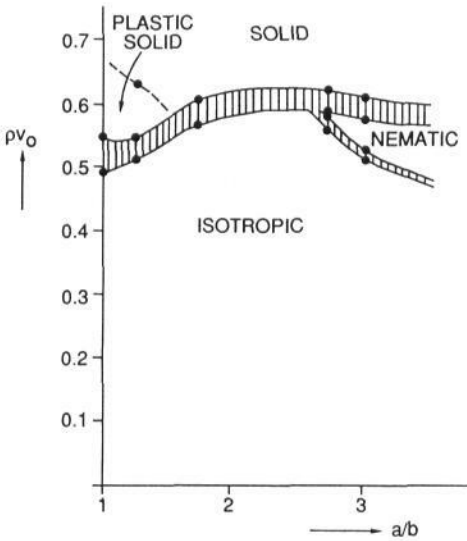

Figure 5. Phase diagram for prolate hard ellipsoids obtained by computer simulation (see text).

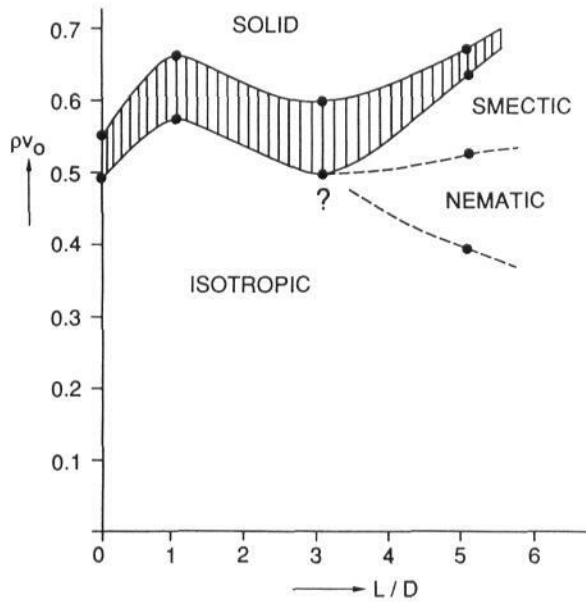

Figure 6. Phase diagram for hard spherocylinders obtained by computer simulation (see text).

For the somewhat artificial system of parallel HSC computer simulations (Stroobants *et al* 1986b, 1987) indicated that for $L/D \gtrsim 0.5$ a thermodynamically stable smectic phase occurs between the nematic and solid phases. Subsequent simulations on HSC with full translational and orientational freedom revealed that for HSC with $L/D \leqslant 3$ no stable liquid crystal phases occur. In these systems only a transition from the isotropic fluid to the solid state takes place. However, for $L/D = 3$ simulations (Veerman and Frenkel 1990) already indicate the existence of

a metastable smectic phase between the isotropic fluid and solid state. Upon further increase of the length-to-diameter ratio to 5, simulations (Frenkel *et al* 1988, Frenkel 1988) provide clear evidence that now both a (thermodynamically stable) nematic and smectic phase occur between the isotropic fluid and solid state. In table 5 we give the densities and pressures for the phase transitions and in figure 6 we present the 'phase diagram' for a fluid of HSC based on the simulation results obtained so far. We note that a simple fluid of HSC displays at least two liquid crystalline phases, namely a nematic and a smectic-A phase. Actually it is very well possible that, for larger L/D values, further liquid crystalline phases (e.g. phases with hexagonal lateral order such as the smectic-B phase or columnar phase) may be observed. However, as computer simulations for HSC with larger L/D become increasingly more sluggish and the unequivocal establishment of these partially ordered/partially disordered phases requires a large number of particles, it is not an easy matter to pursue these questions.

Table 5. Simulation results for phase transitions in a fluid of hard spherocylinders (sol, solid; sm, smectic). For the sake of completeness we have added the case $L/D = 0$ (hard spheres).

L/D	Phase transition $\alpha - \beta$	$(\rho v_0)_\alpha$	$(\rho v_0)_\beta$	Pv_0/kT
0[a]	iso–sol	0.494	0.545	6.13
1[b]	iso–sol	0.579	0.662	15.75
3[b]	iso–sol	0.502	0.601	9.9
5[c]	iso–nem	0.40		4.9
	nem–sm	0.53		7.9
	sm–sol	0.64	0.67	13.8

[a] Hoover and Ree (1968).
[b] Veerman and Frenkel (1990).
[c] Frenkel *et al* (1988). The transition densities for the isotropic–nematic and nematic–smectic transition were obtained from an analysis of the long-range orientational and positional correlations in the phases.

3.3. Incorporation of higher virial coefficients into the Onsager theory of the isotropic–nematic transition

3.3.1. The third virial coefficient. As discussed in section 2 Onsager's (second virial) theory of the isotropic–nematic transition is an exact theory for $L/D \to \infty$. The question then arises 'how long should the rods be for the theory to have quantitative validity?'. In order to quantify the necessary length Straley (1973b) estimated the first correction term (the third virial coefficient) to the Onsager theory. This is not an easy calculation because B_3 must be evaluated for all possible relative orientations of triplets of particles. Straley approximated B_3, arguing that for an estimation of the lowest order (in D/L) correction to the Onsager theory the evaluation of the third virial coefficient does not have to be particularly accurate, provided that adequate precautions are taken to ensure that the significant features of the function are not overlooked. Straley estimates that up to $L/D \simeq 20$ the contribution of the third virial term to the free energy (evaluated at the transition density) is at least comparable to the contribution of the second virial term. For L/D values

as high as 100 he finds that the contribution of the third virial term is still about 10% of the second term. Using the simulation results of Frenkel for the higher virial coefficients of hard spherocylinders (table 1) and the transition densities given by equation (59) in the virial expansion of the free energy (equation (24)) we see that for $L/D = 100$ the Straley's estimate is remarkably accurate but that for the lower L/D values he is slightly too pessimistic about the quantitative accuracy of the Onsager theory. For example for $L/D = 10$ the contribution of the third virial term is certainly not more than 50% of that of the second virial term. Furthermore it can be seen from table 1 that—whereas the contribution of B_3 remains substantial up to $L/D \simeq 10^2$—the contributions of the higher virial terms decrease very quickly with increasing elongation. This raises hopes that for intermediate elongations the incorporation of B_3 in the Onsager theory of the isotropic–nematic phase transition suffices to make the theory quantitatively accurate. Such calculations were performed by Tjipto-Margo and Evans (1990) for HE of length-to-breadth ratios $a/b = 5$ and 10. They evaluated B_2 and B_3 both in the isotropic and anisotropic phase with high accuracy. As can be seen from table 6 the transition densities calculated incorporating the third virial coefficient are in accord with the Monte Carlo results of Allen *et al* (1989).

Table 6. Isotropic–nematic phase transition densities for hard ellipsoids calculated with the virial expansion using B_2 and B_3 compared with Monte Carlo (MC) simulation results.

	$B_2 + B_3$ theory[a]		MC[b]
a/b	$(\rho v_0)_{iso}$	$(\rho v_0)_{nem}$	$(\rho v_0)_{transition}$
5	0.388	0.426	0.37
10	0.199	0.233	0.21

[a] Tjipto-Margo and Evans (1990).
[b] Allen and Wilson (1989).

For elongations below five the second and third virial terms do not suffice to make the theory for the isotropic–nematic phase transition quantitatively accurate. In fact it may be surmised that all higher virial coefficients have to be somehow incorporated in the theory. Unfortunately at the present time the statistical mechanics of fluids of rodlike particles is nowhere near sufficiently well developed to provide confident answers on how to do this. Nevertheless, a number of interesting attempts have been made to incorporate the higher virial coefficients. We present some of these theoretical works although they generally have an *ad hoc* character and we know of no fundamental reasons why they should work.

3.3.2. The y-expansion. First of all we would like to mention the 'y'-expansion of Barboy and Gelbart (1979). In the y-expansion theory the free energy is expressed in terms of the variable

$$y = \rho/(1 - \rho v_0) \tag{98}$$

where v_0 is the volume of the hard particle. Specifically one requires that the virial expansion of the free energy can be rewritten in the form

$$\frac{\Delta F}{NkT} = \frac{\mu^0}{kT} + \ln \rho - 1 + \sigma[f] + B_2[f]\rho + \tfrac{1}{2}B_3[f]\rho^2 + \cdots \tag{99}$$

$$= \frac{\mu^0}{kT} + \ln y - 1 + \sigma[f] + C_2[f]y + \tfrac{1}{2}C_3[f]y^2 + \cdots. \quad (100)$$

The relation of the C_n coefficients to the traditional virial coefficients is easily obtained from this relationship:

$$C_2 = B_2 - v_0 \quad (101)$$

$$C_3 = B_3 - 2v_0B_2 + v_0^2 \quad (102)$$

For hard spheres, where $B_2 = 4v_0$ and $B_3 = 10v_0^2$ one finds $C_2 = 3v_0$ and $C_3 = 3v_0^2$. Terminating the y-expansion at the C_3 term one obtains for the free energy (and thus also for the other thermodynamic quantities such as the pressure) exactly the same result as is obtained by the Percus–Yevick and scaled particle theory (Hansen and McDonald 1986) for hard spheres.

Mulder and Frenkel (1985) were the first to use the y-expansion for the treatment of the isotropic–to–nematic phase transition in a fluid of HE. Rather than obtaining the exact third virial coefficient with all of its attendant orientation angles Mulder and Frenkel approximated B_3 which has consequences for the accuracy of the calculated transition densities and pressure. They found a reasonable agreement with simulation results. Recently Tjipto-Margo and Evans (1990) repeated the calculations of Mulder and Frenkel, although this time evaluating B_3 with a high degree of accuracy. As may be seen from table 7 the agreement with MC data is now considerably better. Indicating that the precise dependence of B_3 on the orientations of triplets of particles plays an important role and that approximation of these features is a subtle problem.

Table 7. Isotropic–nematic phase transition densities for hard ellipsoids calculated with the y-expansion compared with Monte Carlo simulation results.

	Elongation $a/b = 2.75$			Elongation $a/b = 3.0$		
	$(\rho v_0)_{iso}$	$(\rho v_0)_{nem}$	Pv_0/kT	$(\rho v_0)_{iso}$	$(\rho v_0)_{nem}$	Pv_0/kT
y-expansion[a] (approximate B_3)	0.449	0.475	6.55	0.420	0.438	5.31
y-expansion[b] (accurate B_3)	0.495	0.509	10.15	0.465	0.481	8.11
MC[c]	0.561	0.570	15.71	0.507	0.517	9.79

[a] Mulder and Frenkel (1985).
[b] Tjipto-Margo and Evans (1990).
[c] Frenkel and Mulder (1985).

3.3.3. Scaled particle theory. While discussing the y-expansion, we mentioned in passing the scaled particle theory (SPT). This simple and successful theory originally put forward by Reiss *et al* (1959) for the hard sphere system was generalized to fluids of hard rodlike particles by several workers (Gibbons 1969, Cotter and Martire 1970a,b, Lasher 1970, Timling 1974, Cotter 1974, 1977, 1979). Here we will focus on the work of Cotter (1977) who presented a thermodynamically consistent scaled particle treatment for both the isotropic and the nematic phase of fluids of HSC and used it to locate the isotropic–nematic phase transition. The basic idea of SPT is to obtain the excess part of the chemical potential by calculating the work W it requires

to insert at some fixed position an additional particle into the system. The way this work is calculated is by expanding (scaling) the particle to be inserted from zero to its final size. In the case of a spherocylinder this expansion can be described in terms of two scaling parameters λ_1 for the length and λ_2 for the diameter. So the scaled particle has a length $\lambda_1 L$ and diameter $\lambda_2 D$.

In the limit $\lambda_1, \lambda_2 \to 0$ the work it requires to insert a spherocylinder with orientation Ω can be easily calculated by realizing that $e^{-W/kT}$ is equal to the probability that the added particle does not overlap with any of the particles present in the system (Widom 1963). Since for $\lambda_1, \lambda_2 \to 0$ we only have to take into account overlaps of two particles, one finds

$$e^{-W(\Omega;\lambda_1,\lambda_2)/kT} = 1 - \rho \int f(\Omega') v_{\text{excl}}(\Omega, \Omega'; \lambda_1, \lambda_2)\, d\Omega'. \tag{103}$$

Here $v_{\text{excl}}(\Omega, \Omega'; \lambda_1, \lambda_2)$ is the excluded volume of the added 'scaled' HSC with orientation Ω and a HSC of the fluid with orientation Ω':

$$\begin{aligned} v_{\text{excl}}(\Omega, \Omega'; \lambda_1, \lambda_2) &= \tfrac{1}{6}\pi D^3(1+\lambda_2)^3 + \tfrac{1}{4}\pi D^2 L(1+\lambda_2)^2(1+\lambda_1) \\ &\quad + DL^2\lambda_1(1+\lambda_2)|\sin\gamma(\Omega,\Omega')|. \end{aligned} \tag{104}$$

From (103) we obtain

$$W(\Omega; \lambda_1, \lambda_2) = -kT \ln\left[1 - \rho \int f(\Omega') v_{\text{excl}}(\Omega, \Omega'; \lambda_1, \lambda_2)\, d\Omega'\right] \qquad (\lambda_1, \lambda_2 \ll 1). \tag{105}$$

For large values of the scaling parameters λ_1 and λ_2 the work required to insert an additional particle is just the work required to create the volume of the scaled particle against the pressure P exerted by the fluid

$$W(\Omega; \lambda_1, \lambda_2) = \left[\tfrac{1}{4}\pi D^2 L \lambda_2^2 \lambda_1 + \tfrac{1}{6}\pi D^3 \lambda_2^3\right] P \qquad (\lambda_1, \lambda_2 \gg 1). \tag{106}$$

Now, in the scaled particle treatment it is *assumed* that the work to add a particle with arbitrary values of the scaling parameters can be obtained by expanding (105) in a Taylor series around $\lambda_1 = \lambda_2 = 0$ up to quadratic terms and adding (106) as the third-order term.

$$W(\Omega; \lambda_1, \lambda_2) = \sum_{p,q=0}^{2} \frac{1}{p!q!} \frac{\partial^{(p+q)} W}{\partial \lambda_1^p \partial \lambda_2^q} \lambda_1^p \lambda_2^q + \left[\tfrac{1}{4}\pi D^2 L \lambda_2^2 \lambda_1 + \tfrac{1}{6}\pi D^3 \lambda_2^3\right] P. \tag{107}$$

The excess chemical potential of a HSC with length L and diameter D is obtained by setting $\lambda_1 = \lambda_2 = 1$ in this expression and integrating over all possible orientations with the orientation distribution function

$$\mu^{\text{ex}} = \int f(\Omega) W(\Omega; 1, 1)\, d\Omega. \tag{108}$$

The pressure can now be obtained by using the Gibbs–Duhem equation

$$\left(\frac{\partial P}{\partial \rho}\right)_T = 1 + \rho\left(\frac{\partial \mu^{ex}}{\partial \rho}\right)_T \tag{109}$$

Finally the Helmholtz free energy can be obtained from the relation

$$\Delta F = N\mu - PV. \tag{110}$$

The expression for the free energy can be conveniently written in terms of the variable y (see equation (98))

$$\frac{\Delta F}{NkT} = \frac{\mu^0}{kT} + \ln y - 1 + \sigma[f] + A[f]y + \tfrac{1}{2}B[f]y^2 \tag{111}$$

where

$$A[f] = \left(3 + \frac{3(\gamma-1)^2}{(3\gamma-1)}\rho[f]\right)v_0 \tag{112}$$

and

$$B[f] = \left(\frac{12\gamma(2\gamma-1)}{(3\gamma-1)^2} + \frac{12\gamma(\gamma-1)^2}{(3\gamma-1)^2}\rho[f]\right)v_0^2. \tag{113}$$

In this section $\gamma \equiv 1 + L/D$ (not to be confused with angle γ). By setting $\gamma = 1$ (and $f = 1/4\pi$) one recovers the well known expression for the free energy of a hard sphere fluid in the scaled particle approximation. One of the remarkable features of the scaled particle treatment of hard spheres is that in addition to B_2 (which is really put into the theory) the third virial coefficient B_3 is reproduced exactly. In view of the earlier discussion, where it transpired that B_3 plays a key role in constructing an accurate theory for the isotropic–nematic phase transition, one might ask how accurately B_3 is given in the scaled particle treatment for rodlike fluids. Using equations (101) and (102), relating A and B to the traditional virial coefficients B_2 and B_3 one obtains

$$B_2 = \left(4 + \frac{3(\gamma-1)^2}{(3\gamma-1)}\rho[f]\right)v_0 \tag{114}$$

and

$$B_3 = \left(7 + \frac{12\gamma(2\gamma-1)}{(3\gamma-1)^2} + \left[\frac{6(\gamma-1)^2}{(3\gamma-1)} + \frac{12\gamma(\gamma-1)^2}{(3\gamma-1)^2}\right]\rho[f]\right)v_0^2. \tag{115}$$

The fact that B_3 only depends on the angle between two rods clearly reveals the nature of the scaled particle approach as a 'renormalized' two-particle theory.

In table 8 we compare B_3/B_2^2 given by SPT for the isotropic phase ($\rho[f] = 1$) with the simulation results of Frenkel. The approximation is not bad but certainly not quantitatively accurate. In order to get an impression of the accuracy of the results of SPT (Cotter 1979) for the isotropic–nematic phase transition we compare them with available computer simulation results for $L/D = 3$ and 5. For $L/D = 3$ SPT

Table 8. Comparison of reduced third virial coefficients of isotropic hard spherocylinders calculated from scaled particle theory (SPT) or from the Parsons approach with accurate numerical results.

	B_3/B_2^2		
L/D	SPT[a]	Parsons[b]	Numerical[c]
0	0.625	0.625	0.625
5	0.3503	0.2972	0.4194
10	0.2481	0.1869	0.3133
10^2	0.0323	0.0242	0.0698
10^3	0.00332	0.00249	0.0106

[a] Cotter (1977).
[b] Parsons (1979) or Lee (1987).
[c] Frenkel (1987a).

yields an isotropic–nematic phase transition with coexisting volume fractions 0.47–0.49. Computer simulations do not find an isotropic–nematic transition for this L/D ratio but an isotropic–solid transition with coexisting volume fractions 0.502–0.601. For $L/D = 5$ SPT yields an isotropic–nematic phase transition with coexisting volume fractions 0.36–0.39 and a coexistence pressure $Pv_0/kT = 4.50$. Simulations show an isotropic–nematic phase transition at a volume fraction 0.40 and at a pressure $Pv_0/kT = 4.89$. In view of its simplicity and clarity one might argue that SPT provides a useful extension of the Onsager theory. However, the fact that already the third virial contribution is only approximately included in the theory prevents it from being quantitatively accurate.

3.3.4. The Parsons approach. In this section we want to mention an approach which is similar to SPT in the fact that it may be considered a renormalized two-particle theory. Although this approach is sometimes attributed to Lee (1987, 1988), it had in fact already been given in the paper by Parsons (1979). Lee used this expression to calculate the isotropic–nematic phase transition in solutions of HSC (Lee 1987) and HE (Lee 1988). In section 4.3.5 the derivation by Parsons is described in somewhat more detail, here we only give the result. The approach may be considered an extension of the semi-empirical Carnahan–Starling equation for hard spheres (Hansen and McDonald 1986). The excess part of the Carnahan–Starling free energy is given by

$$\frac{F_{\mathrm{CS}}^{\mathrm{ex}}}{NkT} = \frac{\phi(4-3\phi)}{(1-\phi)^2} \tag{116}$$

with ϕ the volume fraction as usual. For hard rodlike particles this excess free energy is multiplied by the factor

$$\frac{\langle\langle v_{\mathrm{excl}}\rangle\rangle(\text{rodlike particle})}{8v_0(\text{rodlike particle})} \tag{117}$$

where

$$\langle\langle v_{\mathrm{excl}}\rangle\rangle \equiv \int\int v_{\mathrm{excl}}(\Omega,\Omega')f(\Omega)f(\Omega')\,\mathrm{d}\Omega\,\mathrm{d}\Omega' \tag{118}$$

and v_0 is the volume of the rodlike particle. The factor of 8 is needed to reduce equation (117) to 1 for spheres. This construction clearly leads to the correct second virial coefficient and for the third virial coefficient one obtains in the case of HSC

$$B_3 = \left(10 + \frac{15}{2}\frac{(\gamma-1)^2}{(3\gamma-1)}\rho[f]\right) v_0^2. \tag{119}$$

To check the quality of this approximation we present data in table 8 for B_3/B_2^2 calculated with this approximation for B_3 and compare it with the simulation data of Frenkel. Although the results for B_3 are not particularly impressive, the transition densities and pressure one obtains with this method are quite reasonable. For example for HSC with $L/D = 5$ Lee (1987) obtains for the volume fractions of the coexisting isotropic and nematic phase 0.3995 and 0.4172 and for the pressure at the transition $Pv_0/kT = 5.361$. Simulations show an isotropic–nematic phase transition at a volume fraction 0.40 at a pressure 4.89.

For HE Lee (1988) obtains for $a/b = 2.75$ coexisting volume fractions of 0.5443 and 0.5518 (simulation results 0.561 and 0.570) at a reduced pressure $Pv_0/kT = 13.19$ (simulation result 15.71) and for $a/b = 3$ coexisting volume fractions 0.5081 and 0.5173 (simulation results 0.507 and 0.517) at a reduced pressure $Pv_0/kT = 10.00$ (simulation result 9.786). Although clearly a successful approach in terms of predicting fairly accurate values for the quantities characterizing the isotropic–nematic phase transition it is difficult to see what the basic reason for this success is. However, in section 4.3.5 we will demonstrate a certain connection with other approaches to be discussed in the next sections.

For the sake of completeness we note that Khokhlov and Semenov (1985) also constructed a free energy for higher densities on the basis of the Parsons approach:

$$\frac{F^{ex}}{NkT} = 4\phi_{max}\ln(1-\phi/\phi_{max})^{-1}\frac{\langle\langle v_{excl}\rangle\rangle}{8v_0} \tag{120}$$

with ϕ_{max} the volume fraction at closest packing of the particles. This expression is chosen for its similarity to the Flory expression of the free energy (Khokhlov and Semenov 1985, Flory 1956).

4. Density functional theory of liquid crystals

Up to now we only discussed theories for the isotropic–nematic transition. In this section we describe the so called density functional theory (DFT) which is also applicable to partially ordered phases like the smectic state or completely ordered phases like the crystalline state. Although most of the applications of DFT to liquid crystals followed those on the freezing transition of liquids, it is noteworthy that the first formulation of DFT for liquid crystals actually preceded the seminal work of Ramakrishnan and Yussouff (1977, 1979) on the freezing transition of hard spheres: the paper by Workman and Fixman (1973) included all essential ingredients for what was later to be called DFT. Prior to a discussion of the results for liquid crystals we give a short exposition of the basic ideas of DFT (for more detailed reviews see e.g. Hansen and McDonald (1986), Evans (1979), Haymet and Oxtoby (1986), Baus (1987, 1990)).

The name of density functional theory originates from the fact that the thermodynamic potentials of an inhomogeneous system may be considered as *functionals* of

the inhomogeneous (one-particle) *density* $\rho(\boldsymbol{x})$. Since we will be dealing with liquid crystals $\boldsymbol{x}$ may represent both positional and/or orientational coordinates. As an example the Helmholtz free energy can be written as follows†

$$F[\rho(\boldsymbol{x})] = F^{\mathrm{id}}[\rho(\boldsymbol{x})] + F^{\mathrm{ex}}[\rho(\boldsymbol{x})] \tag{121}$$

This expression contains an ideal part

$$F^{\mathrm{id}}[\rho(\boldsymbol{x})] = kT \int \rho(\boldsymbol{x}) \left[\ln(\Lambda^3 \rho(\boldsymbol{x})) - 1\right] \mathrm{d}\boldsymbol{x} \tag{122}$$

which is a straightforward generalization to inhomogeneous systems of the ideal entropy term $N[\ln(\Lambda^3\rho) - 1]$ in the free energy, cf equation (7). The second term in (121) represents an excess free energy as a result of interactions between particles. It may be shown that this excess free energy is related to the (two-particle) direct correlation function $c^{(2)}(\boldsymbol{x}, \boldsymbol{x}'; [\rho])$ via its second functional derivative (Hansen and McDonald 1986)

$$\frac{\delta^2 F^{\mathrm{ex}}[\rho]}{\delta\rho(\boldsymbol{x})\delta\rho(\boldsymbol{x}')} = -kTc^{(2)}(\boldsymbol{x}, \boldsymbol{x}'; [\rho]) \tag{123}$$

or—more generally—to the n-particle direct correlation functions $c^{(n)}(\boldsymbol{x}_1, \cdots, \boldsymbol{x}_n; [\rho])$

$$\frac{\delta^n F^{\mathrm{ex}}[\rho]}{\delta\rho(\boldsymbol{x}_1)\cdots\delta\rho(\boldsymbol{x}_n)} = -kTc^{(n)}(\boldsymbol{x}_1, \ldots, \boldsymbol{x}_n; [\rho]) \tag{124}$$

since these are interrelated via functional differentiations as well. In the foregoing—as in the rest of the article—we often write $[\rho]$ as a shorthand notation for a functional dependence $[\rho(\boldsymbol{x})]$.

The Helmholtz free energy is related to the grand potential Ω through a Legendre transformation

$$\Omega[\rho] = F[\rho] - \mu \int \rho(\boldsymbol{x}) \, \mathrm{d}\boldsymbol{x} \qquad (= F - \mu N) \tag{125}$$

where μ is the chemical potential as usual. In equations (125) and (121) $\Omega[\rho]$ and $F[\rho]$ are functionals of the density $\rho(\boldsymbol{x})$. The basic principle of DFT is that it can be proven that the equilibrium density $\rho^{\mathrm{eq}}(\boldsymbol{x})$ is given by that specific density which minimizes $\Omega[\rho]$, i.e.

$$\left.\frac{\delta\Omega[\rho]}{\delta\rho(\boldsymbol{x})}\right|_{\rho(\boldsymbol{x})=\rho^{\mathrm{eq}}(\boldsymbol{x})} = 0 \tag{126}$$

† To prove that it is possible to write the free energy as a unique functional of density $\rho(\boldsymbol{x})$, it is necessary to consider our system in an externally applied field. This introduces an extra term in equation (121), which we do not take along here because it vanishes upon reducing the strength of this field to zero. From a formal point of view, however, this term is of importance and we refer the reader to Hansen and McDonald (1986) and Baus (1987) for a discussion.

and the corresponding $\Omega[\rho^{eq}]$ and $F[\rho^{eq}]$ are the (equilibrium) grand potential and Helmholtz free energy respectively. By substituting (125) in (126) we may just as well formulate a minimum principle for the Helmholtz free energy

$$\left.\frac{\delta F[\rho]}{\delta \rho(\boldsymbol{x})}\right|_{\rho(\boldsymbol{x})=\rho^{eq}(\boldsymbol{x})} = \mu \tag{127}$$

to find the equilibrium density. Comparing (127) with equation (30) we realize that chemical potential μ in this equation may be interpreted as a Lagrange multiplier associated with the normalization condition

$$\int \rho(\boldsymbol{x})\,\mathrm{d}\boldsymbol{x} = N \tag{128}$$

and the development of DFT closely resembles the procedure described in section 2.4 for the virial theories. Many papers about DFT use grand potential Ω with equation (126) as a starting point, here we prefer the equivalent method of using Helmholtz free energy F with equation (127) to stress the analogy with the rest of our article. Before developing DFT any further however, we first turn to a simpler problem which may be easily discussed within this context.

4.1. Stability analysis

Equation (127) is a necessary though not a sufficient condition to find the minimum of the free energy. To ensure an extremum found with equation (127) is a minimum a further condition is required:

$$\iint \frac{\delta^2 F}{\delta\rho(\boldsymbol{x})\delta\rho(\boldsymbol{x}')}\delta\rho(\boldsymbol{x})\delta\rho(\boldsymbol{x}')\,\mathrm{d}\boldsymbol{x}\,\mathrm{d}\boldsymbol{x}' > 0 \tag{129}$$

for arbitrary variations in the particle distribution, $\delta\rho(\boldsymbol{x})$. Expression (129) may also be used separately to determine when a given phase ceases to be stable. In the context of density functional formalism this was first done by Stecki and Kloczkowski (1979, 1981). Using equations (122) and (123) they transformed (129) to

$$\iint \left[\frac{\delta(\boldsymbol{x}-\boldsymbol{x}')}{\rho(\boldsymbol{x})} - c^{(2)}(\boldsymbol{x},\boldsymbol{x}';[\rho])\right]\delta\rho(\boldsymbol{x})\delta\rho(\boldsymbol{x}')\,\mathrm{d}\boldsymbol{x}\,\mathrm{d}\boldsymbol{x}' > 0. \tag{130}$$

Considering the stability of the isotropic state towards nematic perturbations as an example, we may write $\rho(\boldsymbol{x}) = \rho_0/4\pi$ for an isotropic density and

$$c^{(2)}_{iso}(\boldsymbol{r},\boldsymbol{r}',\Omega,\Omega';[\rho]) = c^{(2)}_{iso}(|\boldsymbol{r}-\boldsymbol{r}'|,\Omega_{\Delta r},\Omega,\Omega';\rho_0) \tag{131}$$

with $\Omega_{\Delta r}$ being the solid angle defining the direction of $\boldsymbol{r}-\boldsymbol{r}'$. An arbitrary nematic perturbation may be expanded in Legendre polynomials

$$\delta\rho(\boldsymbol{x}) = \rho_0 \sum_{n=0}^{\infty} a_{2n} P_{2n}(\cos\theta). \tag{132}$$

Now, substitution of these expressions in equation (130) and some manipulation yields

$$\sum_n a_{2n}^2 \left[\frac{1}{4n+1} - \rho_0 \iiint c_{\text{iso}}^{(2)} P_{2n}(\cos\theta) P_{2n}(\cos\theta') \frac{\mathrm{d}\Omega}{4\pi} \frac{\mathrm{d}\Omega'}{4\pi} \mathrm{d}(\boldsymbol{r}-\boldsymbol{r}') \right] > 0. \tag{133}$$

The fact that only terms with equal n for $\delta\rho(\boldsymbol{x})$ and $\delta\rho(\boldsymbol{x}')$ appear may be derived using the angular expansion (136) and (137) for an isotropic direct correlation function. Because of the quadratic form in a_{2n} of equation (133), the factor in square brackets in (133) must be positive for each n separately. As soon as one of these factors changes sign, the isotropic state loses its stability.

To show the connection to the bifurcation analysis of section 2.4.2 we may employ the lowest order term in the density expansion (142) of $c^{(2)}$

$$\int c_{\text{iso}}^{(2)} \mathrm{d}(\boldsymbol{r}-\boldsymbol{r}') \simeq \int \Phi \, \mathrm{d}(\boldsymbol{r}-\boldsymbol{r}') \overset{(20)}{=} -v_{\text{excl}}(\gamma) \tag{134}$$

which—applied in equation (133)—again leads to the bifurcation density of equation (46).

4.2. The isotropic direct correlation function

As we shall see the direct correlation function plays a key role in DFT (cf equation (123)). Since we are dealing with liquid crystals this will be an anisotropic function, which is generally not known. Therefore, in all current versions of DFT, an approximative form is used, derived in one way or another from the direct correlation function in the isotropic state. However, even this function is not so easily obtained for anisometric particles since it not only involves the distance r but also their mutual orientations represented by two direction vectors (see figure 7).

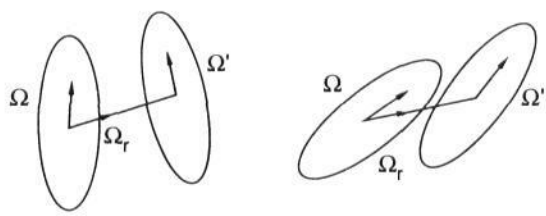

Figure 7. *Illustration of the need to use two unit vectors to describe an isotropic* $c^{(2)}$: if we know the direction ($\widehat{\boldsymbol{\Omega}}_r$) of the vector connecting the centres of both molecules, the correlation will still depend on their directions ($\widehat{\boldsymbol{\Omega}}$ and $\widehat{\boldsymbol{\Omega}}'$) as is clear from these illustrations both having the same $\widehat{\boldsymbol{\Omega}}_r$ and r. In an isotropic state the direct correlation function must be invariant under rotations, which implies it does not explicitly depend on $\widehat{\boldsymbol{\Omega}}_r$ when the two direction vectors $\widehat{\boldsymbol{\Omega}}$ and $\widehat{\boldsymbol{\Omega}}'$ are specified with respect to the direction of $\widehat{\boldsymbol{\Omega}}_r$. If $\widehat{\boldsymbol{\Omega}}$ and $\widehat{\boldsymbol{\Omega}}'$ are specified in a space-fixed coordinate system $c^{(2)}$ also depends on $\widehat{\boldsymbol{\Omega}}_r$.

Formally, $c^{(2)}$ is defined by the Ornstein–Zernike equation (Hansen and McDonald 1986)

$$h(\boldsymbol{x}_1, \boldsymbol{x}_2) = c^{(2)}(\boldsymbol{x}_1, \boldsymbol{x}_2) + \int \rho(\boldsymbol{x}_3) c^{(2)}(\boldsymbol{x}_1, \boldsymbol{x}_3) h(\boldsymbol{x}_3, \boldsymbol{x}_2) \, \mathrm{d}\boldsymbol{x}_3 \tag{135}$$

which relates the pair correlation function $h(\boldsymbol{x}_1, \boldsymbol{x}_2)$ of two particles to their direct correlation function $c^{(2)}(\boldsymbol{x}_1, \boldsymbol{x}_2)$. While h describes the real correlation between the two particles, $c^{(2)}$ only involves their direct correlation, i.e. excluding the indirect correlation which is 'transmitted' through mutual correlations with other particles in the neighbourhood. Equation (135) must be supplemented by a second relation between both correlation functions, a so called closure relation like the Percus–Yevick (PY) or hypernetted chain (HNC) (Hansen and McDonald 1986). The PY closure relation gives good results for hard spheres with the additional advantage of providing an analytical solution of (135).

Unfortunately, the state of affairs is less advanced for non-spherical hard particles because of the extra angular variables and much more complicated integration areas. We now discuss some of the methods used to obtain the isotropic direct correlation function in DFT of liquid crystals.

4.2.1. Integral equation approach. Patey and co-workers (Fries and Patey 1985, Perera *et al* 1987, Perera and Patey 1988) have made extensive studies of solving the Ornstein–Zernike equation for different non-spherical particles. They use an expansion of both correlation functions in so called rotational invariants, Φ^{mnl}, introduced by Blum and Torruella (1972), for example for the direct correlation function

$$c^{(2)}_{\mathrm{iso}}(\boldsymbol{r}, \Omega, \Omega') = \sum_{mnl} c^{mnl}(r)\Phi^{mnl}(\Omega_r, \Omega, \Omega'). \tag{136}$$

This expression makes use of the fact that all angle-dependent functions may be expanded in a complete set of basis functions. One set, the Legendre polynomials $P_{2n}(\cos\theta)$, we encountered in section 2 for functions solely depending on angle θ. For axially symmetrical particles we need two angles (θ and φ) to characterize their direction and the corresponding set of basis functions are the spherical harmonics $Y_l^\lambda(\Omega)$. Now, $\Phi^{mnl}(\Omega_r, \Omega, \Omega')$ are combinations of products of three spherical harmonic functions (one set for each direction) which are invariant under simultaneous (arbitrary) rotations of all three directions (cf the discussion of figure 7). They may be written as follows

$$\Phi^{mnl}(\Omega_r, \Omega, \Omega') \equiv \text{constant} \sum_{\mu\nu\lambda} \begin{pmatrix} m & n & l \\ \mu & \nu & \lambda \end{pmatrix} Y_m^\mu(\Omega) Y_n^\nu(\Omega') Y_l^\lambda(\Omega_r) \tag{137}$$

with $\begin{pmatrix} m & n & l \\ \mu & \nu & \lambda \end{pmatrix}$ a $3j$ Wigner symbol. The coefficients $c^{mnl}(r)$ of these rotational invariants in (136) are still dependent on the centre-to-centre distance r and are evaluated by intricate numerical calculations. Because of this, expansion (136) had to be truncated rather soon in Perera *et al* (1987) and Perera and Patey (1988) which raises some doubts about the degree of convergence of the series, especially at higher concentrations.

As may be seen by substituting (136) in equation (133) the stability of the isotropic state towards a nematic (P_2) perturbation is determined by the behaviour of $\rho_0 \int c^{220}(\boldsymbol{r})\,\mathrm{d}\boldsymbol{r}$. At the density for which this integral exceeds a critical value the isotropic phase gets unstable. Perera *et al* (1987) and Perera and Patey (1988) located this (spinodal) point by extrapolating the results for this integral at lower densities (because of the use of rotational invariants, the correlation functions are forced to be isotropic, which will probably cause convergence problems near the spinodal

point). Surprisingly, it appeared that the PY closure relation gave bifurcation points beyond the freezing transition both for ellipsoids $a/b = 2, 3, 5$ and spherocylinders $L/D = 1, 2, 5$, whereas the HNC closure relation predicted reasonably situated bifurcation points. However, the fit of the data for the equation of state did not indicate a preference for either of the closure relations (Talbot *et al* 1990).

4.2.2. Decoupling approximation. This method consists of making an educated guess for the direct correlation function based upon the analytically known PY direct correlation function for hard spheres of diameter σ_0 at volume fraction ϕ, $c_{\mathrm{PY}}^{(2)}(r/\sigma_0; \phi)$ (Hansen and McDonald 1986). This function is a spherical symmetric function, so it only depends on the centre-to-centre distance r. Pynn (1974a, b) suggested extending the use of this function to anisometric particles by scaling r differently for each direction, namely with the distance of nearest approach of the two particles $\sigma(\Omega_r, \Omega, \Omega')$ in the configuration involved.

$$c_{\mathrm{iso}}^{(2)}(\boldsymbol{r}, \Omega, \Omega'; \phi) = c_{\mathrm{PY}}^{(2)}\left(\frac{r}{\sigma(\Omega_r, \Omega, \Omega')}; \phi\right). \tag{138}$$

The angular dependence thus introduced possesses plausible characteristics just because of this coupling to σ, on the other hand Lado (1985) showed that it has the deficiency of giving an isotropic value for $c^{(2)}(r \to 0)$, which is contrary to reality. Lado also tested the decoupling approximation by comparing it with the integral equation approach for hard dumbbells and found excellent agreement for the case of a separation of 0.4 times the diameter of the composing spheres. We want to stress, however, that this approximation is *ad hoc* and will probably worsen for larger axial ratios and higher densities. In section 4.3.5 we will show why approximation (138) is called the decoupling approximation and show its connection to the Parsons expression for the free energy.

As a last point we want to mention some variations on this approximation. Marko (1988, 1989) introduced an additional angular factor $(1 + \alpha P_2(\hat{\Omega} \cdot \hat{\Omega}'))$ in equation (138) to correct for the problem put forward by Lado. The value of α was determined by formulating a variational principle derived from the Ornstein–Zernike equation (135). Finally, Singh and Singh (1986) used a variation on $c_{\mathrm{PY}}^{(2)}$ in the form of the Waisman–Henderson–Blum DCF (Waisman 1973, Henderson and Blum 1976) which is claimed to work better for spheres.

4.2.3. Factorization. Baus and co-workers introduced a different way to relate the direct correlation function of ellipsoids to the PY function of spheres (Baus *et al* 1987, Colot *et al* 1988)

$$c_{\mathrm{iso}}^{(2)}(\boldsymbol{r}, \Omega, \Omega'; \phi) = \frac{v_{\mathrm{excl}}(\hat{\Omega} \cdot \hat{\Omega}')}{4\pi\sigma_0^3/3} c_{\mathrm{PY}}^{(2)}(r/\sigma_0; \phi) + \cdots \tag{139}$$

where they represent the translational part by that of a sphere with equal volume

$$\sigma_0^3 \equiv ab^2 \tag{140}$$

and the angular dependence by that of the excluded volume (divided by the excluded volume of the equivalent sphere). In contrast to the decoupling approximation this

method has the advantage of giving an anisotropic direct correlation function at $r = 0$ although at the expense of giving both configurations of figure 7 equal weight. In reality $c^{(2)} = c^{(2)}(\hat{\Omega} \cdot \hat{\Omega}')$ only at low density (see equation (142)).

A more serious problem is the fact that (139) is fundamentally inadequate to describe phases of partial positional order like the smectic state, since the position dependence of (139) is that of a sphere. The angular dependence in (139) is completely decoupled from the positional dependence so that they cannot cooperate to form a smectic state. Note that the decoupling approximation (138) does not involve such a rigorous decoupling but a more restricted decoupling as shown in section 4.3.5.

4.3. Density functional theory

After this preparatory section on the direct correlation function in the isotropic phase, we return to the formalism. The basic relation of DFT is equation (123) which relates the excess free energy F^{ex} to the direct correlation function. Double functional integration of this relation from a reference state of uniform density ρ_R to a final state $\rho(\boldsymbol{x})$ gives us

$$F^{ex}[\rho(\boldsymbol{x})] = F^{ex}[\rho_R] - kTc^{(1)}[\rho_R] \int d\boldsymbol{x}_1 \, \Delta\rho(\boldsymbol{x}_1) - kT \int d\boldsymbol{x}_1 \int d\boldsymbol{x}_2 \int_0^1 d\lambda \times \int_0^\lambda d\lambda' \, c^{(2)}(\boldsymbol{x}_1, \boldsymbol{x}_2; [\rho_R + \lambda' \Delta\rho(\boldsymbol{x})]) \Delta\rho(\boldsymbol{x}_1) \Delta\rho(\boldsymbol{x}_2) \tag{141}$$

where $\Delta\rho(\boldsymbol{x}) \equiv \rho(\boldsymbol{x}) - \rho_R$, so $\rho_R + \lambda' \Delta\rho(\boldsymbol{x})$ is the parametrized integration path from the uniform reference state to the non-uniform final state. Further, $F^{ex}[\rho_R]$ and $c^{(1)}[\rho_R]$ are the free energy and one-particle direct correlation function of the uniform reference state (which are constants).

Combined with equations (121) and (122) the above expression for F^{ex} forms the starting point of DFT. Unfortunately, the problem of an unknown free energy has now been shifted to that of an unknown direct correlation function $c^{(2)}(\boldsymbol{x}_1, \boldsymbol{x}_2; [\rho_R + \lambda' \Delta\rho(\boldsymbol{x})])$ of a non-uniform fluid.

In the following, we first show the connection between DFT and the virial expansion (in section 4.3.1). Subsequently, we discuss several ways in which to simplify the general but intractable equation (141):

expansion around a uniform fluid (section 4.3.2); structural mapping (section 4.3.3); and weighted density approximation (section 4.3.4).

Every method either uses one of the isotropic direct correlation functions of section 4.2 or avoids the use of the direct correlation function all together. Then, we draw attention to the fact that many of the different lines of approach are actually closely connected to the Parsons expression for the free energy (section 4.3.5). Finally to really calculate a phase transition there are two more points to be considered:

the parametrization of the density (section 4.3.6); and locating the phase transitions (section 4.3.7).

In section 4.3.8 we summarize results obtained thus far via the different approaches and compare them to available computer simulations.

4.3.1. Low-density expansion. To show the connection between the DFT and the virial expansion we can make a low-density expansion of the direct correlation function

(Hansen and McDonald 1986, McQuarrie 1976)

$$c^{(2)}(\boldsymbol{x}_1, \boldsymbol{x}_2) = \Phi(\boldsymbol{x}_1, \boldsymbol{x}_2) + \int \Phi(\boldsymbol{x}_1, \boldsymbol{x}_2)\Phi(\boldsymbol{x}_2, \boldsymbol{x}_3)\Phi(\boldsymbol{x}_3, \boldsymbol{x}_1)\rho(\boldsymbol{x}_3)\,\mathrm{d}\boldsymbol{x}_3 + \cdots. \tag{142}$$

We may substitute this expansion in (141) with the low-density reference state $\rho_R = 0$, for which $F^{ex}[0] = 0$ and $c^{(1)}[0] = 0$. When we further restrict ourselves to the nematic state (157) we get

$$\frac{F^{ex}[\rho]}{NkT} = -\frac{1}{2}\rho \int \mathrm{d}\Omega_1 \int \mathrm{d}\Omega_2\, \beta_1(\Omega_1, \Omega_2) f(\Omega_1) f(\Omega_2) - \cdots \tag{143}$$

which is the virial expansion of the interaction part of the free energy, where the cluster integral β_1 is defined as in equation (4). We can similarly use (157) in ideal part (122) obtaining

$$\frac{F^{id}[\rho]}{NkT} = \ln(\Lambda^3\rho) - 1 + \int \mathrm{d}\Omega\, f(\Omega) \ln f(\Omega) \tag{144}$$

which completes the link between the DFT and the virial equation (18). The omission of a term $\ln 4\pi$ in the integral in (144) is due to a different point of zero orientational entropy. Both conventions are used in the literature.

4.3.2. Expansion around a uniform liquid. When we have obtained a (positionally or orientationally) non-uniform density which is not too much disturbed from a uniform liquid of density ρ_R, we could try to make a functional Taylor expansion around this state on the basis of equation (124):

$$F^{ex}[\rho(\boldsymbol{x})] = F^{ex}[\rho_R] - kT \int \mathrm{d}\boldsymbol{x}_1\, c^{(1)}(\rho_R)\Delta\rho(\boldsymbol{x}_1) - \tfrac{1}{2}kT \int \mathrm{d}\boldsymbol{x}_1 \int \mathrm{d}\boldsymbol{x}_2 c^{(2)}(|\boldsymbol{x}_1 - \boldsymbol{x}_2|; \rho_R)\Delta\rho(\boldsymbol{x}_1)\Delta\rho(\boldsymbol{x}_2) + \cdots \tag{145}$$

where the higher order terms contain the more-particle direct correlation functions $c^{(3)}, c^{(4)}, \ldots$ of the uniform liquid of density ρ_R. A considerable number of papers applying DFT to liquid crystals use equation (145) as a starting point (Workman and Fixman 1973, Sluckin and Shukla 1983, Lipkin and Oxtoby 1983, Singh 1984, Kloczkowski and Stecki 1985, Singh and Singh 1986, Perera *et al* 1988, Marko 1988, 1989, Singh *et al* 1989). Because $c^{(3)}$ is not known except for a uniform liquid of hard spherical particles (Rosenfeld *et al* 1990) the Taylor series is usually truncated after the quadratic term.

4.3.3. Structural mapping. In this approach the anisotropic state is not expanded about an isotropic state, although the form of its direct correlation function is borrowed from the isotropic state. However, the specifications of this isotropic state are chosen such that its correlation function reflects some essential features of the anisotropic state it must describe. An example for hard spheres is the paper by Baus and Colot (1985), in which the first maximum of the static structure factor of the effective liquid

(the Fourier transform of its direct correlation function) is required to coincide with the smallest reciprocal lattice vector of the solid.

For nematic liquid crystals of hard ellipsoids Colot *et al* (1988) chose to use a PY function with its variable r scaled by the distance at nearest approach of its equivalent sphere system as in equation (139). They furthermore argued that at a given volume fraction ϕ there is, on average, less interaction between the more or less parallel ellipsoids in the nematic state than between the randomly directed ellipsoids in the isotropic state of the same volume fraction. This means that we should take a lower effective volume fraction $\bar{\phi}$ if we want to describe this nematic state with an isotropic direct correlation function. This effective volume fraction $\bar{\phi}$ was fixed by requiring the same value at contact of the direct correlation function in both systems:

$$c_{\mathrm{PY}}^{(2)}\left(\frac{r}{\sigma_0}=1;\phi\right)=c_{\mathrm{PY}}^{(2)}\left(\frac{r}{\sigma_0}=x;\bar{\phi}\right) \tag{146}$$

where the average contact distance in the nematic phase is assumed to be reduced by a factor x compared to the isotropic phase. Regrettably—due to an oversight (Baus 1991)—Colot *et al* (1988) took x to be equal to b/a, which implies the average contact distance in the nematic phase would be smaller than the minor axis of the ellipsoid. Because of this the value of the effective volume fraction was taken to be much too small. Unfortunately, although Singh *et al* (1989) used a more accurate numerical form for $c^{(2)}$ they applied the same recipe for the effective volume fraction in the nematic state, which renders their numerical results for the isotropic–nematic transition useless as well.

4.3.4. Weighted density approximation. Some authors (Poniewierski and Hołyst 1988, Hołyst and Poniewierski 1989a, Somoza and Tarazona 1988, 1989a, 1990, Mederos and Sullivan 1989) take a somewhat deviating standpoint from the foregoing by not starting from the direct correlation function to find F^{ex}, instead they start from a local free energy density $\Delta\psi$. To show the connection with DFT we note that equation (141) with $\rho_{\mathrm{R}}=0$ may be rewritten as

$$F^{\mathrm{ex}}[\rho(\boldsymbol{x})]=\int\rho(\boldsymbol{x})\Delta\psi[\rho(\boldsymbol{x})]\,\mathrm{d}\boldsymbol{x}. \tag{147}$$

Here the local free energy density $\Delta\psi[\rho(\boldsymbol{x})]$ is a *functional* of $\rho(\boldsymbol{x})$, which means it depends upon the density in each point of the system. In the weighted density approximation $\Delta\psi$ is postulated to be a *function* of a local density $\bar{\rho}(\boldsymbol{x})$. This density could not be $\rho(\boldsymbol{x})$ itself since this would preclude interactions between molecules at different points (note that F^{id} of equation (122) is of this form). Therefore they assume that this density is a weighted average of the density in the neighbourhood

$$\bar{\rho}(\boldsymbol{x})\equiv\int W(\boldsymbol{x},\boldsymbol{x}')\rho(\boldsymbol{x}')\,\mathrm{d}\boldsymbol{x}' \tag{148}$$

where the weighting function $W(\boldsymbol{x},\boldsymbol{x}')$ is sometimes taken to depend on $\bar{\rho}(\boldsymbol{x})$ too. Thus, equation (147) is approximated by

$$F^{\mathrm{ex}}[\rho(\boldsymbol{x})]=\int\rho(\boldsymbol{x})\Delta\psi(\bar{\rho}(\boldsymbol{x}))\,\mathrm{d}\boldsymbol{x}. \tag{149}$$

Additional assumptions must be introduced to find W and $\Delta\psi$. Poniewierski and Hołyst (1988) and Hołyst and Poniewierski (1989a) apply a local free energy density which is adapted from the Carnahan–Starling expression for hard spheres

$$\Delta\psi(\rho) = \Delta\psi^{CS}(\phi) + (\rho B_2^{iso} - 4\phi) \tag{150}$$

where $\Delta\psi^{CS} = F_{CS}^{ex}/N$ from the Carnahan–Starling expression (116), which is modified by the term in brackets to provide the right second virial coefficient in the isotropic state. Since this free energy density no longer depends on the angular distribution, they introduced an extra angular integration $d\Omega$ in the definition of $\bar{\rho}(\boldsymbol{x})$, equation (148). Their weighting function is chosen to be proportional to the Mayer function and may as such considered to be a low-density approximation. For the nematic state this gives

$$\bar{\rho} \equiv \rho \frac{\langle\langle v_{excl} \rangle\rangle}{v_{excl}^{iso}} \tag{151}$$

yielding a lower effective density as in the case of structural mapping.

Somoza and Tarazona (1988, 1989a, 1990) prefer to start from a parallel hard ellipsoid (PHE) reference fluid, for which both the free energy density and the weighting function are obtained from those of a hard sphere fluid by expansion of the spheres in one direction. They introduce an angle dependence via a generalization to inhomogeneous systems of the approach by Parsons (1979), equations (116) and (117)

$$F^{ex}[\rho(\boldsymbol{r},\Omega)] = \int d\boldsymbol{r} \int d\Omega\, \rho(\boldsymbol{r},\Omega)\Delta\psi^{CS}[\bar{\rho}(\boldsymbol{r})] \times \frac{\int d\boldsymbol{r}' \int d\Omega\, \rho(\boldsymbol{r}',\Omega')\Phi(\boldsymbol{r}-\boldsymbol{r}',\Omega,\Omega')}{\int d\boldsymbol{r}'\, \Phi_{PHE}(\boldsymbol{r}-\boldsymbol{r}') \int d\Omega\, \rho(\boldsymbol{r}',\Omega')}. \tag{152}$$

They determine the parameters for the reference parallel hard ellipsoids by requiring that the average tensor of inertia in the reference fluid be proportional to that of the fluid to be described and the volumes of the ellipsoids be equal to those of the original particles.

Since in this approach an expression for the excess free energy is given, we can now use equation (123) to obtain an approximate direct correlation function instead of the reverse. This expression may be used to determine the bifurcation density to the smectic state via a method similar to the one described in section 4.1. Somoza and Tarazona (1988, 1989b) do this for the parallel hard spherocylinder fluid, while Poniewierski and Hołyst (1988) apply it to derive the location of the transition nematic–smectic A under the supposition that it is second order.

4.3.5. Connection of various theories to the Parsons approach. Now that we have discussed several approximation paths in DFT, we would like to show a striking similarity with the Parsons expression (116) and (117) for the nematic free energy. By substituting the direct correlation function in the decoupling approximation (138) and a nematic density (157) in the general expression for the free energy (141) we get, after some manipulation,

$$\frac{F^{ex}[\rho(\boldsymbol{x})]}{NkT} = -\int d\Omega \int d\Omega' \int d\Omega_{\Delta r}\, \sigma^3(\Omega_{\Delta r},\Omega,\Omega') f(\Omega) f(\Omega') \cdot \times \rho \int_0^1 d\lambda \int_0^\lambda d\lambda' \int d \left|\frac{\boldsymbol{r}-\boldsymbol{r}'}{\sigma}\right| \left|\frac{\boldsymbol{r}-\boldsymbol{r}'}{\sigma}\right|^2 c_{PY}^{(2)}\left(\left|\frac{\boldsymbol{r}-\boldsymbol{r}'}{\sigma}\right|; \lambda'\phi\right). \tag{153}$$

From this equation we see that by scaling the interparticle distance with $\sigma(\Omega_{\Delta r}, \Omega, \Omega')$ the orientational and positional integrations are *decoupled* (hence the name decoupling approximation for equation (138)). It is easy to verify that

$$\int \mathrm{d}\Omega_{\Delta r}\, \sigma^3(\Omega_{\Delta r}, \Omega, \Omega') = 3v_{\mathrm{excl}}(\Omega, \Omega') \tag{154}$$

while the positional integration may be performed analytically, since $c^{(2)}_{\mathrm{PY}}(r)$ is known. This eventually leads to

$$\frac{F^{\mathrm{ex}}[\rho f(\Omega)]}{NkT} = \frac{\langle\!\langle v_{\mathrm{excl}}(\Omega, \Omega')\rangle\!\rangle}{8v_0}\left[\frac{3\phi - \frac{3}{2}\phi^2}{(1-\phi)^2} - \ln(1-\phi)\right] \tag{155}$$

where the factor in square brackets is the Percus–Yevick expression for the excess free energy of hard spheres obtained via the compressibility route (Hansen and McDonald 1986). Compared with the Parsons expression the only difference appears to be the PY compressibility free energy instead of the semi-empirical Carnahan–Starling free energy.

At this point it is good to mention that Parsons (1979) also used a decoupling approximation, although for the pair distribution function

$$g(\boldsymbol{r}) = g\left(\frac{r}{\sigma(\Omega_{\Delta r}, \Omega, \Omega')}\right). \tag{156}$$

By using the pressure (also called virial) equation (Hansen and McDonald 1986) this function may be related to the pressure and the free energy, ultimately giving (116) in combination with (117).

In the factorization expression (139) used by Colot *et al* (1988) the decoupling of orientational and positional integrations is even more obvious than for (138). This similarly leads to (155). As discussed in section 4.3.3 they chose a lower effective volume fraction in the nematic state.

The approach by Somoza and Tarazona (equation (152)) leads by construction to the Parsons expression for the excess free energy in the nematic state.

4.3.6. Parametrization of the density. Apart from the question of the direct correlation function in a non-uniform system, we must also know how to characterize the non-uniform state $\rho(\boldsymbol{x})$. We are looking for a state which gives the absolute minimum of the Helmholtz free energy, although we do not know beforehand which state we must expect. Therefore, in principle we should choose a parametrization of $\rho(\boldsymbol{x})$ which may describe all possible states; this means not only including all types of liquid crystals, plastic crystals or true crystals but also systems containing liquid–solid interfaces etc. It will be clear that this is too ambitious, so in practice in describing phase transitions only the free energy for a few selected bulk phases is considered. In that case, each bulk phase is parametrized separately and the minimum free energy for each of these phases are compared to find the stable phase. We must always bear in mind that we might overlook another phase which is not contained in our parametrization.

For a (uniaxial) nematic phase we may write

$$\rho(\boldsymbol{x}) = \rho_0 f(\theta) \tag{157}$$

with ρ_0 the uniform density and $f(\theta)$ the usual angular distribution function. For $f(\theta)$ several authors choose an expansion in Legendre polynomials like equation (40) or (41) or truncated versions like

$$f(\theta) = N \exp\{\alpha_2 P_2(\cos\theta)\} \tag{158}$$

or versions which may be reduced to the previously mentioned

$$\begin{aligned} f(\theta) &= N' \exp(\alpha_2' \cos^2\theta + \alpha_4' \cos^4\theta) \\ &= N \exp(\alpha_2 P_2(\cos\theta) + \alpha_4 P_4(\cos\theta)). \end{aligned} \tag{159}$$

Finally, Somoza and Tarazona (1988, 1989a) use a numerical method similar to (42).

For smectic phases of axially symmetric molecules Lipkin and Oxtoby (1983) introduce a distribution function in terms of a combined expansion in spherical harmonics for the angular variation and Fourier components for the spatial variation

$$\rho(\boldsymbol{x}) = \sum_{qlm} \mu_{qlm} Y_l^m(\Omega) \exp(\mathrm{i}\boldsymbol{k}_q \cdot \boldsymbol{r}). \tag{160}$$

Although these authors only give this formal expression, Kloczkowski and Stecki (1985) applied it to the smectic-A phase, where the spherical harmonics reduce to Legendre polynomials and there is only spatial variation in the direction $\theta = 0$. For the smectic-A phase Somoza and Tarazona (1990) again use a numerical solution method while assuming that the angular and spatial variations may be decoupled:

$$\rho(\boldsymbol{x}) = \rho(z, \theta) = \rho(z) f(\theta). \tag{161}$$

This implies a restriction in the sense that molecules at the centre of a smectic layer have the same angular distribution as those which happen to be situated between two layers.

4.3.7. Locating the phase transitions. Having obtained an (approximate) expression for the free energy in terms of one or more types of parametrized density, we now may locate the minimum of the free energy of these different phases by variation of their parameters. In general this is done for different values of the overall density ρ_0 of each phase, resulting in a free energy $\Delta F(\rho_0)$ for each phase. Subsequently, the coexistence relations for the (osmotic) pressure and the chemical potential (cf section 2.4.3) are used to determine possible transitions between the phases of interest. Care must be taken to accept only those transitions which guarantee the lowest overall free energy.

4.3.8. Results and discussion. At the end of this section on density functional theory we want to show some of the results obtained by this approach. To that purpose we have gathered some representative results in tables 9 and 10, which apart from the numerical values summarize the particular approximations which were employed to obtain these results. As a reference we have taken the MC calculations, since these

Table 9. Comparison of theoretical results for the isotropic–nematic phase transition of hard *ellipsoids* of elongation $a/b = 3$ via MC simulation, various forms of DFT and the Parsons approach.

Reference	Method	$(\rho v_0)_{iso}$	$(\rho v_0)_{nem}$	Pv_0/kT	S
Frenkel and Mulder (1985)	a	0.507	0.517	9.79	...
Singh and Singh (1986)	c,f,m	0.309	0.330	4	0.547
Singh and Singh (1986)	c,i,m	0.314	0.335	...	0.547
Colot *et al* (1988)	d,g,k	0.472	0.484	7.76	0.56
Marko (1989)	b,h,l	0.493	0.494	...	0.017
Perera *et al* (1988)	b,j,n	0.418	0.436	...	0.657
Hołyst and Poniewierski (1989a)	e,k	0.454	0.474	4.68	0.485
Singh *et al* (1989)	b,d,f,l	0.475	0.494	...	0.547
Lee 1988	o	0.508	0.517	10.00	0.533

(a) Monte Carlo simulation.
(b) Functional Taylor expansion (to second order).
(c) Functional Taylor expansion (with partial third order).
(d) Structural mapping: effective volume fraction in the nematic phase (unreliable results, see section 4.3.3).
(e) Weighted density approximation.
(f) Decoupling approximation with $c^{(2)}_{PY}$.
(g) Factorization approximation with $c^{(2)}_{PY}$.
(h) Decoupling approximation and a variational angular correction using $c^{(2)}_{PY}$.
(i) Decoupling approximation with $c^{(2)}_{WHB}$ (WHB: Waisman (1973), Henderson and Blum (1976)).
(j) $c^{(2)}_{HNC}$ via an expansion in rotational invariants.
(k) $\rho \simeq N \exp(\alpha_2 P_2(\cos\theta))$.
(l) $\rho \simeq N \exp(\alpha_2 P_2(\cos\theta) + \alpha_4 P_4(\cos\theta))$.
(m) $\rho \simeq N(a_2 P_2(\cos\theta) + a_4 P_4(\cos\theta))$.
(n) $\rho \simeq \sum_n a_{2n} P_{2n}(\cos\theta)$.
(o) Parsons approach.

Table 10. Comparison of theoretical results for the phase transitions of hard *spherocylinders* of $L/D = 5$ via Monte Carlo simulation, various forms of DFT and the Parsons approach (d is the distance between adjacent smectic layers).

Reference	Method	$(\rho v_0)_{iso}$	$(\rho v_0)_{nem}$	Pv_0/kT	S	
Frenkel *et al* (1988)	a	0.40		4.9	...	
Perera *et al* (1988)	b,j,n	0.325	0.338	...	0.635	
Hołyst and Poniewierski (1989a)	e,k	0.38	0.41	2.9	0.59	
Lee (1987)	o	0.400	0.418	5.36	0.667	
		$(\rho v_0)_{nem}$	$(\rho v_0)_{sm\text{-}A}$	Pv_0/kT	S	d/L
Frenkel *et al* (1988)	a	0.53		7.9	...	1.35
Poniewierski and Hołyst (1988)	e,p	0.53	0.53	...	0.88	1.40
Somoza and Tarazona (1990)	e	0.507	0.554	...	0.912/0.985	1.4

For explanation of the methods used see table 9 while (p) is the bifurcation analysis for nematic–smectic-A.

are at present a better touchstone than a direct comparison with experiments in which other (unknown) interactions may play a role.

As may be seen from table 9 for hard ellipsoids of length-to-breadth ratio 3 none of the DFTs provides perfect agreement with the MC simulations. The early version of Singh and Singh (1986) gives an isotropic–nematic transition at too small densities, Marko's version yields almost the right density but shows an extremely small density jump and order parameter (this raises some suspicion about his calculational procedure, since his theory is designed to provide a correction to the decoupling approximation which shows much more realistic values). A similar picture is given by the results for HSC of $L/D = 5$: a qualitative agreement is the best DFT can provide. Note that the only way the nematic–smectic-A transition has been attacked is in the second virial approximation (Kloczkowski and Stecki 1985), which does not give a transition, or via the weighted density approximation (Poniewierski and Hołyst 1988, Mederos and Sullivan 1989, Somoza and Tarazona 1990) which uses an *ad hoc* formulation of the free energy. Other results on more highly ordered liquid crystal phases using DFT have been obtained for the artificial system of parallel hard spherocylinders (Mulder 1987, Somoza and Tarazona 1988, 1989a, 1989b, Hołyst and Poniewierski 1989b, 1990) which we do not discuss here. For the isotropic–nematic transition we have also included in the tables Lee's calculations (Lee 1987, 1988) based on the Parsons approach, which gives better agreement than DFT. Note that the perfect agreement between Lee's results and MC data in table 9 is somewhat misleading: for $a/b = 2.75$ the agreement is less striking although still not bad.

As a conclusion we want to stress that—although DFT is an attractive theoretical framework for determining phase transitions—the actual application to hard-core liquid crystals involves such drastic suppositions and simplifications that its results are *ad hoc* and up to now lack predictive power.

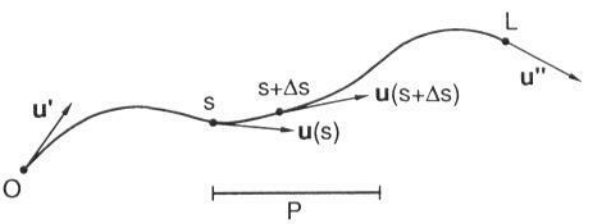

Figure 8. A typical configuration of a wormlike chain of length L and persistence length P. s measures the distance along the contour of the chain and $\boldsymbol{u}(s)$ is the direction vector of the chain at this point.

5. Virial theory of partially flexible polymers

5.1. The free energy for semiflexible chains

Up to now all particles considered were completely rigid. However, in reality most stiff polymers do possess at least some degree of flexibility, with which we may associate a certain configurational entropy. In the nematic phase, all polymers must be more or less parallel to the director, which leads to a considerable loss in configurational entropy. This entropy replaces the orientational entropy (11) for rods and was first derived by Khokhlov and Semenov (1981) as an extension of the Lifshitz theory (Lifshitz 1968, Lifshitz *et al* 1978) for flexible polymers to stiff polymers. The most

useful model of a stiff yet slightly flexible chain is the so-called wormlike chain model (e.g. see Yamakawa 1971) it is sometimes denoted as persistent chain or Kratky–Porod chain (Kratky and Porod 1949). This model presupposes a gradual change of direction of the chain, e.g. due to slight fluctuations in bond lengths or bond angles. The persistence length P is the characteristic length scale on which the direction vector $\boldsymbol{u}$ of the chain changes (see figure 8)

$$\langle \boldsymbol{u}(s) \cdot \boldsymbol{u}(s + \Delta s) \rangle = \langle \cos \theta(\Delta s) \rangle = \exp(-|\Delta s|/P) \tag{162}$$

where $\theta(\Delta s)$ denotes the angle between two direction vectors which are a distance Δs apart. The advantage of the wormlike chain is the fact that it is able to interpolate between a random-flight limit and a rod limit. For many stiff polymers without abrupt changes in direction (kinks) the wormlike chain is a good model, which was tested by several independent methods in dilute solutions (Yamakawa 1984). For so-called semiflexible chains (contour length $L \gg$ persistence length $P \gg$ diameter D), which are locally very stiff but which are so long that they form coils in dilute solution, we sketch the derivation of the configurational entropy in appendix B. The result (per chain) is

$$S_{\text{con}} = k\frac{L}{2P} \int f^{1/2}(\cos\theta) \Delta f^{1/2}(\cos\theta)\, \mathrm{d}\Omega \tag{163}$$

$f(\cos\theta)$ is the angular distribution function of the chain segments—for these long chains independent of the position of the segment on the chain. Δ is a shorthand notation for the two-dimensional $\Delta_{\boldsymbol{u}}$ of equation (203), simplified to

$$\Delta = \frac{\partial}{\partial \cos\theta}(1 - \cos^2\theta)\frac{\partial}{\partial \cos\theta} = \frac{1}{\sin\theta}\frac{\partial}{\partial\theta}\sin\theta\frac{\partial}{\partial\theta} \tag{164}$$

for a nematic phase. When we substitute an isotropic distribution like equation (10) we see that this is the zero point for S_{con}. An anisotropic distribution always leads to a lower entropy, which is seen most clearly by partial integration of equation (163)

$$S_{\text{con}} = -k\frac{L}{8P} \int \frac{1}{f}\left(\frac{\partial f}{\partial\theta}\right)^2 \mathrm{d}\Omega \leqslant 0. \tag{165}$$

Having obtained an expression for the entropy, we need to look into the interaction terms (Khokhlov and Semenov 1981). To obtain the second virial term consider the following. Take a solution of N rods of length L and number density ρ. Its second virial term has been calculated in equations (7), (12) and (22)

$$NB_2\rho = \frac{N^2L^2}{V} D \iint |\sin\gamma| f(\Omega) f(\Omega')\, \mathrm{d}\Omega\, \mathrm{d}\Omega'. \tag{166}$$

When we now divide each rod into L/l (sub)rods of length l, the number of rods increases but their length decreases by the same factor, keeping the combination NL constant (to avoid the influence of end effects we take $l \gg D$). Therefore, this system has the same second virial term as the original system. The conclusion which we can draw is that the second virial term is built up from independent, local, rodlike two-particle interactions. Because on a length scale l ($P \gg l \gg D$) a wormlike

chain is rodlike, two wormlike chains locally interact similarly as rods (configurations where a wormlike chain interacts simultaneously with two segments of another chain are scarce). Therefore equation (166) can also be used in the case of stiff wormlike chains. Correction terms to this expression and higher virial terms in the free energy have not been calculated yet because of the difficult configurational averages involved (most likely they are small in the limit $P \gg D$). There is a calculation by Yamakawa and Stockmayer (1972) for the second virial coefficient of a wormlike bead model. However—since their development does not lead to the right rod limit—it cannot be used to evaluate the correction terms in our case.

In summary, we now have an expression for the free energy of wormlike chains

$$\frac{\Delta F}{NkT} = \text{constant}' + \ln(\Lambda^3\rho) - \frac{L}{2P}\int f^{1/2}(\cos\theta)\Delta f^{1/2}(\cos\theta)\,\mathrm{d}\Omega + \rho L^2 D \iint |\sin\gamma| f(\cos\theta) f(\cos\theta')\,\mathrm{d}\Omega\,\mathrm{d}\Omega' \tag{167}$$

or given per persistence length unit

$$\frac{P\Delta F}{LNkT} = \text{constant} + \sigma_P[f] + c_P\rho[f]. \tag{168}$$

Here we neglected the ideal term $(P/L)\ln(\Lambda^3\rho)$ (we are dealing with very long connected chains, so the translational entropy per persistence length unit is small) and introduced

$$\sigma_P[f] \equiv -\frac{P}{kL}S_{\text{con}} = -\frac{1}{2}\int f^{1/2}(\cos\theta)\Delta f^{1/2}(\cos\theta)\,\mathrm{d}\Omega \tag{169}$$

and scaled concentration

$$c_P \equiv \frac{\pi}{4}PLD\rho = \frac{P}{D}\phi \tag{170}$$

while $\rho[f]$ is the same as in equation (28).

5.2. The isotropic–nematic transition for semiflexible chains

To obtain the phase transition from (168) we may employ similar methods as those described in section 2.4. Here we just summarize some important results.

If we use a Gaussian trial function (32) it is easy to evaluate the configurational entropy by the methods described in appendix A. We find for the entropy per chain (Odijk 1986a)

$$S_{\text{con}} = -\frac{kL}{P}\sigma_P(\alpha) \sim -\frac{kL}{P}\frac{\alpha}{4}. \tag{171}$$

Comparing this with the orientational entropy per rod of $-k\ln\alpha$ (equations (11) and (193)) we see that at the same degree of ordering a semiflexible chain loses much more entropy than a rod. First, because of the much stronger α dependence and second because each segment of the wormlike chain loses configurational entropy (hence the scaling with L) while a rigid particle only loses orientational entropy as

a whole. Minimization of free energy (168) in conjunction with equations (171) and (194) gives the c_P dependence of α

$$\alpha \sim \frac{4c_P^{2/3}}{\pi^{1/3}}. \tag{172}$$

The much weaker concentration dependence of α compared to that of rods (equation (35)) originates from the much stronger entropy loss for wormlike chains as discussed above.

To determine the phase transition we need the coexistence equations which are found similarly as in section 2.4.3

$$c_{P,i}^2 = c_{P,a}^2 \rho(\alpha) \tag{173}$$

$$2c_{P,i} = \sigma_P(\alpha) + 2c_{P,a}\rho(\alpha) \tag{174}$$

and are slightly simpler because of the neglect of the translational entropy $(P/L)\ln\rho$. We are now able to calculate the phase transition in the Gaussian approximation

$$c_{P,\mathrm{i}} = 7.77 \qquad c_{P,\mathrm{a}} = 9.71 \qquad \alpha = 12.34 \qquad S = 0.759. \tag{175}$$

Considering the low value of α we may only expect qualitative results from the asymptotic expansions of appendix A. The Onsager trial function gives a somewhat better result (Odijk 1986a)

$$c_{P,\mathrm{i}} = 5.409 \qquad c_{P,\mathrm{a}} = 6.197 \qquad \alpha = 6.502 \qquad S = 0.610. \tag{176}$$

Finally, we may also perform a formal minimization of ΔF along the lines of section 2.4. In this case, we obtain an integrodifferential equation

$$\Delta\phi_0(\cos\theta) = \left[\lambda + \frac{16c_P}{\pi}\int |\sin\gamma|\phi_0^2(\cos\theta')\,\mathrm{d}\Omega'\right]\phi_0(\cos\theta) \tag{177}$$

which is formulated in terms of the square root of the distribution function (see equation (208))

$$\phi_0(\cos\theta) = f^{1/2}(\cos\theta) \tag{178}$$

λ is the usual Lagrange multiplier which is determined by the normalization condition (209). If we compare equation (177) with the eigenvalue equation (204) we can identify the integral term as a kind of mean field originating from the surrounding polymers

$$U_{\mathrm{scf}}[\cos\theta] \equiv kT\frac{L}{P}\frac{8c_P}{\pi}\int |\sin\gamma(\Omega,\Omega')|\phi_0^2(\cos\theta')\,\mathrm{d}\Omega' \tag{179}$$

the self-consistent field per polymer of length L (this is actually the same self-consistent field as for rods, equation (38), taking into account definitions (26), (170) and (178)).

To solve this nonlinear integrodifferential equation an expansion of $\phi_0(\cos\theta)$ in Legendre polynomials is especially suitable (Vroege and Odijk 1988), since the Legendre polynomials are eigenfunctions of Δ

$$\Delta P_n(\cos\theta) = -n(n+1)P_n(\cos\theta). \tag{180}$$

Combined with the methods from section 2.4.2 this simplifies the calculations considerably, giving (Vroege and Odijk 1988)

$$c_{P,i} = 5.124 \qquad c_{P,a} = 5.509 \qquad S = 0.4617. \tag{181}$$

Finally, the bifurcation point of equation (177) is

$$c_P^* = 6. \tag{182}$$

5.3. Alternative methods and the deflection length

In his review Odijk (1986a) showed several other ways to arrive at equation (171) for the entropy of confined wormlike chains. We shall not try to surpass his exposition, but only elaborate on his scaling method involving the deflection length, because of the clear physical image it invokes. In the isotropic state the persistence length P is the length scale determining the angular correlations along the chain, which may be seen from equation (162) and figure 8. However, in the nematic state the surrounding polymers force the chain to remain within a certain angular range, dependent on the degree of order (see equation (192)), typically

$$\langle \theta^2 \rangle \sim 2/\alpha. \tag{183}$$

Consider a wormlike chain with $\boldsymbol{u}(s) \parallel \boldsymbol{n}$. For small Δs the chain is essentially free and behaves like (162). For these $\theta(\Delta s)$ values (162) may be expanded, giving

$$\langle \theta^2(\Delta s) \rangle \simeq 2|\Delta s|/P. \tag{184}$$

However, as soon as $\langle \theta^2(\Delta s) \rangle$ is near $\langle \theta^2 \rangle$ the chain undergoes the influence of neighbouring chains and is prevented from deviating much further from the director. The length scale λ where this happens is found by comparing equations (183) and (184)

$$\lambda \sim P/\alpha. \tag{185}$$

Because near this length the chain is, as it were, deflected back to the director, Odijk (1984) called it the deflection length λ. As the chain loses its angular correlations through these deflections, the relevant length scale is no longer the persistence length P but the much shorter deflection length λ (since $\alpha \gg 1$). For an illustration of this, see figure 9.

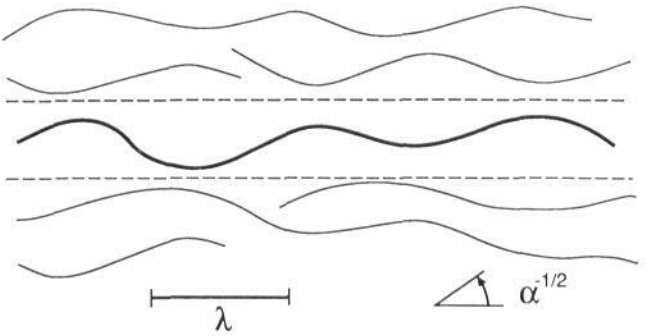

Figure 9. Each chain is confined by its neighbours to remain within an angle of about $\alpha^{-1/2}$ from the (horizontal) director. Therefore the typical length scale of fluctuations is given by deflection length λ (see text).

This observation opened the way to apply simple scaling arguments to different problems in liquid crystals formed by wormlike chains. For instance the configurational entropy is obtained by the fact that a very long chain forms a statistical mechanical system by itself. An extensive quantity like the free energy must therefore

scale like kT (the only available measure of energy) multiplied by the chain length L (as a measure of the system size) divided by the only other relevant length scale λ

$$S_{\text{con}} = \frac{F_{\text{con}}}{T} \sim -k\frac{L}{\lambda} \overset{(185)}{\sim} -k\frac{L}{P}\alpha. \tag{186}$$

Further examples of the scaling approach may be found in Odijk's work (1986a,c, 1988).

Another way to derive equation (171) is given by analysing the fluctuations of a nematically confined wormlike chain and applying the equipartition theorem to its Fourier components. This is analogous to the method of Helfrich (1978, Helfrich and Harbich 1985) for restricted fluctuating membranes. Finally, it is possible to reformulate the confinement of a wormlike chain in the nematic state in terms of a harmonic potential in θ, which enables the connection with the quantum harmonic oscillator and path integral methods to solve it. Note that some very recent papers (Selinger and Bruinsma 1991, Le Doussal and Nelson 1991) on liquid crystalline wormlike chains may be classified as extensions of the last two methods.

5.4. Intermediate chain lengths

In the above we considered two extreme cases, namely the rod limit ($P \gg L \gg D$) and the semiflexible limit ($L \gg P \gg D$). Essential points in the derivation were the two-particle interactions (described by a rodlike second virial term for the locally rodlike interactions) and expressions for the orientational/configurational entropy. In experimental situations we most often encounter an intermediate case where $L \simeq P \gg D$. The difficulty now lies in finding an appropriate formula for the entropy. Khokhlov and Semenov (1982) derived this by an analogous construction as in appendix B, i.e. applying an external field $U_{\text{ex}}(\boldsymbol{u})$, deriving a differential equation for Z, and using this to eliminate U_{ex} from the final expression for $S = (U - F)/T$. This formal expression for S_{con} is too complicated to be of direct use. Therefore, Khokhlov and Semenov calculated the correction terms to the rod limit and the semiflexible limit using Onsager's trial function (31):

$$\begin{aligned} S_{\text{con}} &= -k\left[\frac{L(\alpha-1)}{P} + \ln(\alpha/4) + \cdots\right] \qquad (\alpha L \gg P \text{ or } L \gg \lambda) \\ &= -k\left[\ln\alpha - 1 + \frac{L(\alpha-1)}{6P} + \cdots\right] \qquad (\alpha L \ll P \text{ or } L \ll \lambda). \end{aligned} \tag{187}$$

Note that S_{con} is the configurational entropy of the total system—although given per chain—and therefore reduces to S_{or} per rod in the rod limit. On the basis of these expressions for the entropy, correction terms for the phase transition concentrations can be determined. To acquire a formula valid for arbitrary L/P ratios Khokhlov and Semenov interpolated these results in the form of a Padé approximant. In table 11 we summarize their results (as corrected by Odijk (1986a)). Unfortunately, there is no theoretical justification of the form of the Padé approximant chosen and preliminary numerical calculations seem to indicate that there are some internal inconsistencies in this type of interpolation (Vroege 1991).

By applying the path integral formulation of the problem, Odijk (1986a) was able to derive an exact expression for the leading Gaussian behaviour of the conformational

Table 11. Phase transition concentrations (scaled according to equation (170)) and order parameter S, with $N_P \equiv L/P$ the number of persistence length units within each chain.

	Semiflexible	Rodlike	Padé approximant
$c_{P,i}$	$5.409 + 1.910 N_P^{-1}$	$3.340 N_P^{-1} + 4.99$	$\dfrac{3.34 + 5.97 N_P + 1.585 N_P^2}{N_P(1 + 0.293 N_P)}$
$c_{P,a}$	$6.197 + 1.781 N_P^{-1}$	$4.486 N_P^{-1} - 1.458$	$\dfrac{4.486 + 11.24 N_P + 17.54 N_P^2}{N_P(1 + 2.83 N_P)}$
S	$0.610 - 0.0948 N_P^{-1}$	$0.847 - 1.487 N_P$	$\dfrac{3.34 + 5.97 N_P + 1.585 N_P^2}{N_P(1 + 0.293 N_P)}$

entropy for arbitrary chain lengths. Here we quote his approximate expression which is easily manageable

$$\sigma_P(\alpha) \simeq \ln \alpha + N_P \frac{\alpha - 1}{6} + \frac{5}{12} \ln \left[\cosh \left(N_P \frac{\alpha - 1}{5} \right) \right] - \frac{19}{12} \ln 2. \tag{188}$$

Hentschke (1990) obtained an interpolating formula for the entropy between rod and semiflexible limit in the form of a similar Padé approximant as used in table 11 with virtually the same numerical results as equation (188).

In view of the experimental importance of the intermediate N_P regime, exact numerical results are badly needed.

5.5. Extensions

A first extension within the context of virial theory for semiflexible chains with purely steric interactions is the effect of charge. As discussed below equation (166), as a first approximation the second virial coefficient for stiff chains is equal to the one for rods, and this argument remains valid for charged polymers (at least when deflection length λ exceeds Debye length κ^{-1}). The case of very long semiflexible polyelectrolytes is described in Vroege (1989). In principle, for semiflexible polyelectrolytes the persistence length is larger than for their uncharged counterparts because of the electrostatic repulsion between adjacent charges on the chain (Odijk 1977, Skolnick and Fixman 1977). Since most of the polyelectrolytes showing liquid crystalline behaviour are intrinsically stiff the influence of the charge on the persistence length is generally negligible, although Odijk (1986a) speculates on the possibility of the formation of a nematic phase as a result of electrostatic stiffening of fully flexible polyelectrolytes without any added salt.

For further extension of these theories it is necessary to go beyond the second virial approximation. Unfortunately up to now all attempts have been purely heuristic in character. For the excess (i.e. interaction) part of the free energy a similar equality between rods and semiflexible chains has been postulated as exists for their second virial coefficients. There is no formal justification for this procedure and on top of that even the justification for the equality of the second virial coefficients vanishes for the more concentrated systems to be described. However—since at present there is no satisfactory alternative—we briefly summarize these attempts. Khokhlov and Semenov (1985) use their version of the Parsons approach equation (120) combined with their entropy expression (163) for long semiflexible chains. Moreover they try to include Van der Waals attraction by means of a concentration-dependent Maier–Saupe method

$$U_{\mathrm{VdW}} = -u_0 c - u_a c S P_2(\cos \theta) \tag{189}$$

with u_0 and u_a unspecified constants. Hentschke (1990) started from the Parsons expression (116/117) combined with an interpolation formula for the configurational entropy (see the preceding section). DuPré and Yang (1991) did the same with a slightly modificated version of equation (188). Finally, Sato and Teramoto (1990) combined equations (187) with scaled particle expression (111)–(113).

Another important extension, the effect of polydispersity on the phase transition, has not been treated yet. As may be seen from equations (168)–(170) for very long semiflexible chains the free energy per persistence length is independent of the length L of the polymers. This implies that in this case we expect the phase transition to be independent of polydispersity. However—since there is a strong polydispersity effect for rods (see section 2.5)—it is intriguing to know its influence on the experimentally important case of $L \simeq P$.

6. Comparison with experiments

Lyotropic liquid crystals occur in a wide variety of dispersions of rodlike colloidal particles and solutions of stiff macromolecules. The first examples of these phases were already reported as early as the 1920s for dispersions of inorganic colloids. Colloidal and macromolecular systems giving rise to these phases can be purely synthetic or may be obtained from biological sources. As far as colloidal systems are concerned we mention:

(i) inorganic colloidal particles, e.g. V_2O_5 (Zocher 1925), β-FeOOH (Zocher 1925, Zocher and Heller 1930, Maeda and Hachisu 1983), γ-AlOOH (Zocher and Török 1960, 1962, Bugosh 1961);

(ii) organic microcrystals, e.g. poly(tetrafluoroethylene) 'whiskers' (Folda *et al* 1988), cellulose microcrystals (Marchessault *et al* 1959);

(iii) stiff viruses, e.g. tobacco mosaic virus (TMV) (Bawden *et al* 1936, Bawden and Pirie 1937, Bernal and Fankuchen 1941, Oster 1950, Kreibig and Wetter 1980, Fraden *et al* 1985), fd-virus (Lapointe and Marvin 1973, Maret and Dransfeld 1985, Booy and Fowler 1985);

(iv) rodlike micelles of amphiphiles (Lawson and Flaut 1967, Radley and Reeves 1975, Yu and Saupe 1980, Hendrikx and Charvolin 1981, Boden *et al* 1986);

(v) rodlike aggregates of globular proteins, e.g. sickle cell haemoglobin (Allison 1957).

Stiff polymers that are known to form lyotropic liquid crystals include:

(i) helicoidal polypeptides, e.g. poly(γ-benzyl glutamate) (PBG) (Robinson 1956, Robinson *et al* 1958, Wee and Miller 1971, Miller *et al* 1974, Russo and Miller 1983, Kubo and Ogino 1979, Kubo 1981);

(ii) aromatic polyamides, e.g. poly(1,4-phenylene terephthalamide) (PPTA) (Morgan 1977, Kwolek *et al* 1977, Bair *et al* 1977, Panar and Beste 1988, Northolt and Sikkema 1990);

(iii) polyisocyanates, e.g. poly(n-hexyl isocyanate) (PHIC) (Conio *et al* 1984, Itou and Teramoto 1988);

(iv) polysaccharides, e.g. schizophyllan (Van and Teramoto 1982, Itou and Teramoto 1984a, 1984b, Kojima *et al* 1987), xanthan (Maret *et al* 1981, Milas and Rinaudo 1983, Sato *et al* 1990);

(v) cellulose derivatives, e.g. hydroxypropyl cellulose (Werbowyj and Gray 1976, 1980);

(vi) DNA (Senechal *et al* 1980, Brian *et al* 1981, Trohalaki *et al* 1984, Rill *et al* 1983, Rill 1986, Strzelecka and Rill 1987, 1990, Strzelecka *et al* 1988, Livolant *et al* 1989); and

(vii) imogolite (Kajiwara *et al* 1986a,b).

In the discussion we will focus on experimental results for systems with a well defined size or molecular weight distribution and known molecular or particle parameters such as length, diameter and persistence length. Only for such systems can a meaningful comparison of experimental and theoretical results be made. The liquid crystal transition in a number of systems we will discuss later is in fact an isotropic–cholesteric transition. Assuming that the chiral part of the interparticle interaction that gives rise to a cholesteric rather than a nematic liquid crystal phase represents only a weak perturbation we will interpret the coexisting concentrations with theories that in fact refer to the isotropic–nematic transition.

6.1. Rigid rodlike particles

Probably the best examples of rodlike particles are virus particles such as the tobacco mosaic virus (TMV) and fd-virus. TMV is a cylindrical particle consisting of a rigid protein shell enclosing double stranded RNA, while the cylindrical fd-virus particle consists of a rigid protein shell wound around a single ribbon of single stranded DNA. In table 12 we summarize the particle parameters of TMV and fd in as far as they are relevant for the discussion of the liquid crystal phase transitions that occur in aqueous dispersions of these particles.

Table 12. Particle parameters for the TMV and fd-virus.

Virus particle	M	L (nm)	D (nm)	L/D	Linear charge density (e nm^{-1})
TMV	4×10^7	300	18	17	-1 to -2
fd-virus	16.4×10^6	880	6	147	-5

Note: The linear charge density depends on pH. The values quoted here refer to near neutral pH.

As early as 1939 Best studied the phase diagram of TMV as function of added salt. Without added salt there was coexistence between an isotropic phase of 15 mg ml^{-1} and a nematic phase of 23 mg ml^{-1}. As the ionic strength increased the concentrations of virus in the coexisting phases increased but the ratio of the concentrations remained constant. Recently Fraden *et al* (1989) measured the coexisting isotropic and nematic phases over a wide range of ionic strength (see figure 10). The theoretical results obtained with the Onsager theory including the effect of screened Coulomb interactions (see section 2.6) lie considerably above the experimental values. This is not surprising as the hard-rod dimensions of TMV give a ratio $L/D \simeq 17$, which is certainly not large enough for the Onsager approach to be quantitatively valid (note that the ratio L/D_{eff} is even less). Fraden *et al* showed that replacing the electrostatic potential between TMV particles by a hard-rod interaction with an appropriate effective diameter and subsequently using this effective diameter (and of course the corresponding effective volume fraction) in the Parsons approach (see section 3.3.4)

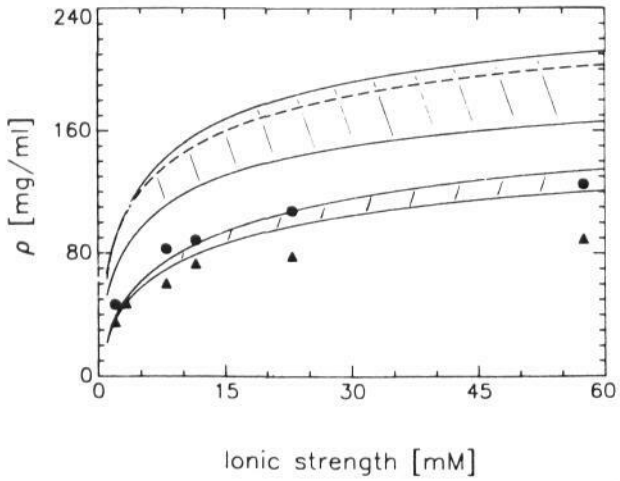

Figure 10. The concentrations of coexisting isotropic (▲) and nematic (●) phases of TMV at pH = 8.0 plotted as a function of ionic strength. The calculated coexistence region is plotted for the second virial theory (negative-sloping hatching, see section 2.6) and the Parsons(–Lee) theory with an effective diameter (positive-sloping hatching, see section 3.3.4) (reproduced with permission from Fraden *et al* (1989)).

gives a reasonably good description of their experimentally observed phase boundaries. The ratio of the coexisting concentrations predicted this way is however much smaller than the experimental value. This indicates that there is clearly a need for a theory that takes into account the effect of electrostatic interactions on third and higher virial terms.

Contrary to the case for TMV the second virial approximation is expected to work well for the fd-virus as the L/D ratio for this slender virus is sufficiently high. The (cholesteric) liquid crystal phase as seen by the onset of optical anisotropy (Maret and Dransfeld 1985) appears in aqueous solution of ionic strength 0.01 M above a critical concentration of 11 mg ml^{-1}. Assuming fd to be highly charged we have $D_{eff} = 20$ nm and $h \simeq 0.15$ letting the specific volume of the virus having a reasonable value of 0.6 ml g^{-1}. Figure 4 predicts the onset of liquid crystal formation at 12 mg ml^{-1} compared with 11 mg ml^{-1} experimentally (Maret and Dransfeld 1985).

In addition to nematic (cholesteric) liquid crystal phases there is clear evidence for layerlike ordering in systems of monodisperse rigid rodlike particles at sufficiently high concentration. In 1950 Oster reported for the first time indications for layerlike ordering in dispersions of TMV. He noted that from the bottom layer of the cholesteric phase of a salt free TMV dispersion an 'iridescent' gel formed. Oster interpreted the iridescence as being due to Bragg diffraction of white light from a structure with a periodicity of the order of optical wavelengths. He determined the distance of the reflecting planes composing the iridescent structure to be 340 nm. Since TMV is 300 nm long this points to a structure formed of layers of TMV oriented perpendicular to the scattering planes. This still leaves open several possible structures, like a smectic-A phase (long-range order perpendicular to the layers but no order within the layers), a smectic-B phase (long-range order perpendicular to the layers and within the layers but no registry of the ordering between the layers) and finally a true crystal phase with long-range order in three dimensions.

Kreibig and Wetter (1980) systematically investigated the iridescent gel for a

number of different TMVs with optical diffraction and found good agreement with the results obtained by Oster (1950). Using x-ray measurements Fraden *et al* (1982) showed that the iridescent phase of TMV in pure water (no salt) is either colloidal crystalline or smectic-B. More recently, Wen *et al* (1989) using a combination of optical and x-ray diffraction demonstrated that under conditions of high salt a smectic-A phase was formed. At higher volume fractions coexistence between a crystalline and smectic-A phase was observed.

6.2. Semiflexible polymers

6.2.1. Neutral semiflexible polymers: monodisperse systems. There are few neutral semiflexible polymers that have sufficiently good solubility such that concentrated solutions may be studied without added complications such as aggregation, gelation and crystallization. Systems that have been studied extensively using fairly monodisperse samples are:

(i) poly(γ-benzyl L-glutamate) (PBLG) in dimethylformamide (DMF) (Wee and Miller 1971, Miller *et al* 1974, Russo and Miller 1983, Kubo and Ogino 1979, Kubo 1981);

(ii) poly(n-hexyl isocyanate) (PHIC) in toluene and dichloromethane (DCM) (Conio *et al* 1984, Itou and Teramoto 1988); and

(iii) schizophyllan in water (Van and Teramoto 1982, Itou and Teramoto 1984a, 1984b, Kojima *et al* 1987).

In table 13 we indicate the range of molecular weights investigated and the relevant parameters that determine the phase behaviour (L, D and P). In figures 11 and 12 we compare the measured isotropic–nematic (cholesteric) coexistence concentrations with the values calculated with the theoretical expressions given in table 11. Clearly the overall agreement between theory and experiment is quite satisfactory.

Table 13. Systems of neutral semiflexible polymers and their molecular parameters.

System	$M \times 10^{-3}$	L (nm)	D (nm)	P (nm)	L/D	L/P
PBLG/DMF	23.8–570	16–390	1.6	80	10–250	0.2–5
PHIC/Toluene	11.4–524	15–708	1.25	40	12–560	0.4–18
PHIC/DCM	11.4–524	15–708	1.25	20	12–560	0.8–36
Schizophyllan/ water	105-478	49–223	1.7	200	30–130	0.25-1.1

Note: There is a considerable variation in the literature for the values quoted for P and D. The values given above may be considered as representative.

The heuristic extensions of the theory to go beyond the second virial approximation mentioned in section 5.5 (Hentschke 1990, Sato and Teramoto 1990, DuPré and Yang 1991) have been used to further analyse the data. Although improved agreement between theory and experiment has been claimed, it is hard to assess the significance of this improvement as the values of D and to a lesser extent P have frequently been used as parameters to improve the fit.

For temperatures below 20 °C the system PBLG/DMF can no longer be considered to be athermal. In order to explain the phase behaviour the attraction between PBLG chains must be taken into account. Using a (generalized) Van der Waals approach

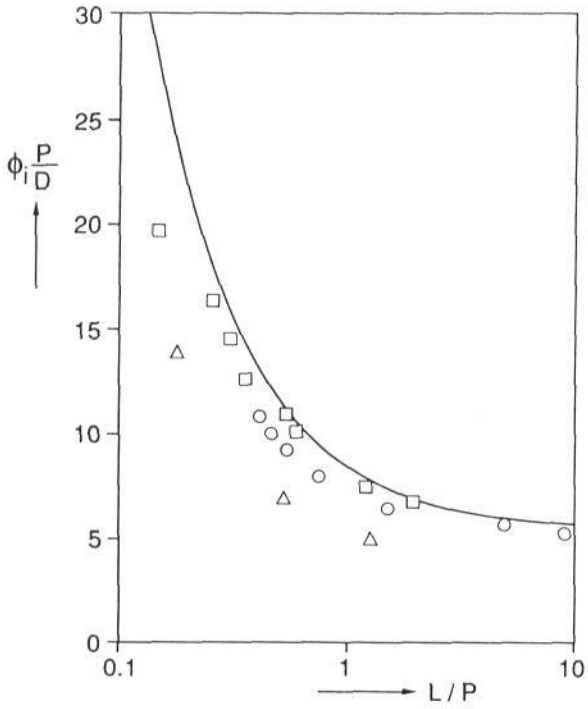

Figure 11. Scaled isotropic volume fraction at the phase transition ($\phi_i P/D = c_{P,i}$—see equation (170)) plotted against L/P: experimental results for PBLG/DMF, (Δ); PHIC/toluene, (○); schizophyllan/water, (□); drawn line, theoretical result according to table 11.

Khokhlov and Semenov (1985) showed that for semiflexible chains with $L/D \gtrsim 125$ there exists a temperature region where two nematic phases coexist. Russo and Miller (1983) carefully verified the equilibrium coexistence of two anisotropic phases using PBLG ($M = 310\,000$, $L/D = 133$) in DMF. Semenov and Khokhlov (1988) compared the experimental results of Russo and Miller with their theory and found reasonable agreement. Recently, there have been reports that systems of PBLG form hexagonal columnar liquid crystals at higher concentrations (Livolant and Bouligand 1986, Lee and Meyer 1990).

Table 14. Bidisperse systems and their phase behaviour. I denotes an isotropic and A an anisotropic phase, double or triple letters represent bi- or triphasic equilibria.

System	M_1 $\times 10^{-3}$	M_2 $\times 10^{-3}$	M_1/M_2	Phase behaviour				
				I	IA	IAA	AA	A
PBLG/benzylalcohol	347	99	3.5	+	+	−	−	+
PHIC/toluene	244	68	3.6	+	+	−	−	+
PHIC/toluene	244	20.9	11.7	+	+	−	−	+
Schizophyllan/water	800	132	6.1	+	+	−	−	+
Schizophyllan/water	800	65.8	12.2	+	+	+	+	+

6.2.2. Neutral semiflexible polymers: bidisperse systems. Bidisperse systems have also been studied for the stiff polymers mentioned above with molecular weight ratios

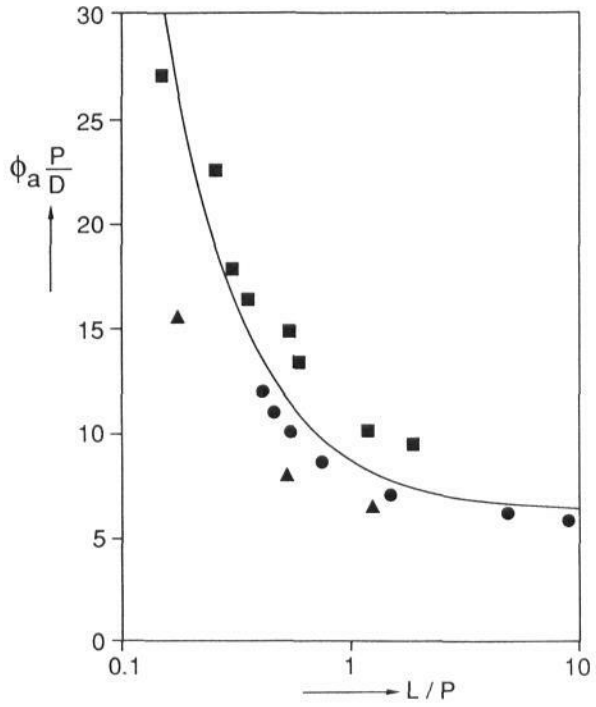

Figure 12. As in figure 11: scaled nematic (cholesteric) volume fraction at the phase transition.

(length ratios) varying from 3 to 12. The systems studied and the observed phase behaviour are summarized in table 14. The data for PHIC/toluene and schizophyllan/water have been analysed (Sato *et al* 1989) using the extension of the Khokhlov–Semenov theory to bidisperse systems worked out by Odijk (1986a). The agreement between theory and experiment is not as good as in the monodisperse case: the theory predicts systematically higher values for the biphasic region than are experimentally observed. This discrepancy can be at least partially traced to the use of the Gaussian approximation. For the stiff polymer schizophyllan at a molecular weight ratio of 12, there is a three-phase region (IAA) in which an isotropic phase coexists with two anisotropic (cholesteric) phases as well as a biphasic region where two anisotropic phases coexist (AA), see figure 13. Such phase behaviour was first predicted by Abe and Flory (1978) on the basis of a lattice model for rigid rods and subsequently by Birshtein *et al* (1988) using the virial approach. At this moment it is not entirely clear if this behaviour may also be expected for wormlike chains.

6.2.3. Semiflexible polyelectrolytes. Polyelectrolytes show good solubility in water. These systems can therefore be studied over an extensive concentration range. Again the limitation is that for a meaningful comparison with theory the systems must be monodisperse and—in addition to the usual parameters L, D and P—the (linear) charge density ν of the polyelectrolyte and the salt concentration in water must be known. Semiflexible polyelectrolytes that have been studied using fairly monodisperse samples are:

(i) xanthan in water (Sato *et al* 1990, Teramoto 1990); and

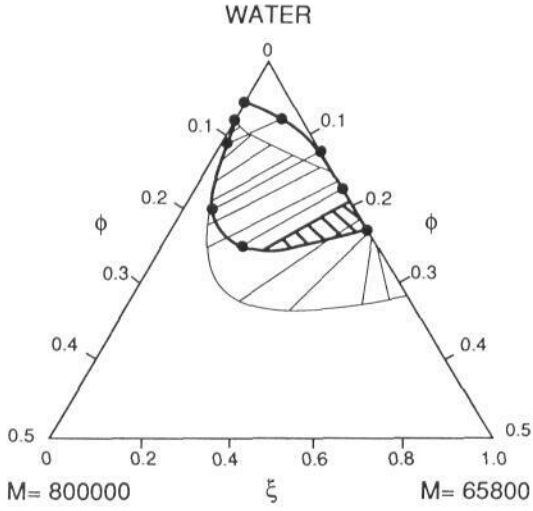

Figure 13. Ternary phase diagram for the system schizophyllan (M = 800 000)/ schizophyllan (M = 65 800)/ water: bold curves, experimental regions of phase separation (triphasic region indicated by negative-sloping hatching); thin curves, theory according to Odijk (1986a) (after Sato *et al* (1989)).

(ii) DNA (fragments) in water (Brian *et al* 1981, Rill *et al* 1983, Rill 1986, Strzelecka and Rill 1987, 1990, Strzelecka *et al* 1988, Livolant *et al* 1989).

In table 15 we indicate the range in molecular weight investigated and the relevant molecular parameters.

Table 15. Molecular parameters of semiflexible polyelectrolytes.

System	$M \times 10^{-3}$	L (nm)	D (nm)	P (nm)	ν (e nm^{-1})
Xanthan/water	106–980	55–500	2.2	120	−3
DNA/water	97–288	50–150	2.4	50	−6

The experimental data on xanthan for a sample with molecular weight 614 000 (L = 316 nm, L/P = 2.6) in salt solutions with concentrations varying from 0.005–1 M have been analysed by Sato *et al* (1990) using the theory of Stroobants *et al* (1986a) discussed in section 2.6, though modified to wormlike chains. As the salt concentration increases, c_i and c_a increase sigmoidally approaching values comparable to those for neutral stiff polymer solutions (see figure 14). The agreement between theory and experiment is almost quantitative. Livolant and Bouligand (1986) also report a columnar liquid crystalline phase for xanthan.

As far as DNA is concerned, the most extensive data available are those of 146 base pair DNA fragments (L = 50 nm) obtained by Rill and coworkers. For 0.21 M NaCl and 20 °C c_i = 125 mg ml^{-1} and c_a = 155 mg ml^{-1} (Strzelecka and Rill 1987) and for 2 M NaCl and 25 °C c_i = 175 mg ml^{-1} and c_a = 210 mg ml^{-1} (Rill 1986). However for low salt concentrations (0.01 M) the phase behaviour of DNA solutions is considerably more complicated. Strzelecka and Rill (1990) found that decreasing the electrolyte concentration only slightly lowers the DNA concentration at which an anisotropic phase appears for the first time, but significantly increases the

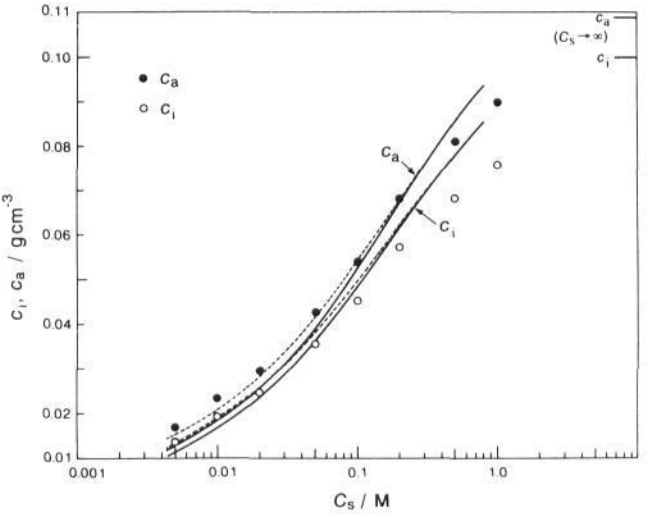

Figure 14. Comparison of experimental and theoretical data on the isotropic–nematic phase separation for xanthan/water as a function of salt concentration: full curves, theoretical expression as described in the text (κ^{-1} calculated at infinite dilution); broken curves, idem with corrected Debye length due to finite concentration (reproduced with permission from Sato *et al* (1990)).

concentration range of coexistence of the isotropic phase with anisotropic phases and even results in the formation of triphasic solutions. Increasing the DNA concentration from 100 to 290 mg ml^{-1} one can distinguish five regions: I, isotropic; II, biphasic (isotropic + precholesteric); III, triphasic (isotropic + precholesteric + cholesteric); IV, triphasic (isotropic + cholesteric + higher order phase); V, fully anisotropic (probably a mixture of cholesteric + higher order phases).

Even the nature of some of the phases involved, such as the precholesteric and the higher order phase, is not entirely clear. The precholesteric phase is weakly birefringent and has a texture intermediate between those of a nematic and a true cholesteric. The nature of the higher order phase is still under active debate. Rill and coworkers (Strzelecka *et al* 1988) describe it as a phase that is two-dimensionally ordered and resembles smectic phases of thermotropic liquid crystals observed with small molecules. On the other hand Livolant *et al* (1989) on the basis of polarizing microscopy, electron microscopy and x-ray diffraction rule out the smectic hypothesis and argue that the highly concentrated liquid crystalline phase of DNA is characterized by a columnar longitudinal order and a hexagonal lateral order with intermolecular distances ranging from 2.8 to 4.0 nm depending on the DNA concentration.

The foregoing shows that polyelectrolytes at low added salt concentrations are still a mysterious subject!

7. Concluding remarks

Looking back upon the preceding sections we may conclude that there are a considerable number of experiments which can be described semi-quantitatively with the Onsager theory and its extensions. Although after nearly 50 years Onsager's explanation of the formation of a nematic phase—a decrease in excluded volume compensating a loss of orientational entropy—remains unassailed, its extension by

Khokhlov and Semenov to semiflexible chains by inclusion of the configurational entropy has considerably widened the range of the theory in terms of applicability to experiments. As we have seen, extensions to higher volume fractions have been given though at the expense of theoretical rigour. In recent years computer simulations have shown that the excluded volume argument of Onsager gives rise to rich phase diagrams for hard particles including more highly ordered liquid crystalline phases, some of which have now also been observed in lyotropic systems.

One important aspect, which in our opinion has not been included in the theoretical framework in a very satisfactory way, is the effect of attractive interaction between particles. At present it remains difficult to predict for which experimental systems attraction plays an important role. Some other theoretical points which require further attention are:

(i) an extension of the theory for charged particles beyond the second virial approximation;
(ii) a more precise (numerical?) expression for the configurational entropy for semiflexible particles of chain length comparable to the persistence length;
(iii) a more convincing way to extend the second virial theory of semiflexible chains to higher volume fractions; and
(iv) a more extensive analysis of bi- and tri-phasic equilibria involving two nematic (cholesteric) phases both for neutral and charged systems.

Apart from these questions concerning nematic phases, more highly ordered phases also offer challenges. For rigid systems the trend was set by computer simulations followed by density functional theory—although not entirely convincingly yet. Therefore further simulations would be welcome, especially for

(i) systems with an additional soft interaction like electrostatic repulsion;
(ii) bidisperse systems; and
(iii) semiflexible systems.

On the experimental side there is need for several more model systems to test the theories, these include:

(i) uncharged rods of different axial ratios, since the well-characterized rodlike model systems available thus far show the additional complication of being charged; and
(ii) charged wormlike polymers of different linear charge densities.

Clearly, a lot of work has to be done before the rich but complicated phase behaviour of DNA given in section 6.2.3 will be completely understood.

Acknowledgments

This work was supported by the Stichting voor Fundamenteel Onderzoek der Materie (Foundation for Fundamental Research on Matter) which is part of the Nederlandse Organisatie voor Wetenschappelijk Onderzoek (Netherlands Organization for the Advancement of Research). We thank Paul van der Schoot for critically reading the manuscript.

Appendix A. Gaussian distribution functions

For large α Gaussian distribution function (32) is sharply peaked, which offers the opportunity to make an *asymptotic expansion* of the integrals concerned. This amounts to assuming that all other functions in the integrand are slowly varying within the peak of f_G and may be approximated by Taylor expansions. Thus the normalization condition (9) yields

$$\begin{aligned} 1 &= \int_0^{2\pi}\int_0^{\pi} f_G(\theta)\sin\theta\,d\theta\,d\varphi \\ &= 2\times 2\pi\int_0^{\pi/2} N\exp\left(-\tfrac{1}{2}\alpha\theta^2\right)\sin\theta\,d\theta \\ &\sim 4\pi N\int_0^{\infty}\exp\left(-\tfrac{1}{2}\alpha\theta^2\right)\left[\theta-\tfrac{1}{6}\theta^3+\cdots\right]d\theta \\ &\sim \frac{4\pi N}{\alpha}\left(1-\frac{1}{3\alpha}+\cdots\right). \end{aligned} \tag{190}$$

Note that the integration may be extended to ∞ because the Gaussian function is extremely small in that region (correction terms are $\mathcal{O}(e^{-\alpha})$). So we find the following expression for N

$$N\sim\frac{\alpha}{4\pi}\left(1+\frac{1}{3\alpha}+\cdots\right). \tag{191}$$

Similarly, we may determine the average value for θ^2

$$\langle\theta^2\rangle\equiv\int f_G(\theta)\theta^2\,d\Omega\sim\frac{2}{\alpha}. \tag{192}$$

These expressions are helpful in determining the orientational entropy term (see equation (11))

$$\sigma[f_G]=\sigma(\alpha)=\langle\ln(4\pi N)\rangle-\tfrac{1}{2}\alpha\langle\theta^2\rangle\sim\ln\alpha-1. \tag{193}$$

On the contrary, the average of $|\sin\gamma|$ is more difficult since it involves the distribution functions of both rods concerned. However, its dependence on α is simply guessed: for sharply peaked distributions $\sin\gamma\simeq\gamma$ and γ (angle between the two rods) will be of the same order of magnitude as θ (angle of a single rod with the director). This means we find a similar α dependence as of the square root of equation (192). It is also possible to determine the coefficient in front of it, whence

$$\rho[f_G]=\rho(\alpha)=\frac{4}{\pi}\iint|\sin\gamma|f_G(\Omega)f_G(\Omega')\,d\Omega\,d\Omega'\sim\frac{4}{\sqrt{\pi\alpha}}. \tag{194}$$

Appendix B. Configurational entropy of wormlike chains

The most useful model for stiff polymers which Khokhlov and Semenov (1981, 1982) considered is the so called *wormlike chain*, which may be described as a limiting case of the *freely rotating chain*. A freely rotating chain consists of N segments of fixed length a which may rotate freely with respect to each other as long as the consecutive segments retain a fixed bond angle θ. The wormlike chain is obtained by taking the so called worm limit

$$\lim_{\text{worm}} = \lim_{N\to\infty} \lim_{a\to 0} \lim_{\theta\to 0} \tag{195}$$

such that

$$\lim_{\text{worm}} Na = L \tag{196}$$

gives the contour length of the polymer while the ratio

$$\lim_{\text{worm}} \frac{a}{\cos\theta - 1} = \lim_{\text{worm}} \frac{2a}{\theta^2} \equiv P \tag{197}$$

defines the *persistence length* P (Yamakawa 1971). From this definition (197) we see that P is the typical length over which the chain changes its direction appreciably and therefore indicates the stiffness of the chain. Because of the continuous nature of the wormlike chain its direction changes gradually, whence it is a good model for stiff polymers which bend through small fluctuations in its valency angles and bond lengths.

We will now briefly sketch the derivation by Khokhlov and Semenov (1981) of the configurational entropy of the wormlike chain. As a first step, we need to go from the recursion relation of the configurational partition function Z of a freely rotating chain in an external field to a differential equation for Z of the wormlike chain. For long chains, Z may then be approximated by the method of the dominant eigenvalue for this differential equation. Finally, the entropy S is obtained by comparing the free energy F and the internal energy U of the system. The final expression for S does not depend on the applied external field (which therefore only serves as an intermediary).

Let us consider a freely rotating chain in an external orientational field $U_{ex}(\boldsymbol{u})$ (this is the potential energy per unit chain length when its direction is given by unit vector $\boldsymbol{u}$). We now start from an expression for $Z(\boldsymbol{u}', \boldsymbol{u}''; 0, N)$ which is the configurational partition function for a chain with fixed starting direction ($\boldsymbol{u}'$ at segment no 0) and fixed ending direction ($\boldsymbol{u}''$ at segment no N)

$$Z(\boldsymbol{u}', \boldsymbol{u}''; 0, N) = \int \prod_{j=0}^{N} \mathrm{d}\boldsymbol{u}_j \, g(\boldsymbol{u}_j, \boldsymbol{u}_{j+1}) \times \exp[-aU_{ex}(\boldsymbol{u}_j)/kT]\delta(\boldsymbol{u}_0 - \boldsymbol{u}')\delta(\boldsymbol{u}_N - \boldsymbol{u}'') \tag{198}$$

where the external potential energy of each segment appears explicitly in a Boltzmann factor and a (normalized) bond probability $g(\boldsymbol{u}_j, \boldsymbol{u}_{j+1})$ ensures the connectivity of the chain according to the freely rotating model. The delta functions fix both end

directions of the chain. When we extend this chain by one segment it is simple to verify the following recursion relation

$$Z(\boldsymbol{u}', \boldsymbol{u}; 0, N+1) = \exp[-aU_{\text{ex}}(\boldsymbol{u})/kT]\langle Z(\boldsymbol{u}', \boldsymbol{u}''; 0, N)\rangle$$
$$= \exp[-aU_{\text{ex}}(\boldsymbol{u})/kT] \int g(\boldsymbol{u}, \boldsymbol{u}'') Z(\boldsymbol{u}', \boldsymbol{u}''; 0, N)\, \mathrm{d}\boldsymbol{u}''. \tag{199}$$

Because in the worm limit the adding of one segment involves only an infinitesimally small change, we may Taylor expand all functions

$$Z(\boldsymbol{u}', \boldsymbol{u}; 0, N+1) = Z(\boldsymbol{u}', \boldsymbol{u}; 0, N) + \frac{\partial Z(\boldsymbol{u}', \boldsymbol{u}; 0, N)}{\partial N}$$

$$\langle Z(\boldsymbol{u}', \boldsymbol{u}''; 0, N)\rangle = Z(\boldsymbol{u}', \boldsymbol{u}; 0, N) + \langle \delta \boldsymbol{u}\rangle \cdot \frac{\partial}{\partial \boldsymbol{u}} Z(\boldsymbol{u}', \boldsymbol{u}; 0, N)$$
$$+ \frac{1}{2}\langle \delta \boldsymbol{u} \delta \boldsymbol{u}\rangle : \frac{\partial}{\partial \boldsymbol{u}} \frac{\partial}{\partial \boldsymbol{u}} Z(\boldsymbol{u}', \boldsymbol{u}; 0, N)$$

$$\exp[-aU_{\text{ex}}(\boldsymbol{u})/kT] = 1 - aU_{\text{ex}}(\boldsymbol{u})/kT \tag{200}$$

where $\langle \delta \boldsymbol{u}\rangle \equiv \langle \boldsymbol{u}'' - \boldsymbol{u}\rangle$ and $\langle \delta \boldsymbol{u} \delta \boldsymbol{u}\rangle$ are easily evaluated from properties of the wormlike chain (see figure 15).

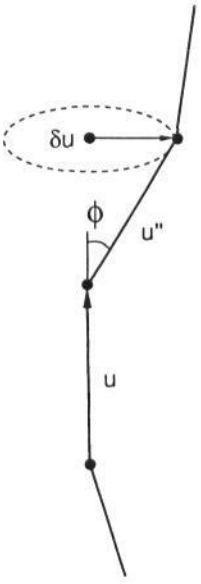

Figure 15. Two consecutive segments of the freely rotating chain. $\langle \delta \boldsymbol{u}\rangle \equiv \langle \boldsymbol{u}'' - \boldsymbol{u}\rangle = 0$ because of the freely rotating character; $\langle \delta u_x^2\rangle = \langle \delta u_y^2\rangle = \frac{1}{2}\langle \delta \boldsymbol{u}^2\rangle \simeq \frac{1}{2}\theta^{2\,(197)} \simeq a/P$ and $\langle \delta u_x \delta u_y\rangle = \langle \delta u_x\rangle\langle \delta u_y\rangle = 0$ in the worm limit, so $\langle \delta \boldsymbol{u} \delta \boldsymbol{u}\rangle = (a/P)\boldsymbol{I}$.

Combining (200) with (199) and (196) gives a differential equation for $Z(\boldsymbol{u}', \boldsymbol{u}; 0, L)$ (in the worm limit we use the contour length L as a variable instead of N)

$$\frac{\partial Z}{\partial L} = \frac{1}{2P}\Delta_{\boldsymbol{u}} Z - \frac{U_{\text{ex}}(\boldsymbol{u})}{kT} Z \tag{201}$$

with the natural boundary condition

$$\lim_{L\to 0} Z(\boldsymbol{u}', \boldsymbol{u}; 0, L) = \delta(\boldsymbol{u}' - \boldsymbol{u}). \tag{202}$$

Equation (201) is actually a diffusion equation (with L in the role of time) which describes the diffusive behaviour of the chain direction if we are following the chain. Because only the direction varies, this diffusion takes place on a unit sphere and the Laplacian $\Delta_{\boldsymbol{u}}$ is therefore restricted to this unit sphere

$$\Delta_{\boldsymbol{u}} = \frac{\partial^2}{\partial \boldsymbol{u}^2} = \frac{\partial}{\partial \cos\theta}(1 - \cos^2\theta)\frac{\partial}{\partial \cos\theta} + \left\{\frac{1}{\sin^2\theta}\frac{\partial^2}{\partial \varphi^2}\right\}. \tag{203}$$

In the case of a (uniaxial) nematic the azimuthal variation (within braces) is zero.

A possible way to solve equations (201)–(203) is to use an eigenfunction expansion in orthonormal eigenfunctions $\phi_n(\boldsymbol{u})$ of

$$\frac{1}{2P}\Delta_{\boldsymbol{u}}\phi_n - \frac{U_{\text{ex}}}{kT}\phi_n = \lambda_n \phi_n \tag{204}$$

with eigenvalues λ_n. Then

$$Z(\boldsymbol{u}', \boldsymbol{u}; 0, L) = \sum_n \mathrm{e}^{\lambda_n L}\phi_n(\boldsymbol{u}')\phi_n(\boldsymbol{u}). \tag{205}$$

Here we will only consider the limit $L \to \infty$ (or $L \gg P$) in which case the largest eigenvalue (supposedly λ_0) will dominate the problem

$$Z(\boldsymbol{u}', \boldsymbol{u}; 0, L) \sim \mathrm{e}^{\lambda_0 L}\phi_0(\boldsymbol{u}')\phi_0(\boldsymbol{u}). \tag{206}$$

Now, there is a simple connection with the angular distribution function of the chain, since $Z(\boldsymbol{u}', \boldsymbol{u}; 0, s)$ may also be interpreted as an (unnormalized) probability that a chain starting with direction $\boldsymbol{u}'$ will point in direction $\boldsymbol{u}$ after a contour length of s. Because of the Markov character of the chain, two consecutive chain sections may be considered as separate chains with one common end vector $\boldsymbol{u}$

$$f(\boldsymbol{u}, s) = \frac{\int\int Z(\boldsymbol{u}', \boldsymbol{u}; 0, s) Z(\boldsymbol{u}, \boldsymbol{u}''; 0, L - s)\,\mathrm{d}\boldsymbol{u}'\,\mathrm{d}\boldsymbol{u}''}{\int\int\int\int Z(\boldsymbol{u}', \boldsymbol{u}; 0, s) Z(\boldsymbol{u}, \boldsymbol{u}''; 0, L - s)\,\mathrm{d}\boldsymbol{u}'\,\mathrm{d}\boldsymbol{u}''\,\mathrm{d}\boldsymbol{u}\,\mathrm{d}s} \tag{207}$$

which gives on substitution of (206):

$$f(\boldsymbol{u}, s) = f(\boldsymbol{u}) = \phi_0^2(\boldsymbol{u}). \tag{208}$$

This distribution function does not depend on s (at least when s is not too near the chain ends, which is generally the case for these long chains) and it is normalized

$$\int f(\boldsymbol{u})\,\mathrm{d}\boldsymbol{u} = \int \phi_0^2(\boldsymbol{u})\,\mathrm{d}\boldsymbol{u} = 1. \tag{209}$$

Finally, the free energy of the chain is now very simple

$$\begin{aligned} F &= -kT \ln \int\int Z(\boldsymbol{u}', \boldsymbol{u}; 0, L)\,\mathrm{d}\boldsymbol{u}'\,\mathrm{d}\boldsymbol{u} \\ &\overset{(206)}{=} -\lambda_0 kTL + \mathcal{O}(kT) \end{aligned} \tag{210}$$

while the (internal) energy U of the chain as a consequence of the external potential $U_{ex}(\boldsymbol{u})$ is

$$U = L \int U_{ex}(\boldsymbol{u}) f(\boldsymbol{u}) \, \mathrm{d}\boldsymbol{u} \tag{211}$$

whence the (configurational) entropy is

$$\begin{aligned} S = \frac{U - F}{T} &= kL \int \left[\lambda_0 + \frac{U_{ex}(\boldsymbol{u})}{kT} \right] \phi_0^2(\boldsymbol{u}) \, \mathrm{d}\boldsymbol{u} \\ &\overset{204}{=} k \frac{L}{2P} \int \phi_0(\boldsymbol{u}) \Delta_{\boldsymbol{u}} \phi_0(\boldsymbol{u}) \, \mathrm{d}\boldsymbol{u}. \end{aligned} \tag{212}$$

The important point of this expression is the fact that the externally applied field is completely eliminated from the final result and S only depends on the angular distribution function $f(\boldsymbol{u}) = f(\cos\theta)$. In section 5 we use this entropy to describe the polymer in the nematic field of the neighbouring chains. In the main text we use $\mathrm{d}\Omega$ to denote $\mathrm{d}\boldsymbol{u}$.

References

Abe A and Flory P J 1978 *Macromolecules* **11** 1122
Abramowitz M and Stegun I A 1964 *Handbook of Mathematical Functions* (Washington: NBS)
Allen M P, Frenkel D and Talbot J 1989 *Comput. Phys. Rep.* **9** 301
Allen M P and Wilson M R 1989 *J. Comput. Aided Mol. Design* **3** 335
Allison A C 1957 *Biochem. J.* **65** 212
Bair T I, Morgan P W and Killian F L 1977 *Macromolecules* **10** 1396
Barboy B and Gelbart W M 1979 *J. Chem. Phys.* **71** 3053
Baus M 1987 *J. Stat. Phys.* **48** 1129
—— 1990 *J. Phys.: Condens. Matter* **2** 2111
—— 1991 private communication
Baus M and Colot J L 1985 *Mol. Phys.* **55** 653
Baus M, Colot J L, Wu X G and Xu H 1987 *Phys. Rev. Lett.* **59** 2184
Bawden F C and Pirie N W 1937 *Proc. R. Soc.* B **123** 274
Bawden F C, Pirie N W, Bernal J D and Fankuchen I 1936 *Nature* **138** 1051
Bernal J D and Fankuchen I 1941 *J. Gen. Physiol.* **25** 111
Best R J 1939 *J. Austral. Inst. Agric. Sci.* **5** 94
Birshtein T M, Kolegov B I and Pryamitsyn V A 1988 *Vysokomol. Soyed.* A **30** 348 (1988 *Polym. Sci. USSR* **30** 316)
Blum L and Torruella A J 1972 *J. Chem. Phys.* **56** 303
Blumstein A (ed) 1978 *Liquid Crystalline Order in Polymers* (New York: Academic)
Boden N, Rushby R J, Ferris L, Hardy C and Sixl F 1986 *Liquid Cryst.* **1** 109
Booy F P and Fowler A G 1985 *Int. J. Biol. Macromol.* **7** 327
Brenner S L and Parsegian V A 1974 *Biophys. J.* **14** 327
Brian A A, Frisch H L and Lerman L S 1981 *Biopolymers* **20** 1305
Bugosh J 1961 *J. Phys. Chem.* **65** 1791
Chandrasekhar S 1977 *Liquid Crystals* (Cambridge: Cambridge University Press)
Ciferri A, Krigbaum W R and Meyer R B (eds) 1982 *Polymer Liquid Crystals* (New York: Academic)
Ciferri A and Marsano E 1987 *Gazz. Chim. It.* **117** 567
Colot J L, Wu X G, Xu H and Baus M 1988 *Phys. Rev.* A **38** 2022
Conio C, Bianchi E, Ciferri A and Krigbaum W R 1984 *Macromolecules* **17** 856
Cotter M A 1974 *Phys. Rev.* A **10** 625
—— 1977 *J. Chem. Phys.* **66** 1098
—— 1979 *The Molecular Physics of Liquid Crystals* ed G R Luckhurst and G W Gray (London: Academic)

Cotter M A and Martire D E 1970a *J. Chem. Phys.* **52** 1902, 1909
—— 1970b *J. Chem. Phys.* **53** 4500
De Gennes P G 1974 *The Physics of Liquid Crystals* (Oxford: Clarendon)
DiMarzio E A 1961 *J. Chem. Phys.* **35** 658
Doi M and Edwards S F 1986 *The Theory of Polymer Dynamics* (Oxford: Clarendon)
DuPré D B and Yang S 1991 *J. Chem. Phys.* **94** 7466
Earnshaw W C and Casjens S R 1980 *Cell* **21** 319
Evans R 1979 *Adv. Phys.* **28** 143
Feynman R P 1972 *Statistical Mechanics* (Reading: Benjamin)
Fixman M and Skolnick J 1978 *Macromolecules* **11** 863
Flory P J 1956 *Proc. R. Soc.* A **234** 60, 73
—— 1978 *Macromolecules* **11** 1138, 1141
—— 1984 *Adv. Polym. Sci.* **59** 1
Flory P J and Abe A 1978 *Macromolecules* **11** 1119
Flory P J and Frost R S 1978 *Macromolecules* **11** 1126
Flory P J and Ronca G 1979 *Mol. Cryst. Liquid Cryst.* **54** 289, 311
Folda T, Hoffmann H, Chanzy H and Smith P 1988 *Nature* **333** 55
Fraden S, Caspar D L D and Phillips W C 1982 *Biophys. J.* **37** 94a
Fraden S, Hurd A J, Meyer R B, Cahoon M and Caspar D L D 1985 *J. Physique* **46** C3 85
Fraden S, Maret G, Caspar D L D and Meyer R B 1989 *Phys. Rev. Lett.* **63** 2068
Frenkel D 1987a *J. Phys. Chem.* **91** 4912 (erratum: 1988 **92** 5314)
—— 1987b *Mol. Phys.* **60** 1
—— 1988 *J. Phys. Chem.* **92** 3280 (erratum: 1988 **92** 5314)
—— 1989 *Liquid Cryst.* **5** 929
—— 1991 *Liquids, Freezing and Glass Transition (Les Houches session LI)* ed J P Hansen *et al* (Amsterdam: North-Holland)
Frenkel D, Mulder B M and McTague J P 1984 *Phys. Rev. Lett.* **52** 287
Frenkel D and Mulder B M 1985 *Mol. Phys.* **55** 1171
Frenkel D, Lekkerkerker H N W and Stroobants A 1988 *Nature* **332** 822
Fries P H and Patey G N 1985 *J. Chem. Phys.* **82** 429
Frost R S and Flory P J 1978 *Macromolecules* **11** 1134
Gibbons R M 1969 *Mol. Phys.* **17** 81
Gordon M and Platé N A (eds) 1984 *Advances in Polymer Science* vol 59–61 (Berlin: Springer)
Grosberg A Yu and Khokhlov A R 1981 *Adv. Polym. Sci.* **41** 53
Hansen J P and McDonald I R 1986 *Theory of Simple Liquids* 2nd edn (London: Academic)
Haymet A D J and Oxtoby D W 1986 *J. Chem. Phys.* **84** 1769
Helfrich W 1978 *Z. Naturforsch.* A **33** 305
Helfrich W and Harbich W 1985 *Chem. Scr.* **25** 32
Henderson D and Blum L 1976 *Mol. Phys.* **32** 1627
Hendrikx Y and Charvolin J 1981 *J. Physique* **42** 1427
Hentschke R 1990 *Macromolecules* **23** 1192
Herzfeld J, Berger A E and Wingate J W 1984 *Macromolecules* **17** 1718
Hill T L 1955 *Arch. Biochem. Biophys.* **57** 229
—— 1956 *Statistical Mechanics* (New York: McGraw–Hill)
Hołyst R and Poniewierski A 1989a *Mol. Phys.* **68** 381
—— 1989b *Phys. Rev.* A **39** 2742
—— 1990 *Mol. Phys.* **71** 561
Hoover W G and Ree F H 1968 *J. Chem. Phys.* **49** 3609
Itou T and Teramoto A 1984a *Macromolecules* **17** 1419
—— 1984b *Polym. J.* **16** 779
—— 1988 *Macromolecules* **21** 2225
Jackson W J Jr and Kuhfuss H F 1976 *J. Polymer Sci. Polym. Chem. Ed.* **14** 2043
Kajiwara K, Donkai N, Hiragi Y and Inagaki H 1986a *Makromol. Chem.* **187** 2883
Kajiwara K, Donkai N, Fujiyoshi Y and Inagaki H 1986b *Makromol. Chem.* **187** 2895
Kamerlingh Onnes H 1901 *Proc. Sec. Sci. Kon. Ned. Akad. Weten. Amsterdam* **4** 125
Kayser R F and Raveché H J 1978 *Phys. Rev.* A **17** 2067
Khokhlov A R 1979 *Vysokomol. Soyed.* A **21** 1981 (1979 *Polymer Sci. USSR* **21** 2185)
Khokhlov A R and Semenov A N 1981 *Physica* A **108** 546

—— 1982 *Physica* A **112** 605
—— 1985 *J. Stat. Phys.* **38** 161
Kloczkowski A and Stecki J 1985 *Mol. Phys.* **55** 689
Kojima T, Itou T and Teramoto A 1987 *Polymer J.* **19** 1225
Kratky O and Porod G 1949 *Rec. Trav. Chim.* **68** 1106
Kreibig U and Wetter C 1980 *Z. Naturforsch.* **35** C 750
Kubo K 1981 *Mol. Cryst. Liquid Cryst.* **74** 71
Kubo K and Ogino K 1979 *Mol. Cryst. Liquid Cryst.* **53** 207
Kwolek S L, Morgan P W, Schaefgen J R and Gulrich L W 1977 *Macromolecules* **10** 1390
Kwolek S L, Morgan P W, Schaefgen J R 1987 *Encyclopedia of Polymer Science and Engineering* 2nd edn vol 9, ed H F Mark *et al* (New York: Wiley) p 1
Lado F 1985 *Mol. Phys.* **54** 407
Lapointe J and Marvin D A 1973 *Mol. Cryst. Liquid Cryst.* **19** 269
Lasher G 1970 *J. Chem. Phys.* **53** 4141
Lawson K D and Flaut T J 1967 *J. Am. Chem. Soc.* **89** 5489
Le Doussal P and Nelson D R 1991 *Europhys. Lett.* **15** 161
Lee S D 1987 *J. Chem. Phys.* **87** 4972
—— 1988 *J. Chem. Phys.* **89** 7036
Lee S D and Meyer R B 1990 *Liquid Cryst.* 7 451
Lekkerkerker H N W, Coulon P, van der Haegen R and Deblieck R 1984 *J. Chem. Phys.* **80** 3427
Lifshitz I M 1968 *Z. Eksp. Teor. Fiz.* **55** 2408 (1969 *Sov. Phys.–JETP* **28** 1280)
Lifshitz I M, Grosberg A Yu and Khokhlov A R 1978 *Rev. Mod. Phys.* **50** 683
Lipkin M D and Oxtoby D W 1983 *J. Chem. Phys.* **79** 1939
Livolant F and Bouligand Y 1986 *J. Physique* **47** 1813
Livolant F, Levelut A M, Doucet J and Benoit J P 1989 *Nature* **339** 724
Longuet-Higgins H C and Widom B 1964 *Mol. Phys.* **8** 549
Luckhurst G R and Gray G W (eds) 1979 *The Molecular Physics of Liquid Crystals* (London: Academic)
McMillan W G Jr and Mayer J E 1945 *J. Chem. Phys.* **13** 276
McMullen W E, Gelbart W M and Ben-Shaul A 1985 *J. Chem. Phys.* **82** 5616
McQuarrie D A 1976 *Statistical Mechanics* (New York: Harper and Row)
Maeda Y and Hachisu S 1983 *Colloids and Surfaces* **6** 1, **7** 357
Marchessault R H, Morehead F F and Walter N M 1959 *Nature* **184** 632
Maret G and Dransfeld K 1985 *Strong and Ultrastrong Magnetic Fields and Their Applications* ed F Herlach (Berlin: Springer) pp 160–7
Maret G, Milas M and Rinaudo M 1981 *Polymer Bull.* **4** 291
Marko J F 1988 *Phys. Rev. Lett.* **60** 325
—— 1989 *Phys. Rev.* A **39** 2050
Mayer J E and Mayer M G 1940 *Statistical Mechanics* (New York: Wiley)
Mederos L and Sullivan D E 1989 *Phys. Rev.* A **39** 854
Milas M and Rinaudo M 1983 *Polymer Bull.* **10** 271
Miller W G 1982 *Ann. Rev. Phys. Chem.* **29** 519
Miller W G, Wu C C, Wee E L, Santee G L, Rai J H and Goebel K G 1974 *Pure Appl. Chem.* **38** 37
Morgan P W 1977 *Macromolecules* **10** 1381
Mulder B 1987 *Phys. Rev.* A **35** 3095
Mulder B M and Frenkel D 1985 *Mol. Phys.* **55** 1193
Northolt M G and Sikkema D J 1990 *Adv. Polymer Sci.* **98** 115
Nyrkova I A and Khokhlov A R 1986 *Biofyzika* **31** 771 (1986 *Biophysics* **31** 839)
Odijk T 1977 *J. Polymer Sci. Polym. Phys. Ed.* **15** 477
—— 1986a *Macromolecules* **19** 2313
—— 1986b *Liquid Cryst.* **1** 97
—— 1986c *Liquid Cryst.* **1** 553
—— 1988 *Integration of Fundamental Polymer Science and Technology* vol 2, ed P J Lemstra and L A Kleintjes (London: Elsevier)
—— 1990 *J. Chem. Phys.* **93** 5172
Odijk T and Lekkerkerker H N W 1985 *J. Phys. Chem.* **89** 2090
Onsager L 1933 *Chem. Rev.* **13** 73
—— 1942 *Phys. Rev.* **62** 558
—— 1949 *Ann. NY Acad. Sci.* **51** 627

Oster G 1950 *J. Gen. Physiol.* **33** 445
Panar M and Beste L F 1977 *Macromolecules* **10** 1401
Parsegian V A 1972 *J. Chem. Phys.* **56** 4393
Parsons J D 1979 *Phys. Rev.* A **19** 1225
Perera A, Kusalik P G and Patey G N 1987 *J. Chem. Phys.* **87** 1295
Perera A and Patey G N 1988 *J. Chem. Phys.* **89** 5861
Perera A, Patey G N and Weis J J 1988 *J. Chem. Phys.* **89** 6941
Pershan P S (ed) 1988 *Structure of Liquid Crystal Phases* (Singapore: World Scientific)
Philip J R and Wooding R A 1970 *J. Chem. Phys.* **52** 953
Poniewierski A and Hołyst R 1988 *Phys. Rev. Lett.* **61** 2461
Pynn R 1974a *Solid State Commun.* **14** 29
—— 1974b *J. Chem. Phys.* **60** 4579
Radley K and Reeves L W 1975 *Can. J. Chem.* **80** 174
Ramakrishnan T V and Yussouff M 1977 *Solid State Commun.* **21** 389
—— 1979 *Phys. Rev.* B **19** 2775
Reinitzer F 1888 *Monatsh. Chem.* **9** 421
Reiss H, Frisch H L and Lebowitz J L 1959 *J. Chem. Phys.* **31** 369
Rill R L 1986 *Proc. Natl Acad. Sci. USA* **83** 342
Rill R L, Hilliard P R and Levy G C 1983 *J. Biol. Chem.* **258** 250
Robinson C 1956 *Trans. Faraday Soc.* **52** 571
Robinson C, Ward J C and Beevers R B 1958 *Discuss. Faraday Soc.* **25** 29
Ronca G and Yoon D Y 1982 *J. Chem. Phys.* **76** 3295
—— 1984 *J. Chem. Phys.* **80** 925
—— 1985 *J. Chem. Phys.* **83** 373
Rosenfeld Y, Levesque D and Weis J J 1990 *J. Chem. Phys.* **92** 6818
Russo P S and Miller W G 1983 *Macromolecules* **16** 1690
Samulski E T and DuPré D B 1983 *J. Chim. Phys.* **80** 25
Sato T and Teramoto A 1990 *Mol. Cryst. Liquid Cryst.* **178** 143
—— 1991 *Physica* A **176** 72
Sato T, Ikeda N, Itou T and Teramoto A 1989 *Polymer* **30** 311
Sato T, Kakihara T and Teramoto A 1990 *Polymer* **31** 824
Selinger J V and Bruinsma R F 1991 *Phys. Rev.* A **43** 2910, 2922
Semenov A N and Khokhlov A R 1988 *Usp. Fiz. Nauk* **156** 427 (1988 *Sov. Phys. Usp.* **31** 988)
Senechal E, Maret G and Dransfeld K 1980 *Int. J. Biol. Macromol.* **2** 256
Singh U P and Singh Y 1986 *Phys. Rev.* A **33** 2725
Singh U P, Mohanty U and Singh Y 1989 *Physica* A **158** 817
Singh Y 1984 *Phys. Rev.* A **30** 583
Skolnick J and Fixman M 1977 *Macromolecules* **10** 944
Sluckin T J 1989 *Liquid Cryst.* **6** 111
Sluckin T J and Shukla P 1983 *J. Phys. A: Math. Gen.* **16** 1539
Somoza A M and Tarazona P 1988 *Phys. Rev. Lett.* **61** 2566
—— 1989a *J. Chem. Phys.* **91** 517
—— 1989b *Phys. Rev.* A **40** 4161
—— 1990 *Phys. Rev.* A **41** 965
Stecki J and Kloczkowski A 1979 *J. Physique* **40** C3 360
—— 1981 *Mol. Phys.* **42** 51
Stephen M J and Straley J P 1974 *Rev. Mod. Phys.* **46** 617
Stigter D 1977 *Biopolymers* **16** 1435
Straley J P 1973a *Mol. Cryst. Liquid Cryst.* **22** 333
—— 1973b *Mol. Cryst. Liquid Cryst.* **24** 7
Stroobants A, Lekkerkerker H N W and Odijk T 1986a *Macromolecules* **19** 2232
Stroobants A, Lekkerkerker H N W and Frenkel D 1986b *Phys. Rev. Lett.* **57** 1452
—— 1987 *Phys. Rev.* A **36** 2929
Strzelecka T E and Rill R L 1987 *J. Am. Chem. Soc.* **109** 4513
—— 1990 *Biopolymers* **30** 57
Strzelecka T E, Davidson M W and Rill R L 1988 *Nature* **331** 457
Talbot J, Perera A and Patey G N 1990 *Mol. Phys.* **70** 285
Ten Bosch A, Maïssa P and Sixou P 1983 *J. Chem. Phys.* **79** 3462

Ten Bosch A, Pinton J F, Maïssa P and Sixou P 1987 *J. Phys. A: Math. Gen.* **20** 4531
Teramoto A 1990 private communication
Timling K M 1974 *J. Chem. Phys.* **61** 465
Tjipto-Margo B and Evans G T 1990 *J. Chem. Phys.* **93** 4254
Trohalaki S, Brian A A, Frisch H L and Lerman L S 1984 *Biophys. J.* **45** 777
Van K and Teramoto A 1982 *Polymer J.* **14** 999
Van Kampen N G 1961 *Physica* **27** 783
Veerman J A C and Frenkel D 1990 *Phys. Rev.* A **41** 3237
Vertogen G and De Jeu W H 1988 *Thermotropic Liquid Crystals, Fundamentals* (Berlin: Springer)
Vieillard-Baron J 1974 *Mol. Phys.* **28** 809
Vroege G J 1989 *J. Chem. Phys.* **90** 4560
—— 1991 unpublished results
Vroege G J and Odijk T 1988 *Macromolecules* **21** 2848
Waisman E 1973 *Mol. Phys.* **25** 45
Warner M and Flory P J 1980 *J. Chem. Phys.* **73** 6327
Warner M, Gunn J M F and Baumgärtner A B 1985 *J. Phys. A: Math. Gen.* **18** 3007
Wee E L and Miller W G 1971 *J. Phys. Chem.* **75** 1446
Wen X, Meyer R B and Caspar D L D 1989 *Phys. Rev. Lett.* **63** 2760
Werbowyj R S and Gray D G 1976 *Mol. Cryst. Liquid Cryst.* **34** 97
—— 1980 *Macromolecules* **13** 69
Widom B 1963 *J. Chem. Phys.* **39** 2808
Workman H and Fixman M 1973 *J. Chem. Phys.* **58** 5024
Yamakawa H 1971 *Modern Theory of Polymer Solutions* (New York: Harper and Row)
—— 1984 *Ann. Rev. Phys. Chem.* **35** 23
Yamakawa H and Stockmayer W H 1972 *J. Chem. Phys.* **57** 2843
Yu L J and Saupe A 1980 *Phys. Rev. Lett.* **45** 1000
Zocher H 1925 *Z. Anorg. Chem.* **147** 91
Zocher H and Heller W 1930 *Z. Anorg. Chem.* **186** 75
Zocher H and Török C 1960 *Kolloid Z.* **170** 140, **173** 1
—— 1962 *Kolloid Z.* **180** 41